INVESTIGATING THE EFFECTS AND MECHANISMS OF INTERACTION BETWEEN CYTOCHROME P450 2B4, CYTOCHROME P450 2E1 AND CYTOCHROME P450 REDUCTASE

by

Cesar Kenaan

A dissertation submitted in partial fulfillment
of the requirements for the degree of
Doctor of Philosophy
(Chemical Biology)
in The University of Michigan
2012

Doctoral Committee:

Professor Paul F. Hollenberg, Chair
Professor David P. Ballou
Professor William L. Smith
Associate Professor Mark A. Saper
Assistant Professor Garry D. Dotson

To my parents

Acknowledgements

The work accomplished in this thesis could not have been achieved without standing on the shoulders of many exceptional people. Chief among them is my thesis advisor and mentor, Dr. Paul F. Hollenberg. The time I spent in his laboratory has molded me into the scientist I am today. I have benefited immensely from his leadership, attention to detail, scientific curiosity and patience. I am deeply indebted to him for his support and encouragement over the years.

I would also like to thank the members of my dissertation committee, Drs. William Smith, Garry Dotson, Mark Saper and David Ballou. I owe an especially great debt to Dr. Ballou for the many hours he invested in my research and for his unwavering enthusiasm for my thesis projects.

Both past and current members of the Hollenberg laboratory have been central to my graduate training. In particular, I owe my deepest gratitude to Dr. Haoming Zhang for his excellent mentorship over the last four years. It has been an honor and privilege to work with such an exceptional scientist. His support and guidance were critical to my scientific and personal development. I would also like to acknowlege the outstanding technical assistance of Ms. Hsia-lien Lin. Her contagious enthusiasm for research and incredible work ethic has been a positive influence on me. I would like to thank the research assistance provided by Ms. Erin Shea. It has been a joy and pleasure to mentor Erin in the laboratory, and I wish her all the best in medical school. Thank you as well to Chitra Sridar, Dr. Jaime D'Agostino, Dr. Hemali Amunugama, Vyvyca Walker, Dr.

Matthew Pratt-Hyatt, Dr. Natasha Snider, Diane Calinski, and Sarah Ney for making the Hollenberg such a fun and rewarding place to do science.

I would especially like to thank my parents, Ghada and Michel Kenaan and brother, Sami, for their endless support and love over the years. They provided me with an exceptional family life and instilled in me the desire to work hard and pursue my dreams. None of this would have been possible without them. Last but not least, I would like to thank Amber Streit for her love and care. Your impact on my life in general has been amazing and I will always be grateful.

Table of Contents

List of Tables

Table

List of Figures

List of Abbreviations

APBS, adaptive Poisson-Boltzmann solver.
BNZ, benzphetamine
CO, carbon monoxide
CPI, 4-(4-chlorophenyl)imidazole
CPR, cytochrome P450 reductase
CYP, cytochrome P450
Cyt b_5, cytochrome b_5
DLPC, dilauroylphosphatidylcholine
EDC, 1-ethyl-3-[3-(dimethylamino)propyl]-carbodiimide
ER, endoplasmic reticulum
ESI, electrospray ionization
FAD, flavin adenine dinucleotide
FM, fluorescein-5-maleimide
FMN, flavin mononucleotide
HCHO, formaldehyde
HLM, human liver microsomes
ITC, isothermal titration calorimetry
LC, liquid chromatography
MD, molecular dynamics
Mn-cyt b_5, manganese-containing cyt b_5
MS, mass spectrometry
NADPH, nicotinamide adenine dinucleotide phosphate
PB, phenobarbital
PDB, protein data bank
Pdr, putidaredoxin reductase
Pdx, putidaredoxin
p-NP, para-nitrophenol
PR, plastic region
PROD, 7-pentoxyresorufin O-deethylase
P450, cytochrome P450
tBHP, tert-butyl hydroperoxide
TCA, trichloroacetic acid
TFA, trifluoroacetic acid
WT, wild-type
βNF, β-naphthoflavone
ΔG, Gibbs free energy
4-NC, 4-nitrocatechol

Chapter I

Introduction

The cytochrome P450 superfamily

The cytochromes P450 (P450s or CYPs) constitute a superfamily of enzymes that plays numerous roles throughout the biological kingdom (Venkatakrishnan et al., 2001). The prevalence of P450s in all organisms is evident in the fact that more than 11,000 P450 genes have been identified to date, and this number is likely to rise in the future as the accessibility of genomic sequencing technology continues to improve (http://drnelson.uthsc.edu/P450.statsfile.html, 2009). In humans, 57 different P450 isoforms have been identified and they play critical roles in steroid biosynthesis, fatty acid metabolism, chemical toxicity and drug metabolism (Guengerich, 1993; Williams et al., 2000a; Venkatakrishnan et al., 2001).

In P450s, carbon monoxide (CO) binds exclusively to the reduced or ferrous form of their prosthetic heme-iron causing the holoprotein to absorb visible light maximally at 450 nm, hence the name “P450”. This unique spectroscopic property differentiates these enzymes from many other hemo-proteins, which generally absorb at ~ 420 nm when bound to CO. P450s are classified on the basis of sequence homology. Isoforms that share 40% sequence homology are grouped into families (1, 2, 3, etc), and these are divided into subfamilies (1A, B, C, etc.) based on at least 55% (up to 95%) sequence homology in primary structure. Individual P450s are then given a second number based

on the order of their discovery, resulting in a unique name for each isoform, for example, 2B4, 2B6 or 2E1. The majority of human P450s are believed to be involved in the biosynthesis of endogenous compounds; however, the P450s in families 1-3 are also generally involved in xenobiotic metabolism. The majority of the drug metabolizing P450s in families 1-3 are expressed primarily in the liver where they vary greatly in their relative contribution to Phase I drug metabolism. Figure 1.1 illustrates the relative contribution of the various drug-metabolizing P450s to the metabolism of the top 200 drugs prescribed in 2004 (Williams et al., 2004) . Collectively, P450s are responsible for the metabolism of approximately 60% of all clinically prescribed drugs.

The remarkable substrate versatility that these enzymes possess can be attributed to the unique structural flexibility and chemistry present in the P450 active site. Structural studies of P450s by x-ray crystallography in the past decade have provided us with a wealth of information regarding the structural organization, critical active site residues, and proton delivery pathways of P450s (Schlichting et al., 2000; Williams et al., 2000b; Scott et al., 2003). In particular, these structural analyses have consistently shown that certain regions of the P450 structures such as the F/G and B/B-C loops are extremely flexible and can undergo large conformational changes to accommodate substrates of various sizes, although the overall folding pattern of all P450s is conserved. For instance, an open conformation was observed in the ligand free CYP2B4 crystal structure, whereas a closed conformation was reported for the 4-(4-chlorophenyl)imidazole (CPI)-bound CYP2B4 (Scott et al., 2003; Scott et al., 2004) (Figure 1.2). The open-to-closed conformational change involves large motions of the F and G-helices and the F/G and B/B-C loops (Figure 1.2). Based on comparisons of the crystal structures of CYP2B4

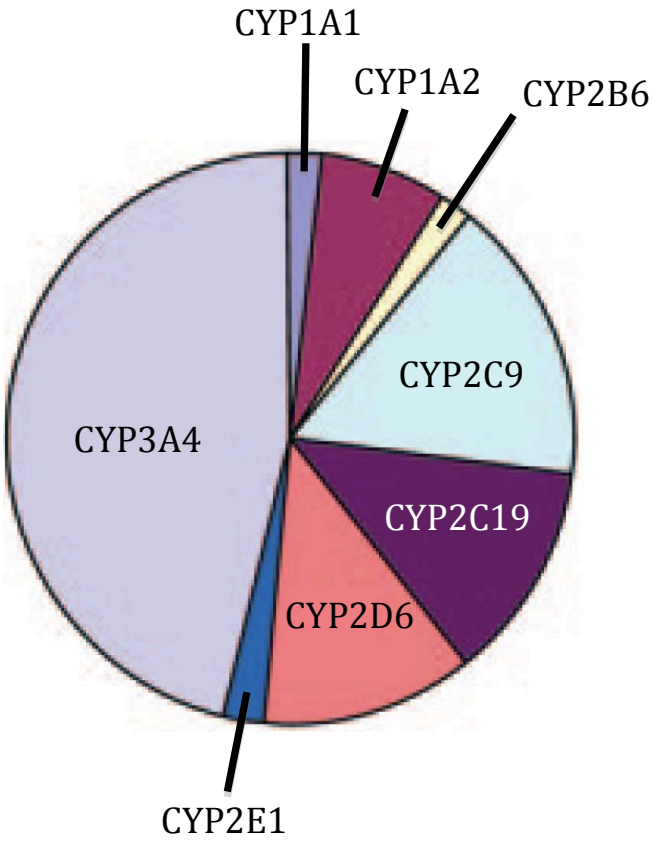

Figure 1.1. The relative contributions of human P450s to the metabolism of the top 200 drugs prescribed in 2000. Adapted from Williams et al., 2004. The percentage of metabolism that each isoform contributes is estimated by the relative size of each section of the corresponding pie chart.

A.

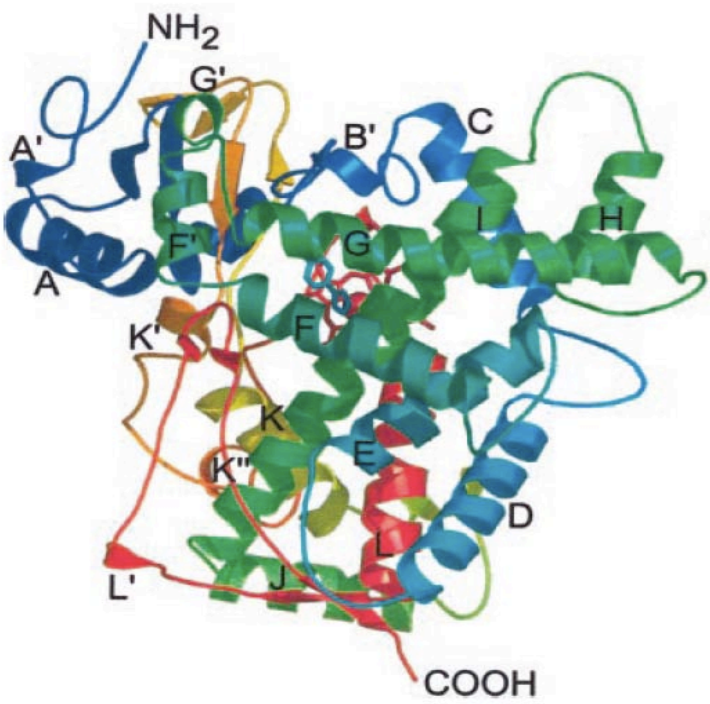

B.

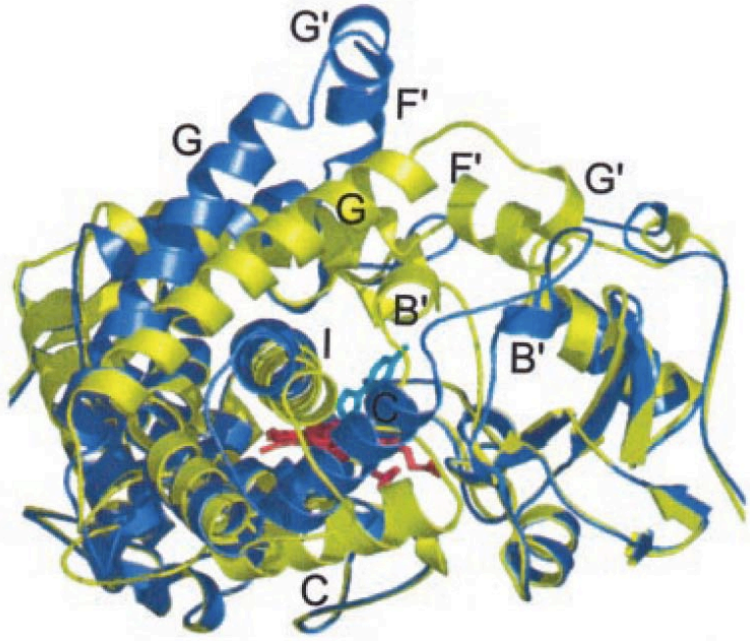

Figure 1.2. Cartoon diagram of the crystal structure of CYP2B4 (PDB ID 1SUO, figure from Scott et al., 2004). A, Structure of CYP2B4 with 4-(4-chlorophenyl)imidazole (CPI) bound to the active site with the major helices and termini labeled. B, The structure of CYP2B4 in an open conformation (blue) superimposed on the structure of CYP2B4 with CPI bound (closed conformation, yellow). The helices that undergo major conformational changes in the presence of CPI are labeled.

bound with inhibitors of different sizes, Zhao et al. (Zhao et al., 2006) identified five plastic regions (PR) in P450s, including the B/B-C loop (PR2) and F/G loop (PR4). Binding of ketoconazole or erythromycin to CYP3A4 led to a large increase in the active site volume (~80% increase) because of conformational changes primarily in the PR4, but interestingly, the F- and G-helices moved in the opposite direction (Ekroos and Sjogren, 2006). These authors proposed that the extreme flexibility of CYP3A4 accounts for its promiscuity, as CYP3A4 metabolizes nearly 50% of all clinically used drugs. The complexity of the conformational flexibility and dynamics are also revealed in a molecular dynamics (MD) simulation study of CYP3A4, 2C9 and 2A6 (Skopalik et al., 2008). Importantly, this MD simulation study shows that the three-dimensional structure of P450s is more flexible in solution than was observed in the crystal structure. Recent studies from our laboratory have shown that limiting conformational dynamics by engineering a disulfide bond into CYP2B1 alters substrate entry and recognition by limiting the conformational states that CYP2B1 can sample in solution (Zhang et al., 2009).

The tremendous catalytic prowess of P450s arises from a unique combination of conformational flexibility with the ability of the P450 heme iron to reduce molecular oxygen, ultimately leading to oxidation of their substrates. This is achieved through a series of steps, which collectively constitute the “consensus P450 catalytic cycle” (outlined in Figure 1.3). In the first step of the catalytic cycle, substrate (denoted as R-H in Figure 1.3) binds to the active site in the vicinity of the heme group and displaces water from its position as the sixth-ligand to the heme iron to produce a high-spin heme

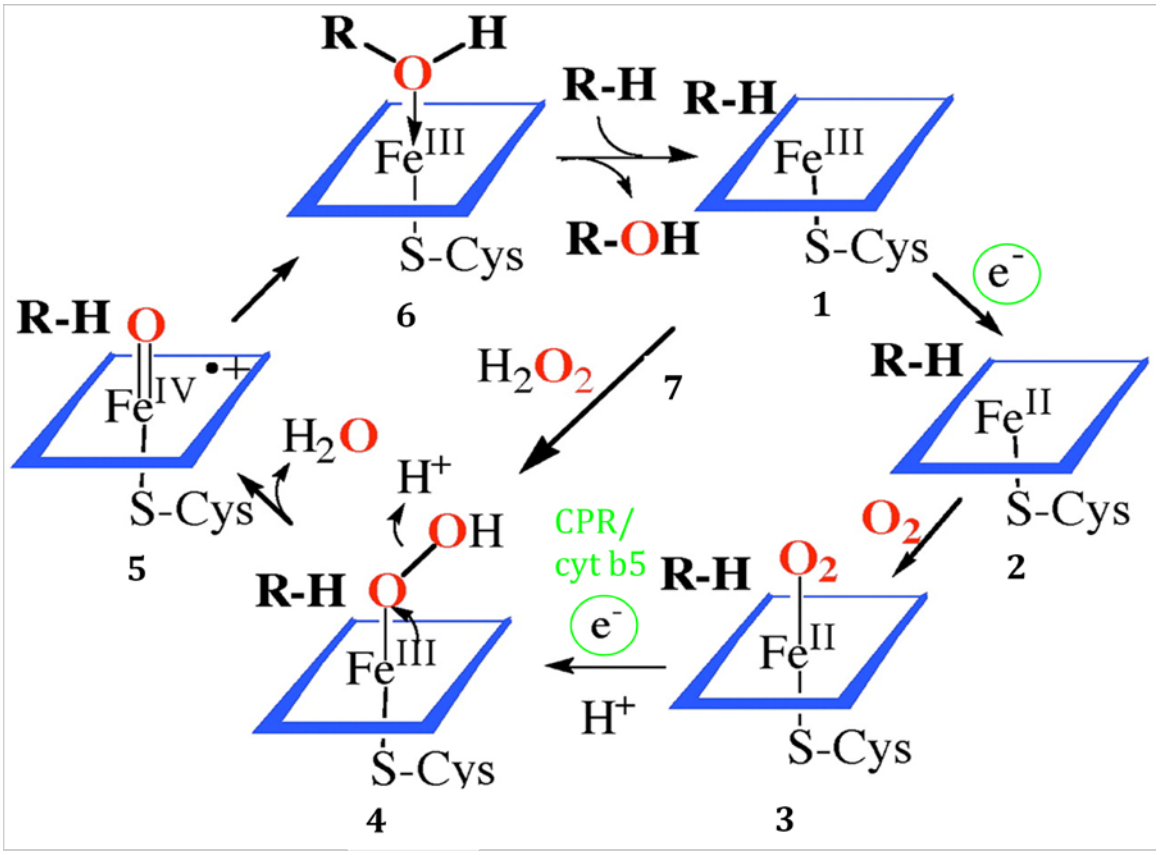

Figure 1.3. Individual steps that constitute the consensus cytochrome P450 catalytic cycle (Adapted from Groves et al. 2003) responsible for oxygen activation and transfer. For simplicity, the porphyrin is depicted as a blue parallelogram while oxygen is shown in red to highlight the fact that only a single oxygen is inserted into the substrate while the second oxygen combines with two protons to form water.

[step 1]. The high-spin heme possesses a more positive redox potential compared to that of its low spin form and with respect to FMN in CPR. This shift in the electronic configuration of the iron valence shell electrons renders the heme more thermodynamically favorable to be reduced by a single electron via CPR to yield a ferrous P450 heme iron [step 2]. Binding of molecular oxygen leads to formation of the ferrous diooxygen complex [step 3], which is followed by the transfer of a second electron from either CPR or cytochrome b_5 (cyt b_5) with subsequent protonation that results in the production of a ferric hydroperoxy complex [step 4]. Heterolytic cleavage of the O-O bond leads to the oxyferryl intermediate [step 5], otherwise known as compound I, which is believed to be the main oxidizing species responsible for the mono-oxidation reactions catalyzed by P450s. Finally, oxidation of the substrate by the oxyferryl intermediate leads to product formation followed by release of the product and regeneration of the resting ferric state of the enzyme [step 6].

In addition to these steps, the peroxide shunt, shown as step 7 (Figure 1.3), is a well-known reaction in the P450 catalytic cycle. In the shunt mechanism, hydrogen peroxide (or other peroxides) bypass the need for molecular oxygen and the transfer of two electrons from NADPH via CPR by donating an activated oxygen atom for substrate hydroxylation. However, occasionally the ferrous-diooxygen or the ferric-hydroperoxy complex can dissociate and release superoxide or hydrogen peroxides, respectively. These reactive species may then react with the heme moiety and cause irreversible damage to the catalytic activity of the P450 under investigation.

Interactions of Cytochrome P450 with CPR

As shown in Figure 1.3 the first step in the P450 catalytic cycle after binding of the substrate, is reduction of the P450 by NADPH via CPR. Since the discovery that the basic components of the P450 system are phospholipid, P450 and CPR, there has been continued interest in the nature of the interactions between P450 and CPR. This interest has been compounded by the realization that P450s exist in a large excess over CPR in the endoplasmic reticulum. This ratio may be 10- to 20-fold, depending on induction levels of the P450. Since CPR has been shown to form a 1:1 functional reductase-P450 complex (Miwa et al., 1979), the disparity in the CPR to P450 ratio raises several questions with regards to how CPR interacts with the many human P450 isoforms.

Peterson et al. (1976) were one of the first to postulate an explanation of how CPR coordinates the efficient transfer of electrons to the large excess of P450 proteins in the endoplasmic reticulum of the liver (Figure 1.4) (Peterson et al., 1976). Their studies showed that the reduction of liver microsomal P450s by CPR is a biphasic process consisting of a fast and slow phase. The fast phase of P450 reduction was attributed to the formation of several P450 clusters around central CPR molecules that could then provide immediate access to electrons from NADPH. It was proposed that the remaining P450s (approximately 30%), which were reduced in the slow phase of the biphasic kinetic process, were not in the vicinity of the CPR but eventually received electrons from CPR following lateral movement of the P450s through the membrane toward CPR. However, subsequent studies showed that biphasic reduction kinetics were still observed under conditions where heteromeric P450 clusters would not be expected to form, (i.e., at saturating or near saturating levels of CPR). Therefore, the formation of P450 clusters

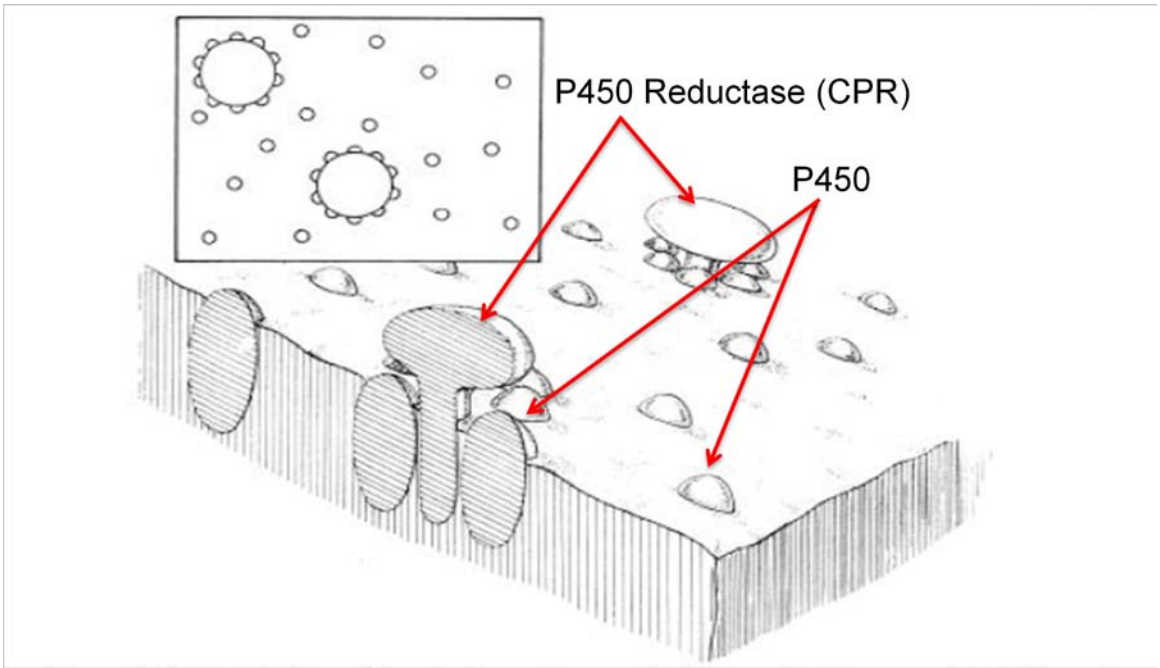

Figure 1.4. Distribution of microsomal P450s and CPR in the membrane of the ER (adapted from Peterson et al. 1976). In the model proposed by Peterson et al (1976), several P450s are envisioned to cluster around a central CPR molecule while a portion of the microsomal P450s are thought to be loosely associated with the CPR and may even be free-floating in the membrane matrix. The disparity in the P450:CPR ratio combined with the likely organization of these microsomal proteins in the membrane suggests that at any given time only a portion of the total microsomal P450s can be in functional complexes with CPR and thus capable of catalyzing the metabolism of drugs.

around a CPR molecule and the distribution of the P450s and CPR in the membrane alone cannot explain by themselves the biphasic reduction kinetics noted by Peterson et al (1976). Nevertheless, this proposed model still remains a valuable working hypothesis as it includes several features that describe the potential interactions and distribution of P450s in the membrane of the ER. Furthermore, the notion that the outcome of P450-mediated metabolism of a drug in a given tissue may not only be a function of the particular P450 that metabolizes the drug, but also its accessibility to CPR, which may be influenced by the presence and abundance of other P450s that may compete for the CPR, is a central principle of their hypothesis. Thus, an understanding of the molecular and kinetic factors that control electron transfer to the complexed and free-floating (uncomplexed) P450s is required in order to attempt to explain the behavior of the drug metabolizing P450s at less than stoichiometric amounts of CPR.

Since microsomal P450s are present in a 10-20 fold molar excess over CPR in the ER, rapid association and dissociation of the P450-CPR complex is likely to be important for the system to work effectively. To this end, there has been continued biochemical and biophysical interest in the interaction of P450s with CPR, and this has been the subject of several studies in the past. A number of lines of evidence suggest that P450-CPR interactions occur via two main processes: electrostatic and hydrophobic intermolecular interactions. For instance, it has been shown that specific basic residues on CYP1A1 are involved in forming an electron transfer complex with CPR (Shimizu et al., 1991). The involvement of Lys residues in the interaction of CYP1A1 with CPR was further demonstrated by site-directed mutagenesis of Lys271 and Lys279 on CYP1A1 (Cvrk and Strobel, 2001). Replacing Lys279 with Ile caused a decrease in CPR supported 7-

ethoxycoumarin deethylase activity, whereas the cumene hydroperoxide-supported reaction was unaffected. Chemical cross-linking studies using the carbodiimide EDC (1-ethyl-3-[3-(dimethylamino)propyl]-carbodiimide)) indicated that a cluster of acidic amino acids on CPR was involved in the interaction with CYP1A1 (Nadler and Strobel, 1991). Evidence also exists to suggest that complementary charge pairing mediates the interaction of CYP2B4 with CPR. For example, chemical modification of lysine residues on CYP2B4 by 2-methoxy-5-nitrotropone (Bernhardt, 1989) led to a decrease in CPR supported activity with virtually no effect on cumene hydroperoxide or hydrogen peroxide-supported activity. Extensive site-directed alanine scanning mutagenesis studies have identified a series of lysine and arginine residues on the proximal surface of CYP2B4 near the heme ligand that interact with CPR (Bridges et al., 1998).

The crystal structure of rat CPR reveals that an FMN-binding domain, an NADPH/FAD-binding domain and a "linker" domain comprise the three catalytic regions of the enzyme (Wang et al., 1997; Hubbard et al., 2001) (Figure 1.5). Since the transfer of electrons proceeds along the pathway from NADPH → FAD → FMN → P450, it is often assumed that the FMN domain of CPR provides the major portion of the docking surface for P450s, although recent studies have shown that orientations of this domain that deviate from the crystal structure shown in Figure 1.5 are likely to also be important in its functional interaction with P450s (Hamdane et al., 2009, (Xia et al., 2011). Electrostatic potential measurements (Figure 1.6) of a recently solved crystal structure of CPR in an open conformation capable of reducing P450 (Hamdane et al., 2009) confirmed that the FMN domain of CPR is highly negatively charged. Within this highly acidic domain, three distinct clusters of acidic residues that could form charge-charge interactions with

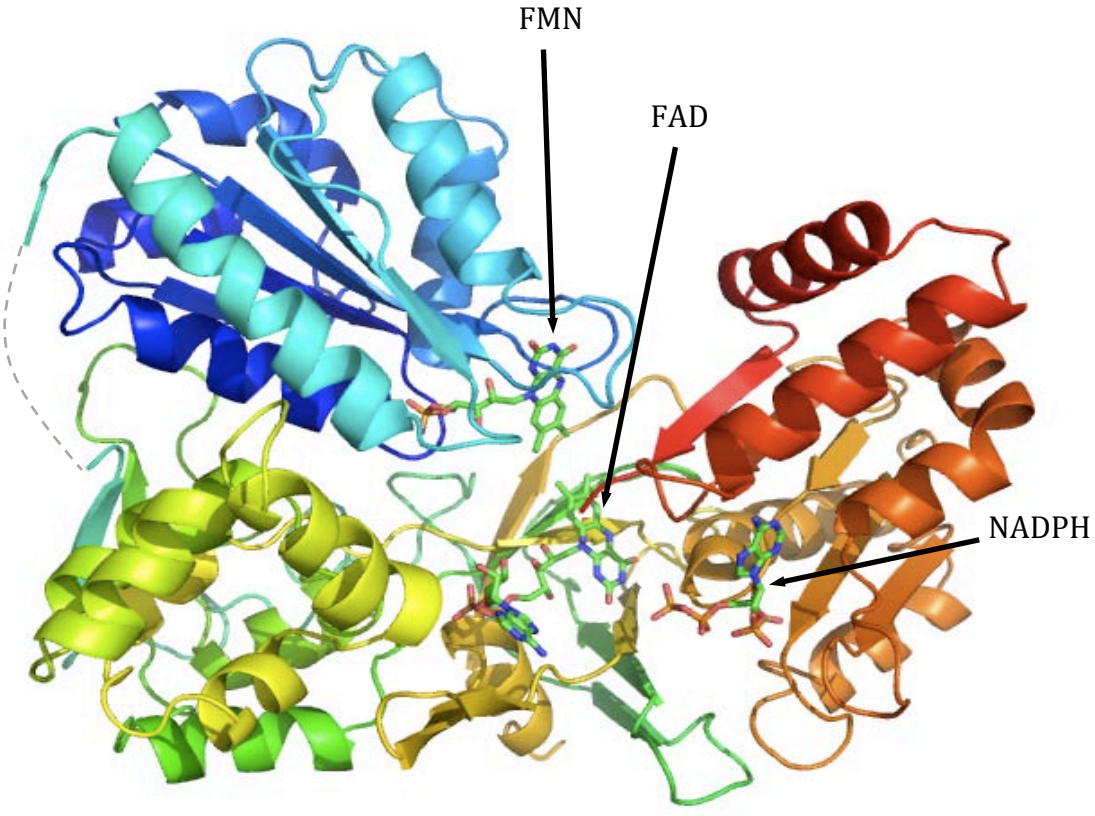

Figure 1.5. The crystal structure of rat CPR (PDB ID 1AMO). Cartoon diagram of the atomic structure of CPR. The co-factors bound to CPR (NADPH, FMN and FAD) are depicted as stick structures.

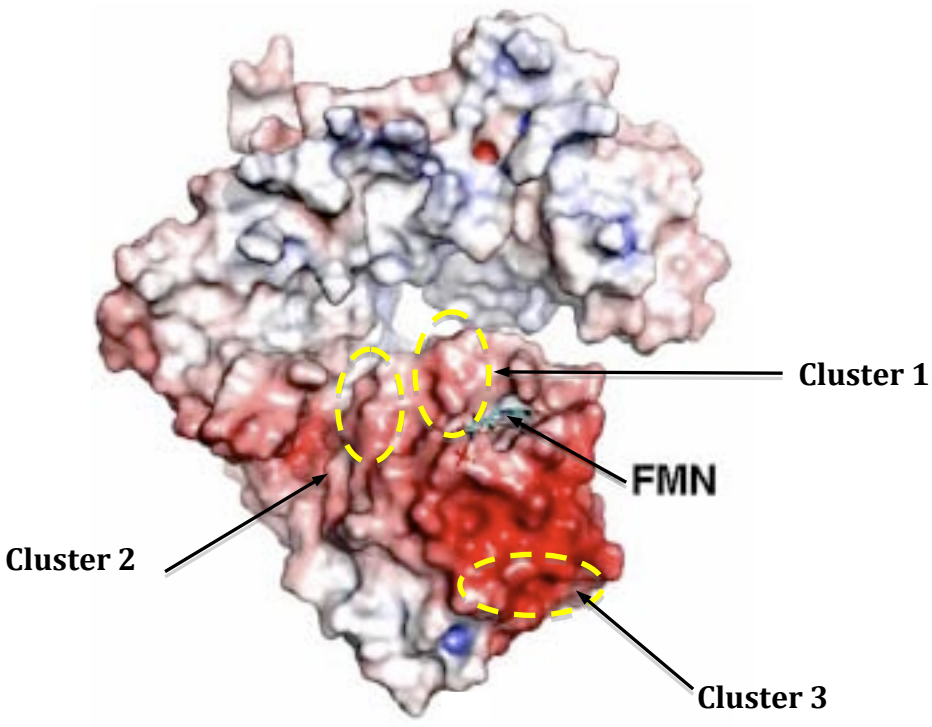

Figure 1.6. Electrostatic surface plot of CPR in an open conformation (PDB ID 3ES9, adapted from Hamdane et al. 2009). Blue, red and gray represent basic, acidic and neutral residues as determined by APBS. The regions containing clusters 1-3 are highlighted with dashed yellow circles.

the basic proximal residues in P450 have been proposed (Shen and Strobel, 1994; Zhao et al., 1999). Cluster 1 contains Asp207, Asp 208, and Asp209; cluster 2 contains Glu213, Glu214, Asp215; and cluster 3 contains Glu142, Asp144 and Asp147. With the exception of cluster 2, these clusters have been shown to play a role in the binding P450 to CPR, although the statistical significance of the observed changes in activity and electron transfer as a result of site-directed mutagenesis varied from one study to another (Shen and Strobel, 1994; Zhao et al. 1999).

While the prevailing hypothesis is that the intermolecular forces that lead to complex formation between P450 and CPR are electrostatic, evidence also exists to support a role for hydrophobic interactions at the P450-CPR interface (Black et al., 1979; Stayton and Sligar, 1990; Rodgers and Sligar, 1991; Voznesensky and Schenkman, 1992; Voznesensky and Schenkman, 1994). For example, studies from the Schenkman lab have questioned the universality of electrostatic pairing interactions and the extent that such interactions contribute to P450-CPR complex formation (Voznesensky and Schenkman, 1992; Voznesensky and Schenkman, 1994). Their results have shown that increasing ionic strength, which should neutralize electrostatic interactions, actually stimulated P450 reduction in an isoform dependent manner, thus suggesting that electrostatic forces do not promote the association of P450 with CPR.

Protein-protein Interactions between Cytochromes P450

Early studies with P450s reported that the rates of substrate metabolism in liver microsomes were significantly different than those observed for purified P450s in

reconstituted systems (West and Lu, 1972; Kaminsky et al., 1983). While there are several factors that may lead to this discrepancy, one explanation for this phenomenon is that interactions between P450s in microsomes were influencing the catalytic activities of the individual P450s. Functional interactions between P450s have been reported for a variety of P450 isoforms. For example, studies by (Tan et al., 1997) showed that by co-expressing CYP2A6 and CYP2E1 in a baculovirus expression system, and varying the expression of CPR, the activity of CYP2A6 was significantly less in the presence of CYP2E1 compared to activity measurements performed in the absence of CYP2E1. Interestingly, increasing the ratio of CPR to P450 could relieve inhibition of CYP2A6 activity by CYP2E1 suggesting that changes in activity likely arise from a simple competition for CPR governed by mass action.

Investigations into whether P450s interact with each other to alter activity have been extended to other human P450 isoforms besides CYP2A6 and CYP2E1. One of the more comprehensive studies on P450-P450 interactions is that of Yamazaki et al (1997), who investigated potential interactions among several recombinant human P450s including CYP1A2, CYP2C10, CYP2D6, CYP2E1, and CYP3A4. While the presence of CYP1A1, CYP2C10, CYP2D6 or CYP2E1 did not affect the CYP3A4-dependent 6β-hydroxylation of testosterone, CYP1A2 enhanced CYP3A4 hydroxylase activity by up to four-fold. The extent of catalytic stimulation varied significantly depending on the species (human, rat or rabbit). These results do not support the suggestion that P450-P450 interactions result from generalized and non-specific protein aggregation effects and suggest that P450-P450 interactions are specific.

Through an elegant series of studies on CYP1A2 and CYP2B4, Backes and co-

workers have shown that functional interactions occur between these two isoforms in both purified and microsomal preparations(Cawley et al., 1995). Using the purified reconstituted system, Cawley et al. compared the activities of CYP2B4 and CYP1A2 in a simple binary reconstitution (consisting of a single P450 and CPR) to a mixed reconstitution (consisting of CPR and two different P450s). The functional interactions between CYP2B4 and CYP1A2 where determined by comparing the sum of the rates of the binary reconstitution to that obtained in the mixed reconstitution. With sub-saturating concentrations of CPR relative to P450, CYP1A2 inhibited the 7-pentoxyresorufin O-deethylase (PROD) activity of CYP2B4. Interestingly, this effect was not observed with the other two CYP2B4 substrates used, benzphetamine (BNZ) and 7-ethoxyresorufin. Therefore, these results established that the presence of another P450 isoform may influence the catalytic activity of the P450 under investigation and that these effects are dependent on the substrate examined. The authors proposed that these results are consistent with CYP1A2 forming a high-affinity complex with CPR which allows CYP1A2 to out-compete CYP2B4 for binding to and subsequent reduction by CPR.

To determine whether these interactions occurred under more physiological conditions than those present in the reconstituted system, the authors extended their studies to rabbit liver microsomes (Cawley et al., 2001). In these experiments, rabbits were pretreated with phenobarbital (PB), β-naphthoflavone (βNF), or PB+βNF to induce the expression of CYP2B4, CYP1A2 or both enzymes, respectively. Both groups treated with PB and βNF displayed similar increases in BNZ demethylation, consistent with the induction of CYP2B4 in both groups. When the PROD activity of CYP2B4 in the PB + βNF treated group was compared to that observed in the PB group, the authors observed

an approximate 75% decrease in activity. The results of the studies in microsomal preparations are consistent with the effect of CYP1A2 on CYP2B4 activity observed in the purified reconstituted system. Taken together, they demonstrate that the interactions observed between P450s, at least in the case of CYP1A2 and CYP2B4, do not result from physical or chemical differences between the artificial conditions present in the reconstituted system and the more natural conditions of the microsomal membranes since the functional interactions could be replicated in microsomes. Therefore, interactions among P450 isoforms may result in significant differences in the metabolic profile of drugs and this may be influenced by the abundance of one isoform relative to another as well as the substrate under investigation.

Cytochrome P450 2B subfamily

The cytochrome P450 2B subfamily plays an important role in drug metabolism (Rendic and Di Carlo, 1997). Human CYP2B6 constitutes approximately 2-10% of the total hepatic P450 (Wang and Tompkins, 2008) but has also been detected in trace amounts in the skin (Du et al., 2004), brain (Gervot et al., 1999), heart (Thum and Borlak, 2000) and kidney (Aleksa et al., 2005). Despite the relatively low expression of CYP2B6, it is estimated that this isoform contributes to the metabolism of approximately 3-12% of clinically used drugs (Wang and Tompkins, 2008) including sertraline, propofol, bupropion, cyclophosphamide, and methadone (Walsky et al., 2006; Wang and Tompkins, 2008). A number of single nucleotide polymorphisms have been found in the *P450 2B6* gene and several of the polymorphic variant proteins have been shown to

exhibit altered rates of metabolism compared to the WT P450s *in vitro* and *in vivo* (Kirchheiner et al., 2003; Zhang et al., 2011). Notably, one clinical study found that *P450 2B6*4* is associated with increased bupropion clearance and with higher plasma levels of hydroxybupropion, the pharmacologically active metabolite produced by CYP2B6 that is responsible for the anti-depressant and smoking cessation effects of bupropion (Kirchheiner et al., 2003). However, higher levels of hydroxybupropion are also thought to be associated with seizures, which occur in 1 in 1000 patients undergoing treatment with bupropion (Wooltorton, 2002).

In addition to its well-established role in drug metabolism, CYP2B6 has been shown to bioactivate several procarcinogens including aflatoxin and nitrosamines derived from tobacco-based products (Ekins and Wrighton, 1999; Dicke et al., 2005). Therefore, given the important role this enzyme plays in determining the pharmacokinetic profile of several drugs, it is important to understand the factors that may contribute to alterations in its activity such as impairments in its binding to and subsequent reduction by CPR.

While the main objective of this thesis project is to better understand the factors that influence the association of human CYP2B6 with CPR, many of the studies reported here were performed initially on rabbit CYP2B4 since the final protein yield from the bacterial overexpression and purification of CYP2B6 is quite low (Scott et al., 2001). However, CYP2B4, the rabbit homologue to the human CYP2B6, is significantly more highly expressed in *E. coli* and shares 88% sequence similarity with CYP2B6, making it a reasonable model system to understand CYP2B6 (Oezguen et al., 2008). Furthermore, CYP2B4 is considered one of the paradigmatic mammalian P450s, as it has been studied extensively by site-directed mutagenesis, and the consequences of mutations intended to

probe the relationship between protein structure and function are more predictable with CYP2B4 than with other P450 isoforms (Zhang et al., 2009). Therefore, the investigations described herein were performed with CYP2B4 unless otherwise noted.

Scope of thesis

Given the discrepancy in the ratio of P450 to CPR, and the relatively low abundance of hepatic CYP2B6, it is likely that CYP2B6 will behave very differently in the presence of other P450 isoforms at limiting concentrations of CPR. It is also likely that the differences between the catalytic activities observed for the individual CYP2B6 when compared to CYP2B6 in the presence of other P450s will have a significant impact on the prediction of *in vivo* drug-drug interactions from *in vitro* CYP2B6 activity data obtained from a simple binary system. Thus, the objective of this thesis is to investigate the effect of the presence of a highly inducible P450 isoform on both the association of CYP2B4 with CPR and the impact this may have on CYP2B4-mediated metabolism. However, an understanding of the molecular factors that control binding to and electron-transfer from CPR is required to begin to explain the behavior of CYP2B4 in the presence of another P450 at less than stoichiometric amounts of CPR. Therefore, this thesis also represents significant progress in the development of novel approaches for studying the roles of specific amino acid residues in CYP2B4 required for binding CPR and explores whether this knowledge can be harnessed to enhance the electron transfer process in CYP2B4. The findings presented here not only have important implications for and applications in the study of redox-partner interactions and bioengineering of P450s

for industrial purposes but, they may also improve our ability to predict *in vivo* drug-drug interactions from *in vitro* data.

References

Aleksa K, Matsell D, Krausz K, Gelboin H, Ito S and Koren G (2005) Cytochrome P450 3A and 2B6 in the developing kidney: implications for ifosfamide nephrotoxicity. *Pediatr Nephrol* **20**:872-885.

Bernhardt R, Kraft, R., and Ruckpaul, K. (1989) *Molecular Mechanism of P450/reductase interaction.* Taylor and Francis, New York.

Black SD, French JS, Williams CH, Jr. and Coon MJ (1979) Role of a hydrophobic polypeptide in the N-terminal region of NADPH-cytochrome P-450 reductase in complex formation with P-450LM. *Biochem Biophys Res Commun* **91**:1528-1535.

Bridges A, Gruenke L, Chang YT, Vakser IA, Loew G and Waskell L (1998) Identification of the binding site on cytochrome P450 2B4 for cytochrome b5 and cytochrome P450 reductase. *J Biol Chem* **273**:17036-17049.

Cawley GF, Batie CJ and Backes WL (1995) Substrate-dependent competition of different P450 isozymes for limiting NADPH-cytochrome P450 reductase. *Biochemistry* **34**:1244-1247.

Cawley GF, Zhang S, Kelley RW and Backes WL (2001) Evidence supporting the interaction of CYP2B4 and CYP1A2 in microsomal preparations. *Drug Metab Dispos* **29**:1529-1534.

Cvrk T and Strobel HW (2001) Role of LYS271 and LYS279 residues in the interaction of cytochrome P4501A1 with NADPH-cytochrome P450 reductase. *Arch Biochem Biophys* **385**:290-300.

Dicke KE, Skrlin SM and Murphy SE (2005) Nicotine and 4-(methylnitrosamino)-1-(3-pyridyl)-butanone metabolism by cytochrome P450 2B6. *Drug Metab Dispos* **33**:1760-1764.

Du L, Hoffman SM and Keeney DS (2004) Epidermal CYP2 family cytochromes P450. *Toxicol Appl Pharmacol* **195**:278-287.

Ekins S and Wrighton SA (1999) The role of CYP2B6 in human xenobiotic metabolism. *Drug Metab Rev* **31**:719-754.

Ekroos M and Sjogren T (2006) Structural basis for ligand promiscuity in cytochrome P450 3A4. *Proc Natl Acad Sci U S A* **103**:13682-13687.

Gervot L, Rochat B, Gautier JC, Bohnenstengel F, Kroemer H, de Berardinis V, Martin H, Beaune P and de Waziers I (1999) Human CYP2B6: expression, inducibility and catalytic activities. *Pharmacogenetics* **9**:295-306.

Guengerich FP (1993) Cytochrome P450 enzymes. *American Scientist* **81**.

Hamdane D, Xia C, Im SC, Zhang H, Kim JJ and Waskell L (2009) Structure and function of an NADPH-cytochrome P450 oxidoreductase in an open conformation capable of reducing cytochrome P450. *J Biol Chem* **284**:11374-11384.

Hubbard PA, Shen AL, Paschke R, Kasper CB and Kim JJ (2001) NADPH-cytochrome P450 oxidoreductase. Structural basis for hydride and electron transfer. *J Biol Chem* **276**:29163-29170.

Kaminsky LS, Guengerich FP, Dannan GA and Aust SD (1983) Comparisons of warfarin metabolism by liver microsomes of rats treated with a series of polybrominated biphenyl congeners and by the component-purified cytochrome P-450 isozymes. *Arch Biochem Biophys* **225**:398-404.

Kirchheiner J, Klein C, Meineke I, Sasse J, Zanger UM, Murdter TE, Roots I and Brockmoller J (2003) Bupropion and 4-OH-bupropion pharmacokinetics in relation to genetic polymorphisms in CYP2B6. *Pharmacogenetics* **13**:619-626.

Miwa GT, West SB, Huang MT and Lu AY (1979) Studies on the association of cytochrome P-450 and NADPH-cytochrome c reductase during catalysis in a reconstituted hydroxylating system. *J Biol Chem* **254**:5695-5700.

Nadler SG and Strobel HW (1991) Identification and characterization of an NADPH-cytochrome P450 reductase derived peptide involved in binding to cytochrome P450. *Arch Biochem Biophys* **290**:277-284.

Oezguen N, Kumar S, Hindupur A, Braun W, Muralidhara BK and Halpert JR (2008) Identification and analysis of conserved sequence motifs in cytochrome P450 family 2. Functional and structural role of a motif 187RFDYKD192 in CYP2B enzymes. *J Biol Chem* **283**:21808-21816.

Peterson JA, Ebel RE, O'Keeffe DH, Matsubara T and Estabrook RW (1976) Temperature dependence of cytochrome P-450 reduction. A model for NADPH-cytochrome P-450 reductase:cytochrome P-450 interaction. *J Biol Chem* **251**:4010-4016.

Rendic S and Di Carlo FJ (1997) Human cytochrome P450 enzymes: a status report summarizing their reactions, substrates, inducers, and inhibitors. *Drug Metab Rev* **29**:413-580.

Rodgers KK and Sligar SG (1991) Mapping electrostatic interactions in macromolecular associations. *J Mol Biol* **221**:1453-1460.

Schlichting I, Berendzen J, Chu K, Stock AM, Maves SA, Benson DE, Sweet RM, Ringe D, Petsko GA and Sligar SG (2000) The catalytic pathway of cytochrome p450cam at atomic resolution. *Science* **287**:1615-1622.

Scott EE, He YA, Wester MR, White MA, Chin CC, Halpert JR, Johnson EF and Stout CD (2003) An open conformation of mammalian cytochrome P450 2B4 at 1.6-A resolution. *Proc Natl Acad Sci U S A* **100**:13196-13201.

Scott EE, Spatzenegger M and Halpert JR (2001) A truncation of 2B subfamily cytochromes P450 yields increased expression levels, increased solubility, and decreased aggregation while retaining function. *Arch Biochem Biophys* **395**:57-68.

Scott EE, White MA, He YA, Johnson EF, Stout CD and Halpert JR (2004) Structure of mammalian cytochrome P450 2B4 complexed with 4-(4-chlorophenyl)imidazole at 1.9-A resolution: insight into the range of P450 conformations and the coordination of redox partner binding. *J Biol Chem* **279**:27294-27301.

Shen S and Strobel HW (1994) Probing the putative cytochrome P450- and cytochrome c-binding sites on NADPH-cytochrome P450 reductase by anti-peptide antibodies. *Biochemistry* **33**:8807-8812.

Shimizu T, Tateishi T, Hatano M and Fujii-Kuriyama Y (1991) Probing the role of lysines and arginines in the catalytic function of cytochrome P450d by site-directed mutagenesis. Interaction with NADPH-cytochrome P450 reductase. *J Biol Chem* **266**:3372-3375.

Skopalik J, Anzenbacher P and Otyepka M (2008) Flexibility of human cytochromes P450: molecular dynamics reveals differences between CYPs 3A4, 2C9, and 2A6, which correlate with their substrate preferences. *J Phys Chem B* **112**:8165-8173.

Stayton PS and Sligar SG (1990) The cytochrome P-450cam binding surface as defined by site-directed mutagenesis and electrostatic modeling. *Biochemistry* **29**:7381-7386.

Tan Y, Patten CJ, Smith T and Yang CS (1997) Competitive interactions between cytochromes P450 2A6 and 2E1 for NADPH-cytochrome P450 oxidoreductase in the microsomal membranes produced by a baculovirus expression system. *Arch Biochem Biophys* **342**:82-91.

Thum T and Borlak J (2000) Gene expression in distinct regions of the heart. *Lancet* **355**:979-983.

Venkatakrishnan K, Von Moltke LL and Greenblatt DJ (2001) Human drug metabolism and the cytochromes P450: application and relevance of in vitro models. *J Clin Pharmacol* **41**:1149-1179.

Voznesensky AI and Schenkman JB (1992) The cytochrome P450 2B4-NADPH cytochrome P450 reductase electron transfer complex is not formed by charge-pairing. *J Biol Chem* **267**:14669-14676.

Voznesensky AI and Schenkman JB (1994) Quantitative analyses of electrostatic interactions between NADPH-cytochrome P450 reductase and cytochrome P450 enzymes. *J Biol Chem* **269**:15724-15731.

Walsky RL, Astuccio AV and Obach RS (2006) Evaluation of 227 drugs for in vitro inhibition of cytochrome P450 2B6. *J Clin Pharmacol* **46**:1426-1438.

Wang H and Tompkins LM (2008) CYP2B6: new insights into a historically overlooked cytochrome P450 isozyme. *Curr Drug Metab* **9**:598-610.

Wang M, Roberts DL, Paschke R, Shea TM, Masters BS and Kim JJ (1997) Three-dimensional structure of NADPH-cytochrome P450 reductase: prototype for FMN- and FAD-containing enzymes. *Proc Natl Acad Sci U S A* **94**:8411-8416.

West SB and Lu AY (1972) Reconstituted liver microsomal enzyme system that hydroxylates drugs, other foreign compounds and endogenous substrates. V. Competition between cytochromes P-450 and P-448 for reductase in 3,4-benzpyrene hydroxylation. *Arch Biochem Biophys* **153**:298-303.

Williams JA, Hyland R, Jones BC, Smith DA, Hurst S, Goosen TC, Peterkin V, Koup JR and Ball SE (2004) Drug-drug interactions for UDP-glucuronosyltransferase substrates: a pharmacokinetic explanation for typically observed low exposure (AUCi/AUC) ratios. *Drug Metab Dispos* **32**:1201-1208.

Williams PA, Cosme J, Sridhar V, Johnson EF and McRee DE (2000a) Mammalian microsomal cytochrome P450 monooxygenase: structural adaptations for membrane binding and functional diversity. *Mol Cell* **5**:121-131.

Williams PA, Cosme J, Sridhar V, Johnson EF and McRee DE (2000b) Microsomal cytochrome P450 2C5: comparison to microbial P450s and unique features. *J Inorg Biochem* **81**:183-190.

Wooltorton E (2002) Bupropion (Zyban, Wellbutrin SR): reports of deaths, seizures, serum sickness. *CMAJ* **166**:68.

Xia C, Hamdane D, Shen AL, Choi V, Kasper CB, Pearl NM, Zhang H, Im SC, Waskell L and Kim JJ (2011) Conformational changes of NADPH-cytochrome P450 oxidoreductase are essential for catalysis and cofactor binding. *J Biol Chem* **286**:16246-16260.

Zhang H, Kenaan C, Hamdane D, Hoa GH and Hollenberg PF (2009) Effect of conformational dynamics on substrate recognition and specificity as probed by the introduction of a de novo disulfide bond into cytochrome P450 2B1. *J Biol Chem* **284**:25678-25686.

Zhang H, Sridar C, Kenaan C, Amunugama H, Ballou DP and Hollenberg PF (2011) Polymorphic variants of cytochrome P450 2B6 (CYP2B6.4-CYP2B6.9) exhibit altered rates of metabolism for bupropion and efavirenz: a charge-reversal mutation in the K139E variant (CYP2B6.8) impairs formation of a functional cytochrome p450-reductase complex. *J Pharmacol Exp Ther* **338**:803-809.

Zhao Q, Modi S, Smith G, Paine M, McDonagh PD, Wolf CR, Tew D, Lian LY, Roberts GC and Driessen HP (1999) Crystal structure of the FMN-binding domain of human cytochrome P450 reductase at 1.93 A resolution. *Protein Sci* **8**:298-306.

Zhao Y, White MA, Muralidhara BK, Sun L, Halpert JR and Stout CD (2006) Structure of microsomal cytochrome P450 2B4 complexed with the antifungal drug bifonazole: insight into P450 conformational plasticity and membrane interaction. *J Biol Chem* **281**:5973-5981.

Chapter II

Hydrophobic Residues V267 and L270 Contribute to Complex Formation Between Cytochrome P450 2B4 and Cytochrome P450 Reductase

Abstract

Cytochrome P450 (CYP or P450)-mediated drug metabolism requires the interaction of P450s with their redox partner, cytochrome P450 reductase (CPR). In this work, we have investigated the role of P450 hydrophobic residues in complex formation with CPR and uncovered novel roles for the surface-exposed residues V267 and L270 of CYP2B4 in mediating CYP2B4-CPR interactions. Using a combination of fluorescence labeling and stopped-flow spectroscopy we have investigated the basis for these interactions. Specifically, in order to study P450-CPR interactions, a single reactive cysteine was introduced in to a genetically engineered variant of CYP2B4 (C79SC152S) at each of 7 strategically selected surface-exposed positions. Each of these cysteine residues was modified by reaction with fluorescein-5-maleimide (FM) and the CYP2B4-FM variants were then used to determine the K_d of the complex by monitoring fluorescence enhancement in the presence of CPR. Furthermore, the intrinsic K_M values of the CYP2B4 variants for CPR were measured and stopped-flow spectroscopy was used to determine the intrinsic kinetics and the extent of reduction of the ferric P450 mutants to the ferrous P450-CO complex by CPR. A comparison of the results from these three approaches reveals that the sites on P450 exhibiting the greatest changes in fluorescence

intensity upon binding CPR are associated with the greatest increases in the K_M values of the P450 variants for CPR and with the greatest decreases in the rates and extents of reduced P450-CO complex formation.

Introduction

The cytochromes P450 comprise a superfamily of heme-containing mono-oxygenases that play central roles in the metabolism of a wide variety of endogenous compounds including drugs and carcinogens. The oxidation of their substrates occurs through a series of steps that collectively constitute the P450 catalytic cycle. An essential component of the cycle is the delivery of two electrons from NADPH-CYP450 reductase (CPR). The first electron reduces the ferric heme to the ferrous state that binds molecular oxygen to produce an oxyferrous complex. The second electron leads to the formation of the peroxo intermediate, which is protonated twice: the first proton serves to yield the hydroperoxo intermediate, and the second to cleave the oxygen-oxygen bond. Finally, oxidation of the substrate by an oxyferryl intermediate leads to product release and regeneration of the resting state of the enzyme (Denisov et al., 2005; Rittle and Green, 2010).

The crystal structure of rat CPR reveals that an FMN-binding domain, an NADPH/FAD-binding domain and a “linker” domain comprise the three catalytic regions of the enzyme(Wang et al., 1997; Hubbard et al., 2001; Hamdane et al., 2009). The FAD serves as an electron acceptor from NADPH, whereas the FMN-binding domain interacts with P450 to transfer electrons. Although we have known for some time that the P450-CPR interaction is required for P450 catalysis, details are lacking with respect to the

fundamental principles that govern redox partner recognition. What is the molecular basis for the rapid association and dissociation of the P450-CPR complex that allows for efficient electron transfer? Since the ratio of CPR to P450 in the endoplasmic reticulum is estimated to be 1:20(Cawley et al., 1995; Backes and Kelley, 2003), how does CPR orchestrate the recognition and reduction of not only multiple P450 isoforms but cytochrome b5 (Enoch and Strittmatter, 1979), cytochrome c (Williams, 1962), heme oxygenase (Kikuchi et al., 2005) and squalene monoxygenase (Ono, 1975) as well?

Currently, it is thought that the association of P450s with CPR is largely driven by charge-pairing interactions between a small cluster of positively charged amino acid residues located on the surface of the side at which the prosthetic heme is ligated to the P450 (proximal), and another cluster of negatively charged amino acid residues located on the FMN domain of CPR (Shen and Kasper, 1995; Hamdane et al., 2009; Jang et al., 2010). For example, Shimizu et al. (1991) mutated a series of Lys and Arg residues in order to identify the binding site of CPR on 1A2. Their studies showed that the mutated residues may form charge interactions with CPR and/or orient the two proteins for functional interaction. Some of these surface-exposed residues were on the proximal side of CYP2B4 and correspond to residues Arg-422, Lys-433, and Arg-443 in CYP2B4, which were investigated extensively by Bridges et al. (1998) using alanine-scanning mutagenesis. In addition to these three basic residues, Bridges et al.'s work demonstrated that CYP2B4 R122A, R126A, R133A, and K139A variants exhibited dramatically weaker binding to CPR. The use of chemical cross-linking reagents coupled with mass spectrometry to investigate CYP interactions with its redox partner has also been recently evaluated (Gao and Nelson, 2006; Bumpus and Hollenberg, 2010). These studies have

shown that key lysine residues on the proximal side of P450 are involved in complex formation. For instance, it has recently been demonstrated through chemical cross-linking studies that residues presumed to be located in the C-helix of CYP2B6 form contacts with residues located in the linker region between the FAD and FMN domains (Bumpus and Hollenberg, 2010). These same residues in the C-helix of CYP2B4 have been shown by mutagenesis to be involved in complex formation.

Although it is generally accepted that the site at which CPR interacts with P450s involves the proximal region of the P450, much of our knowledge regarding the specific residues that mediate this interaction stems from a very limited number of mutagenesis studies. Furthermore, most of these experimental studies have focused on mutating charged residues to neutral ones and measuring changes in activity of the CPR-P450 complex in attempts to identify important residues. A central assumption in these studies is that the mutation does not alter electron transfer and/or the heme's catalytic integrity. However, since CPR affinity is measured indirectly through substrate turnover, it is not possible to distinguish the effect of mutagenesis on protein activity from CPR-P450 complex formation by relying exclusively on steady-state measurements. Additionally, the significant biochemical and crystallographic work performed on the P450cam and P450BM3 redox complexes suggests the likelihood that ionic interactions do not exclusively dominate protein-protein contact regions in all P450s (Sevrioukova and Poulos, 2010). The structure between the heme domain of P450BM3 and its FMN domain is the only available P450-redox partner complex structure and reveals that only a single intermolecular ionic bond mediates domain interaction (Sevrioukova et al., 1999b). The shared role that hydrophobic and ionic interactions play in redox proteins was also

demonstrated in the recent crystal structure of the Pdx-Pdr complex which showed that the interface includes two potential ionic interactions but is predominantly hydrophobic (Sevrioukova et al., 2010). Work from the Schenkman lab has questioned the universality of electrostatic pairing interactions and the extent that such interactions contribute to P450-CPR complex formation (Voznesensky and Schenkman, 1992; Voznesensky and Schenkman, 1994). Their results have shown that for some isoforms, increasing ionic strength actually stimulated P450 reduction, thus suggesting that electrostatic forces inhibit the P450-CPR interaction. These observations, in part, inspired us to investigate the role of hydrophobic residues in P450-CPR interactions.

In an effort to experimentally identify the CPR-P450 interface and the residues that dictate functional interactions at this interface, it is essential that the changes measured by such investigations result directly from protein-protein interactions. Fluorescent probes that can be chemically attached to various sites on P450 and that exhibit varying fluorescence intensities as a function of their proximity to the CPR-P450 binding site are powerful tools for mapping protein-protein interfaces (Drees et al., 1996; Sevrioukova et al., 1999a; Hassan et al., 2008). Additionally, measurements of the kinetics of the reduction of ferric P450 by CPR using a stopped-flow spectrophotometer can be used to determine whether the effect of site-directed mutagenesis is on protein binding or electron transfer. Since the rate of reduction of P450 by CPR can be measured by mixing a preformed P450-CPR complex with NADPH in the presence of CO, then the mutation of residues on P450 that mediate P450-CPR complex formation should decrease the rate of reduction and the extent of P450-CO complex formation.

The results presented in this chapter demonstrate that when fluorescein-5-

maleimide (FM) is attached to the proximal side of CYP2B4 and incubated with excess CPR, this region shows the largest fluorescence enhancement compared to studies where FM was adducted to residues located in regions distal and perpendicular to the axis of the heme-thiolate ligation. The mutation of hydrophobic residues to Cys on the proximal side of 2B4 reduced the extent and rate of P450-CO complex formation to virtually the same extent as a positively-charged proximal residue (R133) that was also mutated to cys and was previously reported to be the single largest contributor to P450-CPR interaction (Bridges et al., 1998).

To our knowledge, this is the first study that circumvents the limitations inherent in identifying residues at protein-protein interfaces exclusively by using mutagenesis and steady-state measurements by complementing those studies with stopped-flow and fluorescence spectroscopy. These results identify a novel role of hydrophobic residues V267 and L270 of CYP2B4 in CPR recognition and suggest that our approach will be informative for acquiring a detailed molecular understanding of protein-protein interactions.

Materials and Method

Chemicals. All chemicals used are of ACS grade, obtained from commercial vendors unless otherwise specified. Benzphetamine, NADPH, sodium dithionite and tert-butyl hydroperoxide were purchased from Sigma. Trifluoroacetic acid and fluorescein-5-maleimide were purchased from Pierce Chemicals. Dilauroylphosphatidylcholine (DLPC) was purchased from Doosan Serdary Research Laboratory (Toronto, Canada).

Carbon monoxide gas (purity >99.5%) was purchased from Cryogenic Gases (Detroit, MI).

Construction of CYP2B4 variants. Site-directed mutagenesis was performed using a QuikChange site-directed mutagenesis kit according to the manufacturer's protocol (Stratagene). The forward and reverse mutagenic primers for C79S, C79SC152S, and the other 7 variants are listed in Table 2.1. These other 7 variants used C79SC152S as a template plasmid with a single additional mutation: V267C, L270C, L420C, R133C, Y484C, H226C or E60C. Each site-specific mutation was confirmed by DNA sequencing at the University of Michigan DNA Sequencing Core.

Overexpression and Purification of CYP2B4 WT and variants. CYP2B4, its variants and CPR were expressed and purified from Escherichia coli as described previously(Zhang et al., 2007). The concentrations of CYP2B4 and its variants were determined using an extinction coefficient of$\Delta\ \varepsilon_{450\text{-}490\ nm}$ of 91 mM cm^{-1} as described by Omura and Sato (Omura and Sato, 1964). The concentration of CPR was determined using an extinction coefficient of 21 mM cm^{-1} at 456 nm for the oxidized enzyme (Vermilion and Coon, 1978).

Labeling of CYP2B4 variants with FM. FM was dissolved in 5% DMF and prepared as a 10 mM stock in 0.1M potassium phosphate buffer, pH 7.1. To determine the optimal concentration for labeling, aliquots of the FM stock solution were added to solutions of CYP2B4 (0.83 μM) in opaque Eppendorf tubes (to protect from light) such that the final concentration of FM was 50-, 100-, 200-, 500- and 1000-fold larger than the

Primer Name	Sequence (5' → 3')
C79S Forward	CCGTGGTCGTGCTGTCTGGGACGG
C79S Reverse	CCGTCCCAGACAGCACGACCACGG
C152S Forward	GAGGAGGCCCGGTCTCTGGTGGAGG
C152S Reverse	CCTCCACCAGAGACCGGGCCTCCTC
E60C Forward	TCCTTCCTGCGGCTCCGATGTAAATACGGGGACGTGTTC
E60C Reverse	GAACACGTCCCCGTATTTACATCGGAGCCGCAGGAAGGA
H226C Forward	CCCGGGCTTCCTAAAGTGCTTTCCTGGCACGCAC
H226C Reverse	GTGCGTGCCAGGAAAGCACTTTAGGAAGCCCGGG
Y484C Forward	CGTGCCCCCGAGCTGCCAGATCCGCTTC
Y484C Reverse	GAAGCGGATCTGGCAGCTCGGGGGCACG
V267C Forward	CTAGGGATTTCATCGACTGCTACCTGCTCCGCATGG
V267C Reverse	CCATGCGGAGCAGGTAGCAGTCGATGAAATCCCTAG
R133C Forward	CGGAGATTCTCCCTGGCCACCATGTGCGACTTCGGCATGGGGAAGCGGAGC
R133C Reverse	GCTCCGCTTCCCCATGCCGAAGTCGCACATGGTGGCCAGGGAGAATCTCCG
L270C Forward	AGGGATTTCATCGACGTCTACCTGTGCCGCATGGAAAAAGACAAGTCCGA
L270C Reverse	TCGGACTTGTCTTTTTCCATGCGGCACAGGTAGACGTCGATGAAATCCCT
L420C Forward	GCCACTTTCTAGATGCCAACGGGGCATGCAAGAGGAATGAAGGCTTTATGCCCTT
L420C Reverse	AAGGGCATAAAGCCTTCATTCCTCTTGCATGCCCCGTTGGCATCTAGAAAGTGGC

Table 2.1. List of primers used for site-directed mutagenesis.

concentration of CYP2B4, and the total volume was 400 µL. The protein samples were either allowed to sit at 4 ^{o}C overnight or for 2 h at room temperature. Any precipitated FM was then removed by centrifuging at 13.2k rpm for 5 min and the molecular masses of the labeled and unlabeled samples were then analyzed using an LCQ ion trap mass spectrometer (ThermoFinnigan, Inc.). Once the optimal concentrations of FM required for labeling each variant were identified, the above steps were repeated on larger samples and the proteins were subsequently dialyzed extensively to remove any free FM from solution. The FM-labeled proteins were dialyzed for 4-5 hr at a time for a number of times and after each dialysis, the fluorescence emission of the dialysis solution was measured to determine the presence of unreacted FM. The dialysis was considered complete when FM could no longer be detected in the dialysis solution.

ESI-LC-MS Characterization of the FM Labeled CYP2B4 variants. The CYP2B4 samples (50 µL) were injected onto an Agilent Zorbax 300SB-C3 column (3.0 X 150 mm; Agilent, Santa Clara, CA). ESI-LC-MS was carried out using a ThermoFinnigan LCQ ion trap mass spectrometer interfaced with a Hewlett Packard 1100 series HPLC system (Hewlett Packard, Palo Alto, CA). The sheath gas was set at 90 (arbitrary units) and the auxiliary gas was set at 30 (arbitrary units). The spray voltage was 3.5 kV and the capillary temperature was 200 ^{o}C. The flow rate was 0.2 ml/min and the initial conditions were 70% 0.1% TFA (v/v) in water (solvent A) and 30% of 0.1% TFA (v/v) in acetonitrile (solvent B). The percentage of B was maintained at 30% for 5 min followed by a linear gradient to 90% B from 5 min to 35 min and maintained at 90% B for another 10 min. The gradient was then lowered from 90% to 30% B in 5 min and

held for 15 min to equilibrate the column.

Characterization of CYP2B4FM Variants. The K_d reported for the CPR-P450 complex is in the range from 0.02 – 0.1 µM (Miwa et al., 1979; French et al., 1980; Davydov, 1996; Bridges et al., 1998). Thus, to ensure that under our experimental conditions >95% of the CYP2B4FM variants were complexed with CPR, final concentrations of 3 µM CPR, 0.1 µM CYP2B4FM and 0.1 mg/ml DLPC were first reconstituted overnight at 4 ^{o}C and then diluted to a final volume of 600 µL in 50 mM potassium phosphate, pH 7.4. Fluorescence measurements of the CYP2B4FM variants were performed on a Shimadzu RF – 5301PC spectrofluorophotometer (Columbia, MD) using 10 nm excitation and 10 nm emission bandwidth slits. The excitation wavelength was set at 490 nm and the emission spectrum was obtained by scanning from 495 nm to 600 nm. The emission intensity of the blank (in the absence of CPR) was subtracted from the intensity in the presence of 3 µM CPR and that difference was divided by the fluorescence intensity in the absence of CPR to give a percent intensity enhancement for each CYP2B4FM – CPR variant complex. The percent fluorescence enhancement of each CYP2B4FM – CPR variant complex was then normalized to the percentage fluorescence enhancement recorded for CYP2B4FM (L420C) to give a relative measure of the fluorescence change as result of reconstituting with CPR.

Determination of the Apparent K_d Values of the CYP2B4FM Variants for CPR. The apparent dissociation constants of the CYP2B4FM variants for CPR were determined by measuring the difference in fluorescence intensity of the CYP2B4FM

variants in the presence and absence of varying concentrations of CPR. These data were normalized to the fluorescence intensity obtained from the concentration of CPR that yielded a plateau in fluorescence enhancement. The fluorescence of the 0.05 µM CYP2B4FM variants was individually recorded in the presence of 0.1 mg/ml DLPC and 50 mM potassium phosphate, pH 7.4, at 22 ^{o}C to obtain initial intensity (I_i) at the emission maximum. Increasing concentrations of CPR were reconstituted overnight at 4 ^{o}C in the presence of 0.05 µM of the CYP2B4FM variant and 0.1 mg/ml DLPC. These samples were diluted in 50 mM potassium phosphate, pH 7.4, to a final volume of 600 µL and the emission of the mixture was recorded to obtain (I). The fluorescence intensity obtained from the concentration of CPR that produced the highest fluorescence intensity was recorded to obtain the maximum intensity (I_{max}).

Assuming the formation of a 1:1 complex, the equilibrium dissociation between CYP2B4FM and CPR can be described by the equation:

CYP2B4FM–CPR complex ↔ CYP2B4FM + CPR

The equilibrium dissociation constant, or K_d is given by the equation:

$$K_d = \frac{[CYP2B4FM][CPR]}{[CYP2B4FM - CPR]} \qquad \text{Eq.1}$$

where [CYP2B4FM] and [CPR] are the free concentrations of CYP2B4FM and CPR, respectively. This can be rewritten as:

$$\frac{[CYP2B4FM - CPR]}{[CYP2B4FM]} = \frac{[CPR]}{K_d + [CPR]} = F \qquad \text{Eq. 2}$$

where F is obtained from the equation:

$$F = \frac{I - I_i}{I_{max} - I_i} \qquad \text{Eq. 3}$$ Eq. 3

K_d can be obtained by plotting F vs [CPR] and fitting the data to a non-linear regression using GraphPad Prism 5.0 from GraphPad software.

Determination of the Apparent K_M and k_{cat} Values for CYP2B4 WT and Variants for CPR Using the N-demethylation of Benzphetamine in the Absence of FM. The K_M and k_{cat} values for CYP2B4 WT and its variants for CPR were determined at 30 ^oC by measuring the rate of formaldehyde formation from the N-demethylation of benzphetamine at a constant P450 concentration with increasing concentrations of CPR. CYP2B4 WT and its variants (0.2 µM) were reconstituted in triplicate with varying concentrations of CPR (0.1, 0.2, 0.3, 0.4, 0.5, 0.6, 1.0 and 1.2 µM) and 0.1 mg/ml DLPC on ice for 1 h. The reconstituted mixtures were then added to 50 mM potassium phosphate buffer, pH 7.4, and 1 mM benzphetamine. After the samples were equilibrated at 30 ^oC for 15 min, the reactions were initiated by adding 7.5 µL of 20 mM NADPH for a final reaction volume of 500 µL. The reactions were allowed to proceed for 5 min at 30 ^oC before they were quenched by the addition of 25 µL of 50% TFA. The protein was precipitated by centrifugation at 13.2k rpm for 5 min and a 500 µL aliquot of the supernatant was assayed for formaldehyde using the Nash reaction (Nash, 1953). The kinetic parameters were determined by fitting the data to the Michaelis-Menten equation using GraphPad Prism 5.0 from GraphPad software (La Jolla, CA).

Characterization of the tert-Butyl Hydroperoxide-supported Metabolism of Benzphetamine by CYP2B4 WT and its Variants in the Absence of FM. To determine the rates for the tert-butyl hydroperoxide–supported metabolism of benzphetamine, final concentrations of 0.25 μM CYP2B4 WT and its variants were each incubated with 0.1 mg/ml DLPC, 50 mM potassium phosphate buffer, pH 7.4, and 1 mM benzphetamine at 30 ^{o}C for 15 min. tert-butyl hydroperoxide (52.5 μL of 1 M) was added to give a final volume of 500 μL and the reactions were allowed to proceed for 5 min, after which, they were terminated by the addition of 25 μL of 50% TFA. The samples were centrifuged at 13.2k rpm for 5 min and 500 μL aliquots of the supernatants were assayed for formaldehyde using the Nash reaction (Nash, 1953).

Determination of the Rate of Electron Transfer from CPR to CYP2B4 WT and its Variants in the Absence of FM. In order to investigate the effects of the mutations on the interactions between the CYP2B4 variants and CPR, the rates of the first electron transfer from CPR to the CYP2B4 WT and its variants were measured. The rates of reduction were determined using a stopped-flow spectrophotometer (Hi-Tech SF61DX2, TgK Scientific, Bradford-on-Avon, UK) to monitor the increase in the absorbance at 450 nm as a result of the formation of the ferrous CYP2B4-CO adduct following reduction of ferric CYP2B4 by CPR at 30 ^{o}C. One syringe contained CYP2B4 WT or a variant (3 μM), CPR (3 μM) and DLPC (0.15 mg/ml) that had been reconstituted on ice for 1 hr before being diluted in 0.1 M potassium phosphate buffer, pH 7.4, to a final volume of 1.5 mL. To determine the effect of saturating concentrations of CPR on the rate and extent of first electron transfer to the WT, the (L270C), or the

(V267C) variant, the reduction experiments were performed using 1.5 µM P450, and 1.5 or 4.5 µM CPR in the presence of 1 mM BNZ. This mixture was then rapidly mixed with an equal volume of 0.1 M potassium phosphate buffer, pH 7.4, and 0.1 mM NADPH from another syringe. Both solutions had been saturated with CO by passing a gentle stream of CO gas over the sample solutions for 5 minutes. The increase in absorbance at 450 nm was monitored over time for 100 sec. The data were then analyzed to determine the apparent rate constants and amplitudes for the rates of electron transfer from CPR to CYP2B4 WT and its variants by fitting the absorbance changes at 450 nm to a three-exponential equation using the KinetAsyst software (Bradford-on-Avon, UK).

Results

Rationale for the Selection of Solvent Exposed Residues for FM Labeling. CYP2B4 is the paradigmatic mammalian P450. It can be expressed and purified in relatively large quantities (Bridges et al., 1998) and has been studied extensively from a structure-function point of view (Coon et al., 1973). Furthermore, a crystal structure is readily available from the Brookhaven National Laboratory Protein Data Bank site (PDB ID 1suo) (Scott et al., 2004) which, along with the work of Bridges et al. (Bridges et al., 1998), guided the selection of solvent exposed residues for mutagenesis.

CYP2B4 WT possesses four Cys residues, two of which (C79 and C152) are solvent exposed. When the WT enzyme was incubated with FM and analyzed using ESI-LC/MS, an increase in molecular mass corresponding to adduct formation by reaction with two FM molecules was observed. Since C152, but not C79, was in a position of interest for our current study, C79 was mutated to a Ser in order to block maleimide

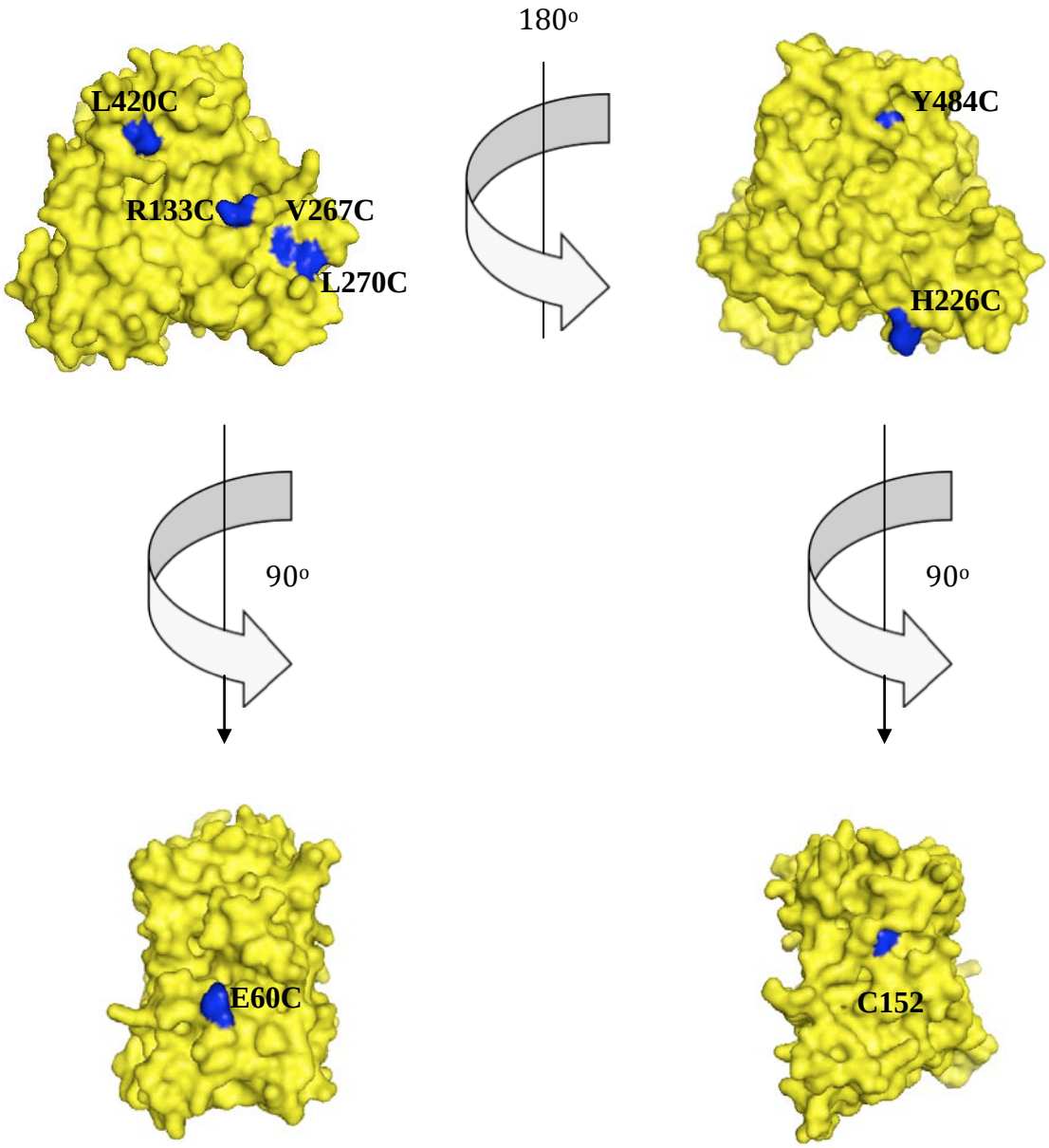

Figure 2.1. Selection of solvent-exposed residues for FM labeling. van der Waals surface representations of CYP2B4 (PDB 1SUO) in the upper left and right corners display the proximal and distal regions of CYP2B4 respectively. The lower left and right structures represent regions perpendicular to the axis of the heme-thiolate ligation. The residues that were selected for cysteine mutagenesis and subsequent FM labeling are shown in blue, while the rest of the structure is shown in maize. Since WT CYP2B4 possesses two surface-exposed cysteines (C79 and C152) almost all of our studies required generating a C79S/C152S template to which cysteine residues were introduced at the sites of interest. However, residue C152 (lower right) was already in a position of interest and studying this site simply required replacing C79 with serine.

labeling, thus leaving C152 available for investigation (Figure 2.1). The additional residues that were selected for FM labeling following cys mutagenesis were E60, H226, Y484, V267, R133, L270 and L420 (Figure 2.1). A double cysteine to serine variant (C79S/C152S) was generated to serve as a starting point for studying the effects of mutation of residues E60, H226, Y484, V267, R133, L270 and L420 to Cys. For simplicity, a specific CYP2B4 such as C79S/C152S/E60C is denoted as CYP2B4 (E60C), while the single C79S mutation is simply denoted as CYP2B4 C79S. All variants containing the FM abbreviation (e.g., (V267C)FM) are P450s that have been chemically labeled by fluorescein-5-maleimide.

In order to determine which hydrophobic residues would be selected for site-directed mutagenesis studies on the proximal region of CYP2B4, we performed an APBS surface electrostatic plot of the crystal structure of CYP2B4 (PDB code 1SUO). This analysis revealed that the solvent-exposed proximal region is composed of a variety of charged and neutral residues (Figure 2.2). Specifically, the center of the proximal region is mostly composed of hydrophobic residues that are surrounded by a series of Arg and Lys. Most notably, we observed a relatively large and concentrated patch of hydrophobic residues near R126, R133 and K274. The hydrophobic patch consists of the following residues: A123, F127, F135, G136, M137, P258, P261, F264, V267, L270 and F283. Of these residues, L270 and V267 are not within van der Waals contact with other amino acids and their roles in CPR binding have yet to be characterized. Therefore, the absence of significant intermolecular interactions between V267 and L270 and their surrounding residues made them good candidates for mutagenesis.

The role of the basic proximal residue R133 in mediating protein-protein

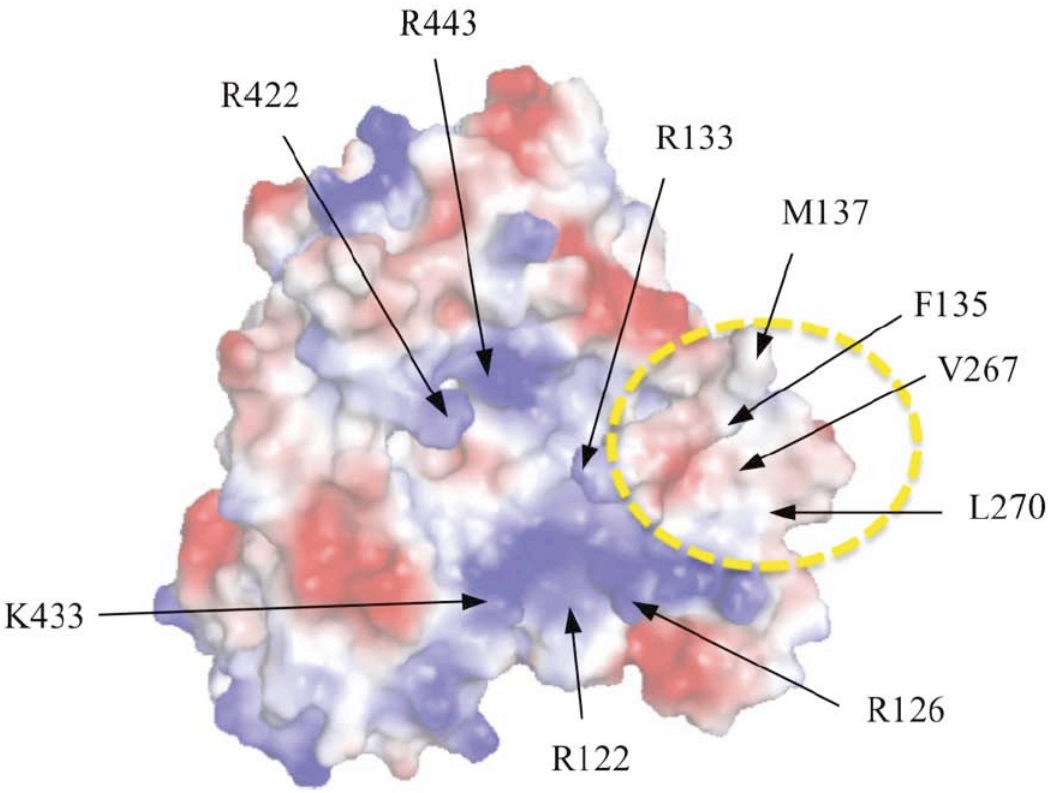

Figure 2.2. Surface electrostatic plot of the proximal region of CYP2B4. Electrostatic surface of CYP2B4 as determined by APBS which shows the central basic residues (R122, R126, R133, R422, K433 and R443) proposed to be involved in CPR binding and a hydrophobic patch that includes V267 and L270 indicated by the dashed yellow circle. Red represents acidic residues while blue represents basic residues on the surface of CYP2B4.

interaction (Bridges et al., 1998). Their study showed that mutating this residue to Ala had the largest impact on increasing the apparent K_d for the CYP2B4-CPR complex. Thus, R133 was also chosen for mutation to Cys due to its previously demonstrated role in complex formation. Furthermore, two more residues, H226 and Y484 were chosen for Cys mutagenesis to investigate the possibility that the distal side of CYP2B4 might serve as a docking site for CPR (Lehnerer et al., 2000).

Generation of CYP2B4 Variants. The site-directed mutations were produced as described in Experimental Procedures. As evidenced by the reduced CO difference spectrum, all of the mutants absorbed predominantly at 450 nm with minimal absorption at 420 nm (~10%). Chemical labeling of the C79S and triple mutants by FM followed by ESI-LC/MS analysis showed that the MW of the variants increased by a mass which corresponded to the adduction with a single FM label and thus suggested they both had a single solvent exposed cysteine. The WT incorporated 2 FM labels while the C79SC152S variant was completely resistant to labeling.

Labeling of the CYP2B4 Mutants with FM. In order to study directly the binding interface of the CYP2B4-CPR complex, we chose FM because it combines an environmentally sensitive fluorescent moiety (fluorescein) (Drees et al., 1996) with the labeling specificity of the maleimide group (Hermanson, 1996). Monitoring the degree of labeling using ESI-LC/MS allowed us to optimize our reaction conditions. Typically, this involved incubating CYP2B4 variants (0.83 μM) each with 41.5, 83, 166, 415, and 830 μM FM overnight at 4 ^{o}C, as described in Experimental Procedures. Each CYP2B4-FM

was dialyzed against 0.1 M potassium phosphate buffer, pH 7.4, until all free flourescein was removed from solution. The crystal structure of CYP2B4 in the closed conformation shows that there are two native solvent-exposed cysteine residues (C79 and C152), and incubation of the WT with FM confirms this observation by incorporating two FM labels. As expected, when C79S and the triple mutants were incubated separately with FM they each reacted with the FM to give a single adduct to the protein, as measured by the increase in mass, while C79SC152S showed no increase in mass This is evidenced by the presence of a peak that corresponds to the mass of a singly labeled CYP2B4-FM variant (± 50 Da) and the absence of a peak that corresponds to an unlabeled CYP2B4 variant (data not shown). The lowest concentration of FM that produced the highest degree of labeling in the given amount of time was chosen for large scale labeling.

Fluorescence Characterization of the CYP2B4FM variants with CPR. In an attempt to study the protein-protein interactions at the binding interface of the CYP2B4-CPR complex, FM, a fluorescent probe that has previously been shown to be sensitive to changes in its local environment was attached to solvent exposed Cys residues on the surface of CYP2B4. When reconstituted with DLPC and CPR, we observed changes in the fluorescence emission intensity of the CYP2B4FM variants, which were dependent on the position of the label. For example, the variants of CYP2B4 labeled on the (L420C), (L270C), (V267C) and (R133C) showed the largest increases in fluorescence intensity in the presence of CPR (Figure 2.3). In contrast, the variants of CYP2B4 labeled on the distal side, (H226C) and (Y484C), showed virtually no fluorescence enhancement, while CYP2B4 (E60C) and C79S showed changes that were intermediate between those

observed for the proximal and distal variants. To test whether the CYP2B4-FM fluorescence enhancement is the result of specific binding of CPR to CYP2B4 and not due to random protein-protein interactions, we tested whether bovine serum albumin (BSA) could, under the same conditions, reproduce the results observed with CPR. The addition of up to a fifty-fold excess of BSA only enhanced the fluorescence emission by 5%, thus demonstrating that the results observed in Figure 2.3 are specific to the interactions of CPR with CYP2B4FM to form a complex (data not shown). To further investigate the specificity of these results, we performed titration studies with CPR to see if the increase in the fluorescence enhancement with increasing CPR would allow us to determine dissociation constants for the complex.

Determination of the K_d Value for the CPR-CYP2B4-FM Complex using Fluorescence Titration. Previous studies have shown that fluorescent compounds can be used as probes to understand the quantitative basis for protein-protein interactions(Davydov, 1996). Since (L420C), (L270C), (V267C) and (R133C) variants of CYP2B4FM showed the largest enhancements in fluorescence emission, they were used to determine the dissociation constants for the complex. The results are presented in Figure 2.4 and Table 2.2. (R133C)FM, (L270C)FM and (V267C)FM showed 3.8-, 5.2- and 5.6-fold increases respectively in their apparent K_d values for CPR compared to (L420C)FM indicating weaker binding of CPR to these variants. The results obtained with (R133C)FM in this assay parallel those for the Ala mutagenesis study reported earlier (Bridges et al., 1998). That is, R133 appears to be an important residue mediating CPR binding. Thus, this residue serves as an excellent positive control for our approach,

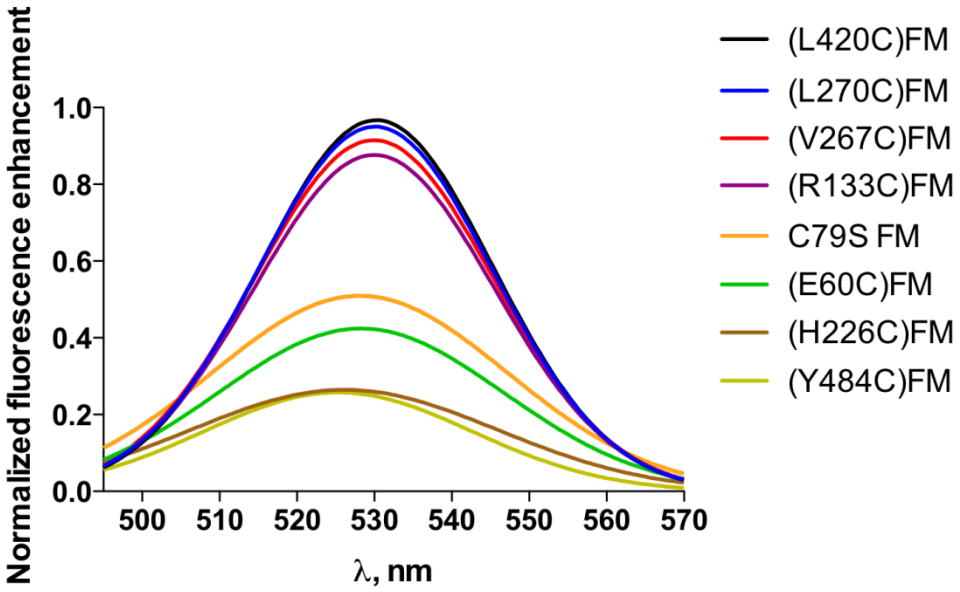

Figure 2.3. Fluorescence emission spectra for all the FM-labeled CYP2B4 variants (0.05 μM) in the presence of 3 μM CPR, 0.1 mg/ml DLPC at 23°C, pH 7.4. When reconstituted with excess CPR, the proximal variants (R133C, V267C, L270C and L420C) showed the greatest increases in fluorescence enhancement, the distal variants (H226C and Y484C) showed the lowest enhancement, while the variants on regions perpendicular to the heme-thiolate ligand (E60C and C79S) exhibited enhancements that were intermediate between the proximal and distal variants.

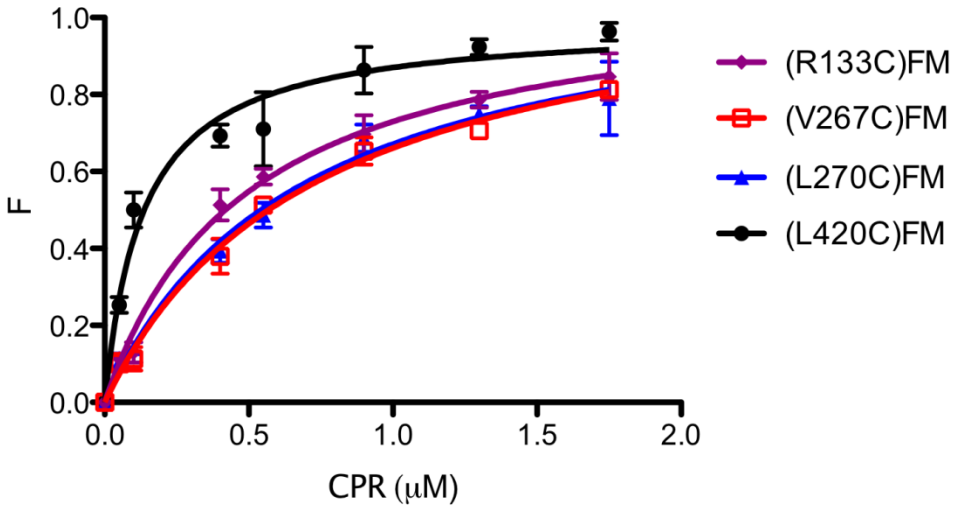

Figure 2.4. Plot of F vs. [CPR] for the CYP2B4-FM proximal variants used to determine the K_d values for CPR. Measurements were carried out in 0.1M potassium phosphate buffer, pH 7.4, with 0.1 mg/ml DLPC at 23 ^{o}C as described under "Materials and Methods". Error bars are the standard deviations for three measurements performed in duplicate.

CYP2B4-FM variant	K_d
(R133C)FM	0.49±0.05
(V267C)FM	0.73±0.07
(L270C)FM	0.68±0.09
(L420C)FM	0.13±0.02

Table 2.2. K_d values for the interactions between the CYP2B4-FM variants on the proximal side of the protein and CPR by fluorescence titration. The fluorescence emission of the 0.05 μM CYP2B4FM proximal variants were recorded in the presence of 0.1 mg/ml DLPC and 50 mM potassium phosphate, pH 7.4, at 22 ^{o} C. The CYP2B4FM samples were then reconstituted with increasing concentrations of CPR. The resulting titration curves were fit to the Michaelis-Menten equation from which K_d values were determined.

and the titration data suggests that L270 and V267 may also be implicated in the interaction of CPR with CYP2B4. If, like R133, L270 and V267 constitute part of the binding interface, we hypothesize that the K_M values of these variants for CPR should also be higher than those for all other variants and WT.

Determination of the K_M and k_{cat} Values for the Interactions of CYP2B4 WT and its Variants with CPR in the Absence of FM. Complex formation between CPR and a CYP is an essential step in the transfer of electrons to the heme that is required for substrate oxidation. It has been proposed that the rate of substrate oxidation is directly proportional to the concentration of the CPR-CYP2B4 complex(Miwa et al., 1979; Bridges et al., 1998). Thus, by measuring the rate of benzphetamine oxidation in the presence of a fixed concentration of CYP2B4 and increasing concentrations of CPR, K_M and k_{cat} values can be determined. By comparing these values with the K_d values that were determined by fluorescence spectroscopy, we can investigate the effect of the mutations on CPR affinity in the absence of FM. The mutation of a residue involved in redox partner recognition should disrupt complex formation and increase the concentration of uncomplexed CYP2B4 which is not able to oxidize substrate. As shown in Figure 2.5 and Table 2.3, the rate of benzphetamine oxidation as a function of varying CPR concentrations follows a rectangular hyperbolic relationship, which can be fit to the Michaelis-Menten equation.

It is apparent that the majority of the mutations did not significantly affect K_M or k_{cat}. Most notable, however were the significant increases in the K_M values observed for CYP2B4 (R133C), (L270C) and (V267C), as well as a decrease in the k_{cat} value for

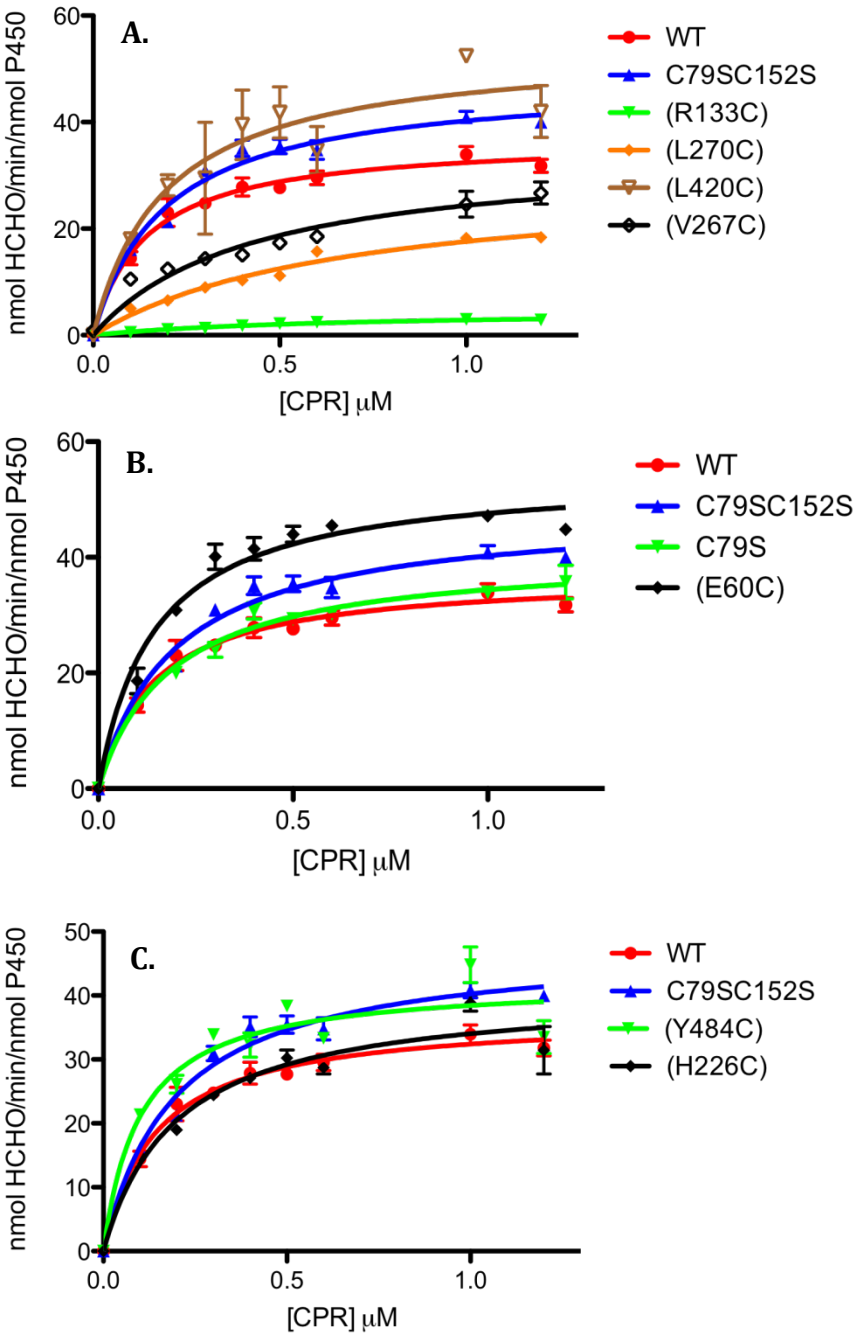

Figure 2.5: Determination of the apparent K_M and k_{cat} values of the CYP2B4 (A) proximal, (B) side and (C) distal variants. The N-demethylation of benzphetamine to produce formaldehyde (HCHO) was measured at a constant concentration of CYP2B4 (0.2 μM) with increasing concentrations of CPR as described under "Materials and Methods". Error bars are the standard deviations from three measurements performed at least in triplicate.

2B4	K_M (μM)	k_{cat} (min^{-1})
WT	0.14±0.022	37±1.5
C79SC152S	0.19±0.023	48±1.7
(E60C)	0.14±0.019	54±1.9
C79S	0.18±0.025	41±1.6
(H226C)	0.20±0.036	41±2.3
(Y484C)	0.10±0.024	42±2.1
(R133C)	0.65±0.11	4.7±0.40
(V267C)	0.43±0.10	34±3.1
(L270C)	0.69±0.12	30±2.5
(L420C)	0.19±0.064	54±5.2

Table 2.3. K_M and k_{cat} values determined for CYP2B4 WT and its variants for CPR. As described under "Materials and Methods", the kinetic parameters were determined by measuring the rate of formaldehyde formation as a result of CYP2B4-mediated N-demethylation of benzphetamine under fixed concentrations of CYP2B4 and excess benzphetamine with increasing concentrations of CPR. The original data are in Figure 2.5.

(R133C). As expected, the K_d values reported in Table 2.2 agree with the increases in the K_M values and this agreement suggests that hydrophobic residues V267 and L270, in addition to charged residues, may also mediate CPR-CYP2B4 interactions. Since the results obtained from this assay rely on substrate metabolism, it might also be argued that a decrease in benzphetamine oxidation may be attributed to an alteration in the P450 active site instead of decreases in the concentrations of the CPR-CYP2B4 variant complex. Such alterations can be assessed by determining the rates for tert-butyl hydroperoxide-supported metabolism of benzphetamine by the CYP2B4 WT enzyme and its variants.

Characterization of the tert-Butyl Hydroperoxide-Supported Metabolism of Benzphetamine by the CYP2B4 WT Enzyme and its Variants in the Absence of FM. In order to determine whether the increase in K_M is due to disruption of the interaction of CYP2B4 with CPR, or another step in the catalytic cycle, the benzphetamine demethylation activity supported by tBHP was characterized and compared to that supported by CPR. As shown in Figure 2.5 and Table 2.3, CYP2B4 (R133C), (L270C) and (V267C) all exhibited increases in the K_M values when titrated with CPR. However, when the reaction was performed in the presence of tBHP, none of the variants displayed any significant changes in benzphetamine activity (Figure 2.6). Since hydroperoxides and other artificial oxygen donors are able to support the catalytic turnover of P450s in the absence of redox partners such as CPR, the decrease in the CPR-supported activity suggests that the increase in K_M occurs as a result of mutations impairing the binding of the CYP2B4 (R133C), (L270C) and (V267C) variants with CPR or electron transfer

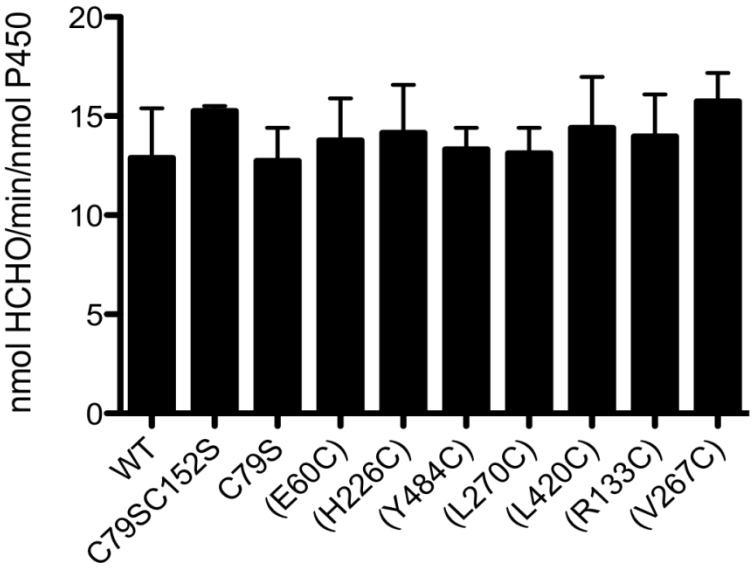

Figure 2.6: Comparison of the tBHP-supported metabolism of benzphetamine by CYP2B4 WT and variants. CYP2B4 WT and its variants were incubated with DLPC, potassium phosphate buffer, pH 7.4, and excess benzphetamine as described under "Experimental Procedures". The reactions were initiated by the addition of tBHP to a final concentration of 0.1M and the rate of formaldehyde formation was assessed spectrometrically after reaction with Nash reagent. The data are an average of two experiments done in duplicate with the error bars representing the standard error of the mean.

pathways. To distinguish between the two we measured the rate and extent of the reduction of the CYP2B4 variants by CPR using stopped-flow spectrophotometry.

Determination of the Rates of Electron Transfer from CPR to CYP2B4 WT and its Variants in the Absence of FM. To test our hypothesis that residues L270 and V267, like R133, are involved in binding to CPR, we measured the rate and extent of reduction of ferric CYP2B4 WT and its variants by CPR under pre-steady state conditions. Using stopped-flow spectrophotometry, we mixed preformed CYP2B4 WT or variant – CPR complexes with NADPH in the presence of CO and monitored the increase in absorbance at 450 nm with time. The production of the reduced-CO complex of P450 absorbing at 450 nm is the result of a series of steps. First NADPH must reduce CPR, which then delivers an electron to P450. This electron reduces the ferric heme to its ferrous state that can bind CO and the ferrous-CO complex absorbs at 450 nm. The binding of CO is very rapid compared to the reduction reaction and has no effect on the rate observed. When the CPR-P450 complex is not pre-formed by lengthy reconstitution, the association reaction and the subsequent reduction of P450 by CPR are very slow(Backes and Eyer, 1989). For this reason, the rate of first electron transfer from CPR to P450 is typically measured by mixing a preformed P450-CPR complex with NADPH. Since formation of the P450-CO complex depends on the amount of ferrous heme, which in turn depends on the concentration of the CPR-P450 complex, the total amplitude of the fast and slow phases is a reflection of the affinity of P450 for CPR. By determining the concentration of the P450-CO complex from the total amplitude of the fast and slow phases and examining the rate constants for those phases we can distinguish the effects of our mutations on

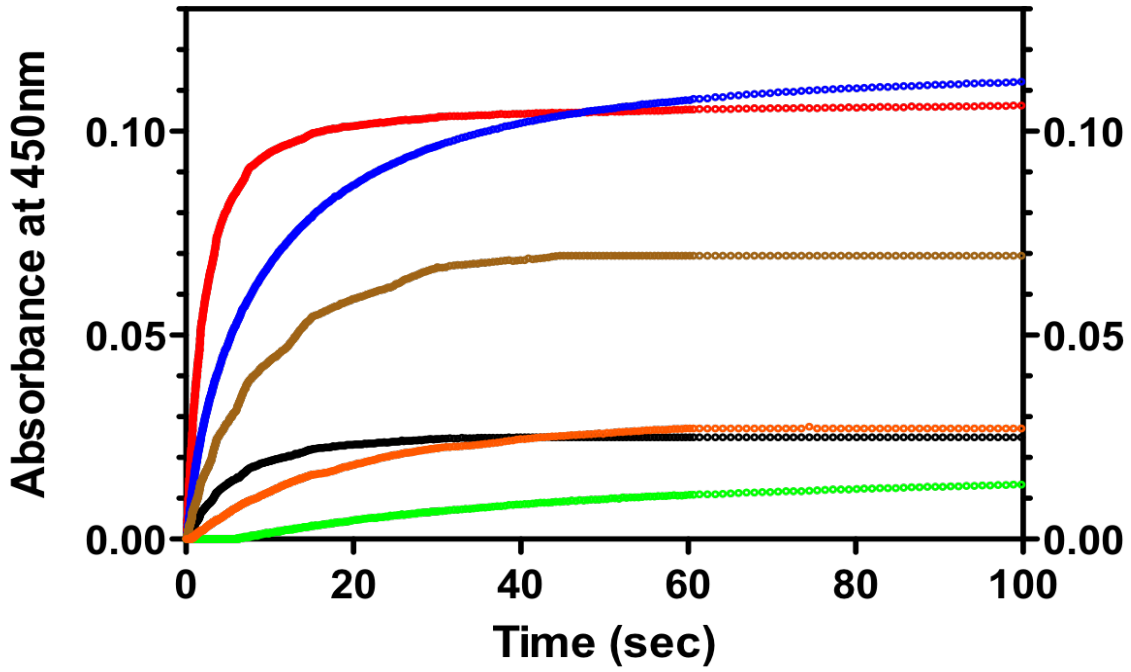

Figure 2.7. Kinetics for the reduction of the CYP2B4 proximal variants by CPR in the presence of NADPH. CYP2B4, CPR and DLPC were reconstituted for 1 hr on ice and mixed with NADPH in a stopped-flow apparatus. After mixing, the final concentrations of CYP2B4 and CPR were 1.5 μM and the NADPH concentration was 50 μM. Experiments were conducted as described under "Materials and Methods" with the solutions in both syringes saturated with CO. For convenience, all of the absorbance data are offset to the same baseline. The traces for CYP2B4 WT and variants are represented by the following colors: Red, WT; Blue, C79SC152S; Brown, (L420C); Orange, (L270C); Black, (V267C); Green, (R133C).

2B4	Kinetic parameters				
	A_T	A_1%	$k_{1,S}^{-1}$	A_2%	$k_{2,S}^{-1}$
WT	0.110	62	0.70	39	0.16
C79SC152S	0.110	28	0.51	72	0.067
(E60C)	0.120	28	0.678	72	0.077
C79S	0.079	18	0.205	82	0.052
(H226C)	0.061	33	0.15	67	0.043
(Y484C)	0.079	21	0.212	79	0.049
(R133C)	0.021	85	0.019	15	0.0031
(V267C)	0.027	64	0.057	36	0.0138
(L270C)	0.029	10	0.032	90	0.0110
(L420C)	0.070	39	0.360	61	0.0035

Table 2.4. Rate constants and amplitudes observed for the reduction of CYP2B4 and its variants by CPR at 23°C. The kinetic parameters were determined from the data in Figure 2.7 as described in "Materials and Methods". The apparent rate constants for the two kinetic phases are k_1 and k_2, respectively, and the relative amplitudes for each phase are expressed as A_1% and A_2% . The total absolute amplitude for the overall reduction is A_T.

protein-protein interactions from studies on P450 reduction. Figure 2.7 shows the increase for the proximal variants, C79SC152S and WT. As expected the reduction rates of all variants and WT exhibited biphasic kinetics. The rate constants of the fast and slow phases for the reduction of CYP2B4 WT in the absence of benzphetamine are 0.70 and 0.16 s^{-1}, respectively, and the fraction of the amplitude in the fast phase is 62%. The final concentration of the CYP2B4WT-CO complex was determined from the total amplitude of the fast and slow phases and the extinction coefficient of CYP2B4. For the WT this was 1.22 μM (81% of the theoretical concentration). Variants C79SC152S, C79S, (E60C) and (Y484C) were all reduced to similar levels and at similar rates as the WT, while (H226C) and (L420C) displayed slightly smaller total amplitudes (by 44% and 36% respectively) and rates compared to WT. As reflected in the total concentration of the reduced CYP2B4-CO complex, variants (V267C), (L270C) and (R133C) had the most significant effect on CPR binding. These variants reduced the total amount of reduced CYP2B4-CO complex by an average of 77% and their kinetic constants for the fast phase of reduction were similarly affected.

In order to more clearly distinguish the effect of the mutations on the altered affinity of the 2B4-CPR complex and the efficiency of electron transfer through the complex at subsaturating and saturating CPR concentrations we repeated the experiment shown in Figure 2.7 and with higher concentrations of CPR and observed no significant increase in the rate of reduction (data not shown). However, the faster phase of reduction for (V267C) and (L270C) is extremely slow and interpreting changes in the fast phase of electron transfer in the presence of 3-fold CPR were somewhat problematic. Therefore, we decided to look at the rate of electron transfer in the presence of benzphetamine since

it is well established that benzphetamine increases the rate of the fast phase of electron transfer from CPR to 2B4 by at least 10-fold and thus would be expected to enhance the accuracy of our rate measurements. We also used half the amount of P450 that we used in the stopped-flow experiments reported previously in this chapter (1.5 μM) to avoid issues of protein aggregation at saturating CPR. The results clearly show that the rate of the fast phase for electron transfer does not increase significantly at saturating CPR concentrations (Figure 2.8, Table 2.5). It is, however, interesting to note the increase in the total amplitude of the reduced (L270C) and (V267C) variants at saturating CPR. This supports our hypothesis that the total amplitude is an indicator of 2B4-CPR affinity since adding more CPR should shift the binding equilibrium in the direction of complex formation and enhance the extent of P450 reduction. Therefore, these data clearly demonstrate that residues V267 and L270 in CYP2B4 are involved in binding CPR.

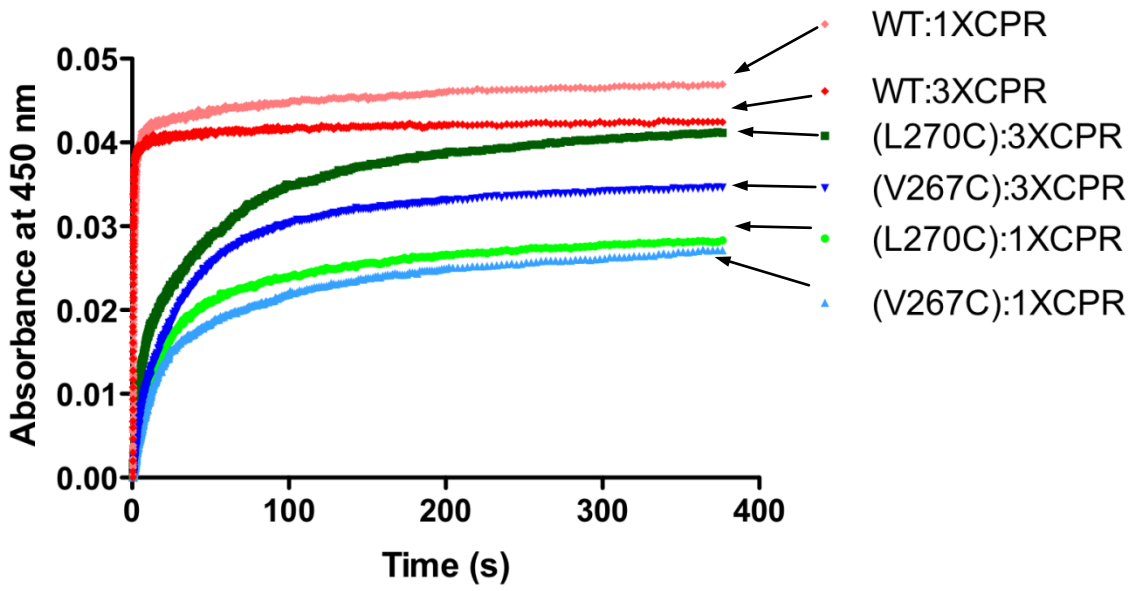

Figure 2.8. Kinetics for the reduction of the CYP2B4 V267C and L270C proximal variants in the presence of saturating and subsaturating amounts of CPR and in the presence of NADPH and BNZ. CYP2B4, CPR and DLPC were reconstituted for 1 hr on ice and mixed with NADPH in a stopped-flow apparatus. After mixing, the final concentration of CYP2B4 was 0.75 μM, NADPH was 50 μM while BNZ was 1 mM. Experiments were conducted as described under "Materials and Methods" with a saturated solution of CO in both syringes. For convenience, all of the absorbance data are offset to the same baseline.

2B4	[CPR]:[2B4]	Kinetic parameters				
		A_T	A_1%	$k_{1,S}^{-1}$	A_2%	$k_{2,S}^{-1}$
WT	1	0.05	91	3.5	9	0.05
WT	3	0.06	97	5.3	3	0.15
(V267C)	1	0.021	81	0.033	19	0.010
(V267C)	3	0.032	84	0.04	16	0.012
(L270C)	1	0.028	64	0.075	36	0.01
(L270C)	3	0.041	64	0.061	36	0.012

Table 2.5. Rate constants and amplitudes observed for the reduction of CYP2B4 WT, (V267C) and (L270C) in the presence of BNZ with subsaturating and saturating concentrations of CPR at 23^{o}C. The kinetic parameters were determined from the data in Figure 2.8 as described in "Materials and Methods". The apparent rate constants for the two kinetic phases are k_1 and k_2, respectively, and the relative amplitudes for each phase are expressed as A_1% and A_2%. The total absolute amplitude for the overall reduction is A_T.

Discussion

The results presented here demonstrate that the likely site for the binding of CPR to CYP2B4 is on the proximal side of CYP2B4, and that mutation of residues L270 and V267 to Cys disrupts the CYP2B4-CPR interaction. To investigate the residues involved in binding, we mutated strategically selected residues on the surface of CYP2B4 to Cys for site-specific labeling with FM and observed that when these P450s were reconstituted with excess CPR and DLPC, the largest fluorescence enhancement was recorded for those variants with labels on their proximal side. With the goal of uncovering whether hydrophobic residues might also be involved in recognition and binding of CPR, we investigated whether the V267C and L270C mutations could result in weaker complex formation by determining the K_M values of the variants for CPR and monitoring the rate and extent of P450 reduction by CPR. We observed significantly larger K_M and diminished rates and extents of P450 reduction for the proximal variants (L270C), (V267C) and (R133C), and virtually no change for (L420C) compared to WT.

Bridges et al. (1998) have previously demonstrated that R133, when mutated to Ala, exhibited the single largest perturbation on the apparent K_d of CYP2B4 for CPR when compared to WT. Therefore, we used this residue as a positive control to evaluate the results obtained using our strategy. Experiments where the CYP2B4FM variants were incubated with CPR revealed that fluorescence enhancement occurs to some extent for each site of FM attachment with the highest extent of fluorescence enhancement occurring with variants (V267C), (L270C), (R133C), and (L420C). It is likely that interactions of the amino acid residues from CPR with the FM label on the P450 increases the quantum yield of the probe by restricting its conformational flexibility and

reducing the amount of energy dissipated as non-radiative decay. This would increase the emission intensity of the probe and explain the observed results. Another, although highly unlikely explanation for the increase in fluorescence emission, is that the binding of CPR to CYP2B4 induces a conformational change in the protein that results in the burial of the probe further into the core of CYP2B4. Thus, the changes observed could possibly be due to some type of allosteric effect rather than direct binding. Although P450s are known to undergo relatively large conformational changes in the presence of substrate (Scott et al., 2003; Scott et al., 2004; Zhang et al., 2009), conformational changes of the magnitude required to internalize FM in CYP2B4 have not been reported. Moreover, the possibility of multiple docking sites for CPR on CYP2B4 is not supported by the data obtained from this study. Instead, our findings support the hypothesis that only a single, proximally located site on CYP2B4 is involved in complex formation.

The spectral results shown in Figure 2.3 led us to investigate the quantitative basis for the CYP2B4-CPR interaction by titrating fixed concentrations of the CYP2B4-FM variants with increasing concentrations of CPR. By plotting the increase in fluorescence intensity as a function of increasing concentrations of CPR and fitting this to Eq. 2, we were able to determine the affinity of the various FM-modified proximal mutants for CPR. As shown in Figure 2.4 and Table 2.2, CYP2B4 (L420C)-FM had the lowest K_d while CYPs (V267C)-, (L270C)-, and (R133C)-FM all displayed similar lower affinities for CPR. Although the addition of two FM labels to the WT P450 prevented us from obtaining fluorescence titration data for an unmutagenized CYP2B4, the K_d obtained for CYP2B4 (L420C)-FM corresponds closely to previously reported K_d values for WT CYP2B4-CPR. Since this variant also exhibited similar K_M and k_{cat} values for CPR as the

WT protein, it not only serves as a reasonable reference for the WT but, also suggests that the FM-labeled L420C residue is close enough to the CPR docking site to exhibit changes in fluorescence enhancement in the presence of CPR but is not involved in mediating CPR binding.

To characterize the effect of mutating the selected residues to cysteines in the absence of the fluorescent probe, we opted to characterize the K_M and k_{cat} values of the mutants for CPR. This approach would not only provide information regarding the possible roles of V267 and L270 in CPR binding in the absence of FM but, would also reveal whether the lack of the fluorescence enhancement observed for the distal and side mutants was due to either a lack of interaction with the reversibly bound CPR or an obliteration of the interaction as a consequence of mutagenesis. Although we expected it was due to the former we needed a definitive way to investigate the latter possibility. By studying the rate of benzphetamine oxidation as a function of increasing concentrations of CPR, an apparent K_M can be determined to assess the affinity of the unmodified variants for CPR. Although this approach has been used in the past, the results obtained from steady-state kinetic analyses of P450 variants do not necessarily directly determine which residues mediate CPR-P450 interaction. For example, electron transfer from CPR to P450 is thought to be mediated by amino acid residues that facilitate electron tunneling through proteins (Gray and Winkler, 1996). The identity of these particular residues is currently unknown, but when mutated to non-functional ones, their effect on protein activity could be indistinguishable from that of residues involved in CPR-P450 interactions. This limitation highlights the need to employ a holistic approach that combines steady-state turnover kinetics with fluorescence and stopped-flow spectroscopy

to the study of residues involved in redox partner recognition and forms the basis on which the experiments presented in this study were conceived.

The hypothesis that residues L270 and V267, like R133, occupy the binding interface is supported by our K_M data and further strengthened by stopped-flow experiments. In the kinetic experiments for the determination of the K_M, all of the proximal mutants with the exception of (L420C) showed increases in K_M values that, based on our studies on the tBHP supported catalytic activity could not be attributed to an altered P450 active site. Furthermore, the possibility that no fluorescence enhancement was observed when the distal FM-labeled variants were incubated with CPR because of complete disruption of complex formation can be conclusively ruled out by the observation that all of the other variants exhibited K_M values that were virtually identical to WT.

Data from measurements of the rate and extent of P450 reduction by CPR argue in favor of the conclusion that the higher K_M and K_d values for (V267C), (L270C) and (R133C) for CPR are due to impaired protein-protein interactions. Disruption of CYP2B4-CPR binding as a result of proximal residue mutagenesis can be inferred from the total amplitude of the slow and fast phases and is critical to our understanding of the roles of L270 and V267 in complex formation. In theory, the binding of CO to ferrous heme should promote further CYP2B4-CPR complex formation by depleting the concentration of ferric heme and shifting the equilibrium between the ferric and ferrous forms in the direction of the ferrous state. However, experimentally, we, and others, find that the association of P450 with CPR is very slow when the complex between the two proteins is not pre-formed by extensive reconstitution (Backes and Eyer, 1989).

Therefore, in this study the concentration of the CYP2B4-CO complex is limited by the concentration of the CYP2B4-CPR complex and the total amplitude of the fast and slow phases is a reflection of the affinity of the protein partners for each other. In the case of residues V267, L270 and R133, only 24, 26 and 19% respectively of the P450 variants was reduced by CPR compared to WT and these results strongly supports the conclusion that these residues are involved in CPR binding.

Since protein-protein interactions between CPR and CYP2B4 appear to involve both complementary charge pairing and hydrophobic interactions, how do the two different intermolecular forces coordinate protein recognition? Jones and Thornton have surveyed the interfaces of protein heterocomplexes with the goal to identify the types of residues that distinguish those found at the interface from those present on the surface of the protein (Jones and Thornton, 1996). They have noted that large hydrophobic and uncharged polar residues were present more often at the binding interface compared to the rest of the solvent exposed surface. Similarly, work on the human growth hormone receptor has demonstrated that when hydrophobic contacts are distributed over a relatively large area they can contribute substantially to the binding energy (Clackson et al., 1998). Shielding these hydrophobic contacts from the influence of water are charged residues that frame the binding interface and are postulated to dictate specificity in the interaction. The notion that hydrophobic residues can dominate the interfaces of redox-partners was recently reinforced by the crystal structure of a chemically cross-linked putidaredoxin reductase (Pdr) and putidaredoxin (Pdx) complex that is essential in the $P450_{cam}$ monooxygenase system. These studies revealed that the Pdr-Pdx interface is

predominantly hydrophobic with a central salt bridge assisting docking and orientation (Sevrioukova et al., 2010).

Since the structure of CYP102A1 (P450BM3) (PDB code 1BVY) represents the only known crystal structure of a P450 complexed with its redox partner (Sevrioukova et al., 1999b), it is interesting to examine whether the residues currently believed to contribute to the CYP2B4-CPR interaction (Bridges et al., 1998) are conserved in the heme domain of P450BM3. The amino acid sequences of CYP2B4 and P450BM3 were subjected to analysis by the EMBOSS Pairwise Alignment Algorithm (http://www.ebi.ac.uk/Tools/emboss/align/index.html), which revealed that the charge of approximately half of the CYP2B4 residues believed to mediate CPR recognition are conserved between these two P450s (Figure 2.9). Specifically, we find that the charges of only R122, F135, M137, L270 and K433 of CYP2B4 are conserved in P450BM3. Interestingly, the P450BM3 counterparts to the CYP2B4 basic amino acids identified by Bridges et al. (1998) to be involved in binding CPR are almost all neutral residues while V267 on CYP2B4 is H237 in P450BM3. Of all the P450BM3 residues presented in Table 2.6 only K98 and Q398 are within the FMN domain binding region. However, only Q396 of BM3's heme domain could potentially form a hydrogen bond with E494 of the FMN domain (although the two are 6.2 Å apart) since K98 of the heme domain likely contributes to the k_{off} of the complex as it forms a charge repulsion interaction with R498 of BM3's FMN domain. Thus, based on the only available crystal structure of a complete P450-redox partner complex, it is difficult to extend our understanding of specific residues of P450BM3 involved in binding to CPR to CYP2B4.

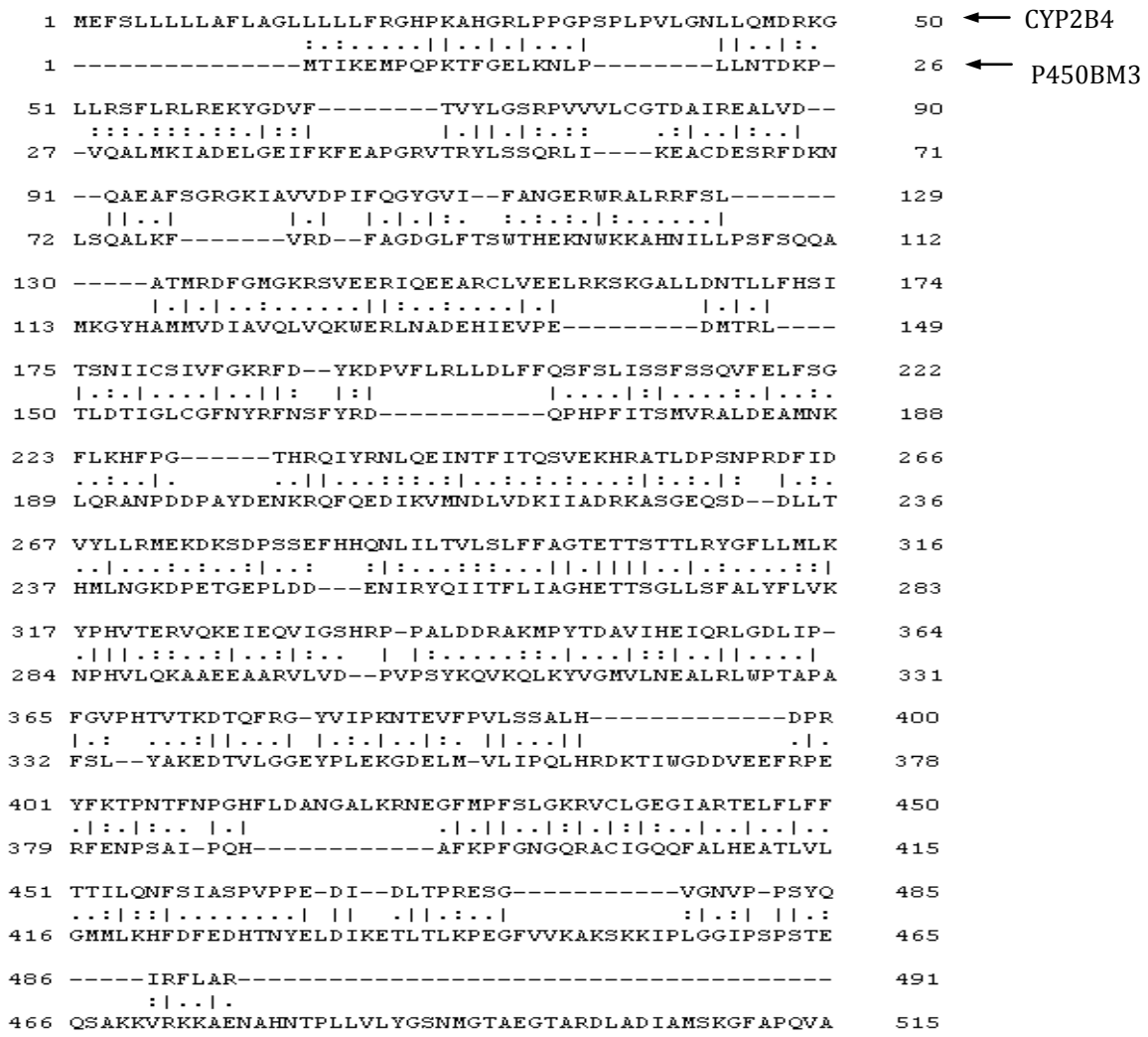

Figure 2.9. EMBOSS Pairwise alignment algorithm output of CYP2B4 (first line in each sequence pair) and P450BM3 (second line in each seqeunce pair) amino acid sequences. The co-crystal structure of P450BM3's heme domain with its FMN domain is the only known crystal structure of a type II P450 with its redox partner. To detemine whether the residues in P450BM3 that appear to be involved in binding the FMN domain are conserved in CYP2B4, a sequence alignment of the two isoforms was performed.

CYP2B4	P450BM3
R122	K98
R126	N102
R133	V121
F135	I123
M137	V125
K139	L127
V267	H237
L270	L239
R422	-
K433	Q398
R443	L408

Table 2.6. CYP2B4 proximal residues, identified by Bridges et al. and this study, to be involved in CPR binding and their corresponding residues in P450BM3. "-" = no equivalent residue identified in P450BM3

Previous studies on CPR-P450 interactions have identified roles for hydrophobic residues and charged residues in mediating complex formation. (Black et al., 1979; Stayton and Sligar, 1990; Rodgers and Sligar, 1991; Shimizu et al., 1991; Voznesensky and Schenkman, 1992; Bridges et al., 1998; Bumpus and Hollenberg, 2010). However, most of these studies relied on steady state turnover kinetics to investigate the binding interface and thus they were not able to distinguish perturbations in electron transfer pathways from binding affinity. To our knowledge, this study is the first to identify roles for L270 and V267 in the interaction between CYP2B4 and CPR using a combination of kinetic and non-kinetic methods.

The residues present at protein-protein interaction sites not only dictate the k_{on} of the association, but the k_{off} of the dissociation as well. This is usually achieved either through steric clashing or electrostatic repulsion. Knowledge regarding the residues responsible for this can be harnessed to create P450 mutants with residues that contribute to the k_{off} re-engineered to promote the k_{on} (Selzer et al., 2000; Xiong et al., 2009). As a result of the modification, we would anticipate changes in the nature of the interaction between CPR and P450, which might lead to faster rates of electron transfer and thus higher P450 catalytic activity. This could be exploited industrially in the P450-mediated biosynthesis of chemicals (Guengerich, 2002). The findings from these studies are discussed in depth in Chapter III.

The insights gained into the roles of selected amino acid residues in the interactions between CYP2B4 and CPR by combining stopped-flow, fluorescence spectroscopy, site-specific mutagenesis, and steady-state kinetics are invaluable. They demonstrate that FM can be used to site-specifically label surface exposed residues on

2B4 and that when reconstituted with CPR, the CYP2B4-FM variants with labels on their proximal side showed the largest fluorescence enhancement compared to other residues on the surface of CYP2B4. These residues were L420C, L270C, V267C and R133C. With the exception of L420C, all the proximal variants showed increased K_d and K_M values for CPR and were reduced by CPR at rates and to extents significantly less than WT. Thus we propose an expanded role for hydrophobic residues in mediating complex formation between CYP2B4 and CPR.

Footnote

This chapter has been published in the journal *Biochemistry* 2011, 50, pages 3957-3967. The authors are Cesar Kenaan, Haoming Zhang, Erin V. Shea and Paul F. Hollenberg from the Chemical Biology Doctoral Program and Department of Pharmacology at The University of Michigan, Medical Sciences Research Building III, 1150 West Medical Center Drive, Ann Arbor, Michigan 48109, United States.

References

Backes WL and Eyer CS (1989) Cytochrome P-450 LM2 reduction. Substrate effects on the rate of reductase-LM2 association. *J Biol Chem* **264**:6252-6259.

Backes WL and Kelley RW (2003) Organization of multiple cytochrome P450s with NADPH-cytochrome P450 reductase in membranes. *Pharmacol Ther* **98**:221-233.

Black SD, French JS, Williams CH, Jr. and Coon MJ (1979) Role of a hydrophobic polypeptide in the N-terminal region of NADPH-cytochrome P-450 reductase in complex formation with P-450LM. *Biochem Biophys Res Commun* **91**:1528-1535.

Bridges A, Gruenke L, Chang YT, Vakser IA, Loew G and Waskell L (1998) Identification of the binding site on cytochrome P450 2B4 for cytochrome b5 and cytochrome P450 reductase. *J Biol Chem* **273**:17036-17049.

Bumpus NN and Hollenberg PF (2010) Cross-linking of human cytochrome P450 2B6 to NADPH-cytochrome P450 reductase: Identification of a potential site of interaction. *J Inorg Biochem* **104**:485-488.

Cawley GF, Batie CJ and Backes WL (1995) Substrate-dependent competition of different P450 isozymes for limiting NADPH-cytochrome P450 reductase. *Biochemistry* **34**:1244-1247.

Clackson T, Ultsch MH, Wells JA and de Vos AM (1998) Structural and functional analysis of the 1:1 growth hormone:receptor complex reveals the molecular basis for receptor affinity. *J Mol Biol* **277**:1111-1128.

Coon MJ, Hoeven TA, Kaschnitz RM and Strobel HW (1973) Biochemical studies on cytochrome P-450 solubilized from liver microsomes: partial purification and mechanism of catalysis. *Ann N Y Acad Sci* **212**:449-457.

Davydov DR, Knyushko, T.V., Kanaeva, I.P., Koen, Y.M., Samenkova, N.F., Archakov, A.I. and Hui Bon Hoa, G. (1996) *Biochimie* **78**:734-743.

Denisov IG, Makris TM, Sligar SG and Schlichting I (2005) Structure and chemistry of cytochrome P450. *Chem Rev* **105**:2253-2277.

Drees BL, Rye HS, Glazer AN and Nelson HC (1996) Environment-sensitive labels in multiplex fluorescence analyses of protein-DNA complexes. *J Biol Chem* **271**:32168-32173.

Enoch HG and Strittmatter P (1979) Cytochrome b5 reduction by NADPH-cytochrome P-450 reductase. *J Biol Chem* **254**:8976-8981.

French JS, Guengerich FP and Coon MJ (1980) Interactions of cytochrome P-450, NADPH-cytochrome P-450 reductase, phospholipid, and substrate in the reconstituted liver microsomal enzyme system. *J Biol Chem* **255**:4112-4119.

Gao Q, Doneanu, C. E., Shaffer, S. A., Adman. E. T., Goodlett, D. R., and and Nelson SD (2006) Identification of the interactions between cytochrome P450 2E1 and cytochrome b5 by mass spectrometry and site-directed mutagenesis. *J Biol Chem* **281**:20404-20417.

Gray HB and Winkler JR (1996) Electron transfer in proteins. *Annu Rev Biochem* **65**:537-561.

Guengerich FP (2002) Cytochrome P450 enzymes in the generation of commercial products. *Nat Rev Drug Discov* **1**:359-366.

Hamdane D, Xia C, Im SC, Zhang H, Kim JJ and Waskell L (2009) Structure and function of an NADPH-cytochrome P450 oxidoreductase in an open

conformation capable of reducing cytochrome P450. *J Biol Chem* **284**:11374-11384.
Hassan AQ, Wang Y, Plate L and Stubbe J (2008) Methodology to probe subunit interactions in ribonucleotide reductases. *Biochemistry* **47**:13046-13055.
Hermanson GT (1996) *Bioconjugate Techniques*. Academic Press, San Diego.
http://www.ebi.ac.uk/Tools/emboss/align/index.html
Hubbard PA, Shen AL, Paschke R, Kasper CB and Kim JJ (2001) NADPH-cytochrome P450 oxidoreductase. Structural basis for hydride and electron transfer. *J Biol Chem* **276**:29163-29170.
Jang HH, Jamakhandi AP, Sullivan SZ, Yun CH, Hollenberg PF and Miller GP (2010) Beta sheet 2-alpha helix C loop of cytochrome P450 reductase serves as a docking site for redox partners. *Biochim Biophys Acta* **1804**:1285-1293.
Jones S and Thornton JM (1996) Principles of protein-protein interactions. *Proc Natl Acad Sci U S A* **93**:13-20.
Kikuchi G, Yoshida T and Noguchi M (2005) Heme oxygenase and heme degradation. *Biochem Biophys Res Commun* **338**:558-567.
Lehnerer M, Schulze J, Achterhold K, Lewis DF and Hlavica P (2000) Identification of key residues in rabbit liver microsomal cytochrome P450 2B4: importance in interactions with NADPH-cytochrome P450 reductase. *J Biochem* **127**:163-169.
Miwa GT, West SB, Huang MT and Lu AY (1979) Studies on the association of cytochrome P-450 and NADPH-cytochrome c reductase during catalysis in a reconstituted hydroxylating system. *J Biol Chem* **254**:5695-5700.
Nash T (1953) The colorimetric estimation of formaldehyde by means of the Hantzech reaction. *Biochem J* **55**:416-421.
Omura T and Sato R (1964) The Carbon Monoxide-Binding Pigment of Liver Microsomes. Ii. Solubilization, Purification, and Properties. *J Biol Chem* **239**:2379-2385.
Ono T, and Bloch, K. (1975) Solubilization and partial characterization of rat liver squalene epoxidase. . *J Biol Chem* **250**:1571-1579.
Rittle J and Green MT (2010) Cytochrome P450 compound I: capture, characterization, and C-H bond activation kinetics. *Science* **330**:933-937.
Rodgers KK and Sligar SG (1991) Mapping electrostatic interactions in macromolecular associations. *J Mol Biol* **221**:1453-1460.
Scott EE, He YA, Wester MR, White MA, Chin CC, Halpert JR, Johnson EF and Stout CD (2003) An open conformation of mammalian cytochrome P450 2B4 at 1.6-A resolution. *Proc Natl Acad Sci U S A* **100**:13196-13201.
Scott EE, White MA, He YA, Johnson EF, Stout CD and Halpert JR (2004) Structure of mammalian cytochrome P450 2B4 complexed with 4-(4-chlorophenyl)imidazole at 1.9-A resolution: insight into the range of P450 conformations and the coordination of redox partner binding. *J Biol Chem* **279**:27294-27301.
Selzer T, Albeck S and Schreiber G (2000) Rational design of faster associating and tighter binding protein complexes. *Nat Struct Biol* **7**:537-541.
Sevrioukova IF, Hazzard JT, Tollin G and Poulos TL (1999a) The FMN to heme electron transfer in cytochrome P450BM-3. Effect of chemical modification of cysteines engineered at the FMN-heme domain interaction site. *J Biol Chem* **274**:36097-36106.

Sevrioukova IF, Li H, Zhang H, Peterson JA and Poulos TL (1999b) Structure of a cytochrome P450-redox partner electron-transfer complex. *Proc Natl Acad Sci U S A* **96**:1863-1868.

Sevrioukova IF and Poulos TL (2010) Structural biology of redox partner interactions in P450cam monooxygenase: A fresh look at an old system. *Arch Biochem Biophys*.

Sevrioukova IF, Poulos TL and Churbanova IY (2010) Crystal structure of the putidaredoxin reductase x putidaredoxin electron transfer complex. *J Biol Chem* **285**:13616-13620.

Shen AL and Kasper CB (1995) Role of acidic residues in the interaction of NADPH-cytochrome P450 oxidoreductase with cytochrome P450 and cytochrome c. *J Biol Chem* **270**:27475-27480.

Shimizu T, Tateishi T, Hatano M and Fujii-Kuriyama Y (1991) Probing the role of lysines and arginines in the catalytic function of cytochrome P450d by site-directed mutagenesis. Interaction with NADPH-cytochrome P450 reductase. *J Biol Chem* **266**:3372-3375.

Stayton PS and Sligar SG (1990) The cytochrome P-450cam binding surface as defined by site-directed mutagenesis and electrostatic modeling. *Biochemistry* **29**:7381-7386.

Vermilion JL and Coon MJ (1978) Purified liver microsomal NADPH-cytochrome P-450 reductase. Spectral characterization of oxidation-reduction states. *J Biol Chem* **253**:2694-2704.

Voznesensky AI and Schenkman JB (1992) The cytochrome P450 2B4-NADPH cytochrome P450 reductase electron transfer complex is not formed by charge-pairing. *J Biol Chem* **267**:14669-14676.

Voznesensky AI and Schenkman JB (1994) Quantitative analyses of electrostatic interactions between NADPH-cytochrome P450 reductase and cytochrome P450 enzymes. *J Biol Chem* **269**:15724-15731.

Wang M, Roberts DL, Paschke R, Shea TM, Masters BS and Kim JJ (1997) Three-dimensional structure of NADPH-cytochrome P450 reductase: prototype for FMN- and FAD-containing enzymes. *Proc Natl Acad Sci U S A* **94**:8411-8416.

Williams CH, Jr. and H. Kamin (1962) Microsomal triphosphopyridine nucleotide-cytochrome c reductase of liver. *J Biol Chem* **237**:587-595.

Xiong P, Nocek JM, Griffin AK, Wang J and Hoffman BM (2009) Electrostatic redesign of the [myoglobin, cytochrome b5] interface to create a well-defined docked complex with rapid interprotein electron transfer. *J Am Chem Soc* **131**:6938-6939.

Zhang H, Im SC and Waskell L (2007) Cytochrome b5 increases the rate of product formation by cytochrome P450 2B4 and competes with cytochrome P450 reductase for a binding site on cytochrome P450 2B4. *J Biol Chem* **282**:29766-29776.

Zhang H, Kenaan C, Hamdane D, Hoa GH and Hollenberg PF (2009) Effect of conformational dynamics on substrate recognition and specificity as probed by the introduction of a de novo disulfide bond into cytochrome P450 2B1. *J Biol Chem* **284**:25678-25686.

Chapter III

Redesigning the CYP2B4-CPR Interface to Create a Complex with a Faster Rate of Electron Transfer and a Higher Catalytic Activity

Abstract

It was demonstrated in Chapter II that the proximal site residues V267 and L270 of CYP2B4 play significant roles in binding CPR. Here we replaced V267 and L270 with Lys, Phe and Glu with the goal of investigating the role of residue charge at the CYP2B4-CPR binding interface. All six variants were successfully expressed in *Escherichia coli* and purified to homogeneity. It was found that CYP2B4 variants V267K and L270K exhibited a ~ 1.6 fold increase in CPR-supported catalytic activity while V267F and L270F remained almost unchanged compared to WT. The most dramatic decrease was observed for the V267E and L270E variants, which showed approximately 72% decreases in maximal activity compared to WT. Interestingly, the changes in steady-state activity results agree with the changes in rates of electron transfer observed with these variants suggesting that the introduction of Lys at the binding interface enhances catalytic activity by enhancing the rate of electron transfer while Glu decreases activity by disrupting the interaction. These results represent new and valuable preliminary progress in engineering a non-covalent CYP2B4-CPR complex with higher rates of electron transfer without jeopardizing catalytic activity.

Introduction

Communication is essential to complex organisms. Biological macromolecules communicate via physical interactions in order to transfer information, such as in signaling pathways or via electrons, such as in P450s. Proteins recognize their partners through biophysical interactions such as electrostatic and hydrophobic interactions at binding interfaces that usually represent only a small fraction of the total surface of the protein partners. The goal of understanding and controlling protein-protein interactions has inspired numerous efforts to modulate the binding of complexes of known structures with high basal affinity interactions (Schreiber and Fersht, 1996; Ivkovic-Jensen et al., 1998; Selzer et al., 2000; Tetreault et al., 2002; Pearl et al., 2008; Schreiber et al., 2009).

For example, the ribonuclease barnase associates with its natural intracellular inhibitor, barstar, with a relatively high rate constant of 10^5 $M^{-1}s^{-1}$ (Schreiber and Fersht, 1996). The co-crystal structure of the complex revealed that the binding interface between these two proteins is dominated by charged amino acids which are thought to mediate long-range electrostatic interactions that lead to the formation of an early low affinity non-specific complex (Buckle et al., 1994). The introduction of two Lys residues in barnase at the protein-protein interaction interface through a double mutant cycle increased the association rate constant to 5 x 10^9 $M^{-1}s^{-1}$ (Schreiber and Fersht, 1996). Since the Einstein-Smoluchowski equation suggests that the maximum rate constant for the collision of molecules in solution is 10^9-10^{10} $M^{-1}s^{-1}$, the rationally engineered enhancement in the association of barnase with barstar represents a significant improvement in the rate of association of the initial encounter complex between these two proteins which approaches the theoretical maximum. Similarly, the association rate

constant for the binding of β-lactamase inhibitor protein (BLIP) and TEM1 β-lactamase was enhanced from 2.2 x 10^5 $M^{-1}s^{-1}$ to 470 x 10^5 $M^{-1}s^{-1}$ with almost no change in the k_{off} by the introduction of four Lys residues in BLIP (Selzer et al., 2000). Therefore, these studies demonstrate that enhanced rates of association between macromolecules that possess relatively high basal rates of association are attainable by the rational replacement of hydrophobic or acidic residues with basic amino acids.

However, to begin such efforts at the other extreme, that is, with a pair of proteins like the mammalian P450s and CPR, which associate relatively weakly and whose co-crystal structure remains to be determined, and attempt to enhance their binding kinetics or the kinetics of other closely associated processes like electron transfer and catalytic activity, offers a different level of challenge. Despite the dearth of information regarding the precise identity of interacting residues in both redox partners, the desire to understand and control protein-protein interactions has encouraged numerous efforts within the P450 field to improve catalytic activity by covalently cross-linking CPR with P450, mostly through genetic means (Fisher et al., 1992; Shet et al., 1993; Hayashi et al., 2000; Deeni et al., 2001). Much of the impetus for this approach stems from biochemical and biophysical studies on P450BM3.

Since its discovery in the late 1980s, P450BM3 has undergone extensive biochemical study and has been widely recognized as an excellent model system for the study of protein-protein interactions in the cytochrome P450 field. The key aspect of the structure of P450 BM3 that led to its rise to prominence is the fact that it was the first prokaryotic P450 recognized to interact with a eukaryotic-like P450 reductase rather than with an iron-sulfur ferredoxin and FAD-containing ferredoxin reductase (Munro and

Lindsay, 1996). Furthermore, P450BM3 is a natural fusion protein with the reductase linked to the P450 (heme) domain as part of a single 119 kDa polypeptide. Analysis of the catalytic activity of P450BM3 revealed it to be a highly active enzyme relative to its eukaryotic fatty acid hydroxylase counterparts with k_{cat} values (min^{-1}) that range up in to the thousands (Boddupalli et al., 1992; Miles et al., 1992). This enhanced activity was ascribed to the efficiency of the covalently associated electron transfer system. For instance, the rate of first electron transfer from CPR to CYP2B4 in the presence of BNZ is approximately 5 s^{-1} (Chapter 2, this thesis), yet these rates apparently approach 600 – 900 s^{-1} in P450BM3 (Ost et al., 2003; deMontellano, 2005).

In attempts to reproduce these greatly enhanced rates in mammalian P450s, several groups have genetically engineered mammalian P450s fused to their redox partners. For instance, Hayashi et al. have attempted the co-expression of human CYP3A4 with yeast CPR and human b_5 (Hayashi et al., 2000). Although they could not achieve the activity levels observed with P450BM3, their findings suggest that genetically fusing these two proteins together enhanced the rate of electron transfer by almost 100-fold (0.38 s^{-1} to 30 s^{-1}); however, the coupling efficiency and catalytic activity of the CYP3A4 were significantly reduced as a result of cross-linking with CPR. Similar observations have been made from attempts to fuse CYP4A1 (from rat liver) and CYP17A (from bovine adrenal glands) with CPR (Fisher et al., 1992). The discrepancy between the rate of electron transfer and the catalytic activity may suggest that the P450 enzyme system is optimally designed to balance rates of electron transfer with auto-oxidation. More recently, investigations with $P450_{cam}$ and a chemically cross-linked Pdr-Pdx complex showed that although the covalently trapped complex was ideal for

reducing cytochrome c, (~150-fold faster than for the individual proteins) it was incapable of transferring electrons to $P450_{cam}$ and thus could not support $P450_{cam}$ activity (Churbanova et al., 2010; Sevrioukova et al., 2010). The inability of covalent fusions between P450 and its redox partner to reproduce the high rates of electron transfer and impressive catalytic activity of P450BM3 likely stems from restrictions in the rotational mobility of the covalently linked proteins. A major assumption in these cross-linking studies, whether chemical or genetic, is that the functional sites for interactions between the two proteins are accessible in spite of the conformational restriction a covalent link imposes. Long-range electrostatic forces are believed to play a major role in stabilizing the transition state, and the consequences of removing conformational freedom by introducing a covalent bond may result in significantly impaired formation of the precursor state leading to association in which the two proteins are correctly oriented towards each other (Schreiber, 2002). Alternatively, irreversibly trapping of CPR and P450 in a functional complex by a covalent bond will lower the dissociation rate constant (k_{off}) to 0, thereby preventing CPR and P450 from disengaging and potentially enhancing the futile cycling of electrons that contributes to uncoupling.

The results discussed in Chapter II suggested an important role for the hydrophobic residues V267 and L270 in the formation of the CYP2B4-CPR complex. That is to say that electrostatic interactions, in conjunction with hydrophobic interactions, likely play an important role at the binding interface of these two redox-partner proteins. Previous studies have shown that neutralization of some of the charged residues by mutation to alanine or acetylation by acetic anhydride reduced the K_d of the complex (Shen and Strobel, 1992; Bridges et al., 1998). However, very little is known about the

effect of replacing hydrophobic residues with charged ones on the rate and extent of electron transfer from CPR to 2B4 as well as its impact on the K_M and k_{cat} for the interaction of CYP2B4 with CPR. The findings reported in this chapter represent preliminary progress in engineering a non-covalent complex between CYP2B4 and CPR with an enhanced rate of electron transfer and catalytic activity while further exploring the potential roles of hydrophobic and acidic residues at the CYP2B4-CPR binding interface.

Materials and Methods

Chemicals. All chemicals used are of ACS reagent grade unless otherwise specified and obtained from commercial vendors. Benzphetamine, NADPH, sodium dithionite and tert-butyl hydroperoxide were purchased from Sigma. Trifluoroacetic acid was purchased from Pierce Chemicals. Dilauroylphosphatidylcholine (DLPC) was purchased from Doosan Serdary Research Laboratory (Toronto, Canada). Carbon monoxide gas (purity >99.5%) was purchased from Cryogenic Gases (Detroit, MI).

Construction of CYP2B4 Variants. Site-directed mutagenesis was performed using a QuikChange site-directed mutagenesis kit according to the manufacturer's protocol (Stratagene). The forward and reverse mutagenic primers for V267F, V267K, V267E, L270F, L270K, and L270E are listed in Table 3.1. Each site-specific mutation was confirmed by DNA sequencing at the University of Michigan DNA Sequencing Core.

Overexpression and Purification of CYP2B4 WT and Variants. CYP2B4, its variants and CPR were expressed and purified from *Escherichia coli* as described previously (Zhang et al., 2007). The concentrations of CYP2B4 and its variants were determined using an extinction coefficient of$\Delta\ \varepsilon_{450\text{-}490\ nm}$ of 91 mM cm^{-1} as described by Omura and Sato (Omura and Sato, 1964). The concentration of CPR was determined using an extinction coefficient of 21 mM cm^{-1} at 456 nm for the oxidized enzyme (Vermilion and Coon, 1978).

Determination of the Rate of Electron Transfer from CPR to CYP2B4 WT and its Variants. In order to investigate the effects of the mutations in CYP2B4 on the interactions between the CYP2B4 variants and CPR, the rates of the first electron transfer from CPR to the CYP2B4 WT and its variants were measured. The rates of reduction were determined using a stopped-flow spectrophotometer (Hi-Tech SF61DX2, TgK Scientific, Bradford-on-Avon, UK) to monitor the increase in the absorbance at 450 nm as a result of the formation of the ferrous CYP2B4-CO adduct following reduction of the ferric CYP2B4 by CPR at 30 ^{o}C in the presence of CO. One syringe contained CYP2B4 WT or a variant (3 µM), CPR (3 µM) and DLPC (0.15 mg/ml) that had been reconstituted on ice for 1 hr before being diluted by half in 0.1 M potassium phosphate buffer, pH 7.4, to a final volume of 1.5 mL. This mixture was then rapidly mixed with an equal volume of 0.1 M potassium phosphate buffer, pH 7.4, and 0.1 mM NADPH from another syringe. Both solutions had been saturated with CO by passing a gentle stream of CO gas over the sample solutions for 5 minutes. The increase in absorbance at 450 nm was monitored over time for 100 seconds. The data were then analyzed to determine the

Primer name	Primer sequence (5’ ∧ 3’)
V267F forward	AACCCCAGGGATTTCATCGACTTCTACCTGCTCCGCATGGAAAAA
V267F reverse	TTTTTCCATGCGGAGCAGGTAGAAGTCGATGAAATCCCTGGGGTT
V267K forward	AACCCCAGGGATTTCATCGACAAGTACCTGCTCCGCATGGAAAAA
V267K reverse	TTTTTCCATGCGGAGCAGGTACTTGTCGATGAAATCCCTGGGGTT
V267E forward	AACCCCAGGGATTTCATCGACGAGTACCTGCTCCGCATGGAAAAA
V267E reverse	TTTTTCCATGCGGAGCAGGTACTCGTCGATGAAATCCCTGGGGTT
L270F forward	AACCCCAGGGATTTCATCGACGTCTACCTGTTCCGCATGGAAAAAGAC
L270F reverse	GTCTTTTTCCATGCGGAACAGGTAGACGTCGATGAAATCCCTGGGGTT
L270K forward	AACCCCAGGGATTTCATCGACGTCTACCTGAAGCGCATGGAAAAAGAC
L270K reverse	GTCTTTTTCCATGCGCTTCAGGTAGACGTCGATGAAATCCCTGGGGTT
L270E forward	GATTTCATCGACGTCTACCTGGAGCGCATGGAAAAAGACAAGTCC
L270E reverse	GCACTTGTCTTTTTCCATGCGCTCCAGGTAGACGTCGATGAAATC

Table 3.1. List of primers used for site-directed mutagenesis.

apparent rate constants and amplitudes for the rates of electron transfer from CPR to CYP2B4 WT and its variants by fitting the absorbance changes at 450 nm to a three-exponential equation using the KinetAsyst software (Bradford-on-Avon, UK).

Determination of the Apparent K_M and k_{cat} Values for CYP2B4 WT and Variants of CPR Using the N-demethylation of Benzphetamine. The K_M and k_{cat} values for CYP2B4 WT and its variants for CPR were determined at 30^{o}C by measuring the rate of formaldehyde formation from the N-demethylation of benzphetamine at a constant P450 concentration with increasing concentrations of CPR. CYP2B4 WT and its variants (0.2 µM) were reconstituted in triplicate with varying concentrations of CPR (0.1, 0.2, 0.3, 0.4, 0.5, 0.6, 1.0 and 1.2 µM) and 0.1 mg/ml DLPC on ice for 1 h. The reconstituted mixtures were then added to 50 mM potassium phosphate buffer, pH 7.4, and 1 mM benzphetamine. After the samples were equilibrated at 30^o C for 15 min, the reactions were initiated by adding 7.5 µL of 20 mM NADPH to give a final reaction volume of 500 µL. The reactions were allowed to proceed for 5 min at 30 ^{o}C before they were quenched by the addition of 25 µL of 50% TFA. The protein was precipitated by centrifugation at 13.2k rpm for 5 min and a 500 µL aliquot of the supernatant was assayed for formaldehyde using the Nash reaction (Nash, 1953). The kinetic parameters were determined by fitting the data to the Michaelis-Menten equation using GraphPad Prism 5.0 from GraphPad software (La Jolla, CA).

Characterization of the tert-butyl hydroperoxide-supported Metabolism of Benzphetamine by CYP2B4 WT and its Variants. To determine the rates for the tert-

butyl hydroperoxide–supported metabolism of benzphetamine, final concentrations of 0.25 µM CYP2B4 WT and its variants were each incubated with 0.1 mg/ml DLPC, 50 mM potassium phosphate buffer, pH 7.4, and 1 mM benzphetamine at 30 ^{o}C for 15 min. 52.5 µL of 1 M tert-butyl hydroperoxide were added to give a final volume of 500 µL and the reactions were allowed to proceed for 5 min after which they were terminated by the addition of 25 µL of 50% TFA. The samples were centrifuged at 13.2k rpm for 5 min and 500 µL aliquots of the supernatants were assayed for formaldehyde using the Nash reaction (Nash, 1953).

Results

Rationale for site-directed mutagenesis of V267 and L270 to F, K and E. The results presented in Chapter II revealed important roles for residues V267 and L270 in the binding of CPR to CYP2B4. Although extensive work has been performed on neutralizing the positive charge composition of the proximal site of CYP2B4 through mutagenesis or chemical means, very little is known about the effect of introducing more basic residues, like Lys, to the proximal site of CYP2B4 on CPR binding and rates of electron transfer. It is conceivable that if dipole-dipole interactions have, on average, higher bond dissociation energies than van der Waals interactions, the intermolecular distance between two atoms that are in a columbic interaction is also likely to be lower. While this type of interaction may not necessarily lead to a tighter complex *per se* with high affinity, it may reduce the distance between the two proteins in the complex and facilitate electron transfer. From a bioengineering standpoint, a redesigned redox-partner complex capable of faster rates of electron transfer and higher activity may be of critical

importance in the P450-mediated biosynthesis of chemicals for industrial purposes (Guengerich, 2002). Since the contribution of hydrophobic residues to the CPR-CYP2B4 interaction has largely been ignored in the past, very little is known about whether V267 and L270 are interchangeable with other hydrophobic residues like Phe. If exchangeable, this would imply that the chemical nature of the residue (i.e., the absence of charge) is more important to binding than the structural contribution of the residue. Since only limited information is available with regard to the role of acidic residues in CPR binding, the effect of mutating V and L to negatively charged residues, like Glu, may shed much needed light on this question.

Characterization of the k_{cat} and K_M of CYP2B4 Variants for CPR using BNZ as a Substrate. Complex formation between CPR and CYP is an essential step in the transfer of electrons to the heme that is required for substrate oxidation. It has been proposed that the rate of substrate oxidation is directly proportional to the concentration of the CPR-CYP2B4 complex (Miwa et al., 1979; Bridges et al., 1998). Thus, by measuring the rate of benzphetamine demethylation in the presence of a fixed concentration of CYP2B4 and increasing concentrations of CPR, K_M and k_{cat} values can be determined. The impact of mutagenesis on these kinetic parameters sheds important light on the role of these residues at the binding interface. The mutation of a residue involved in redox partner recognition should disrupt complex formation and decrease the concentration of complexed CYP2B4 which is capable of oxidizing substrate. As shown in Figures 3.1 and 3.2, the rate of benzphetamine oxidation as a function of varying CPR concentrations follows a rectangular hyperbolic relationship, which can be fit to the

Michaelis-Menten equation. As shown in Table 3.2 the mutations at positions 267 and 270 in CYP2B4 had variable effects on the K_M and k_{cat} values. Their effects can be grouped based on the charge of the residue. When V267 and L270 were replaced by Lys, the change in K_M was almost negligible compared to the WT protein. Introducing a Lys increased the k_{cat} by almost 1.5 fold indicating that the introduction of a single basic residue at the proposed CYP2B4-CPR binding site enhances the k_{cat}/K_M ratio for CPR. Interestingly the replacement of V or L with Phe had almost no effect on either of the kinetic parameters suggesting that the identity of the hydrophobic residues is likely less critical than its charge.

Similar observations have been made from mutagenesis studies on Y422 in CYP2E1 (unpublished data from a collaborative project with Ms. Hsia-lien Lin in the Hollenberg Lab). Notably, the introduction of an acidic residue (Glu) at either position 267 or 270 increased the K_M and significantly decreased the k_{cat}. Since the results obtained from this assay rely on substrate metabolism, it might also be argued that any decrease in the rate of BNZ oxidation may be attributed to an alteration in the P450 active site instead of decreases in the concentrations of the CPR-CYP2B4 complexes. Such alterations can be assessed by determining the tert-butyl hydroperoxide-supported metabolism of BNZ by WT CYP2B4 and its charge variants at residues 267 and 270.

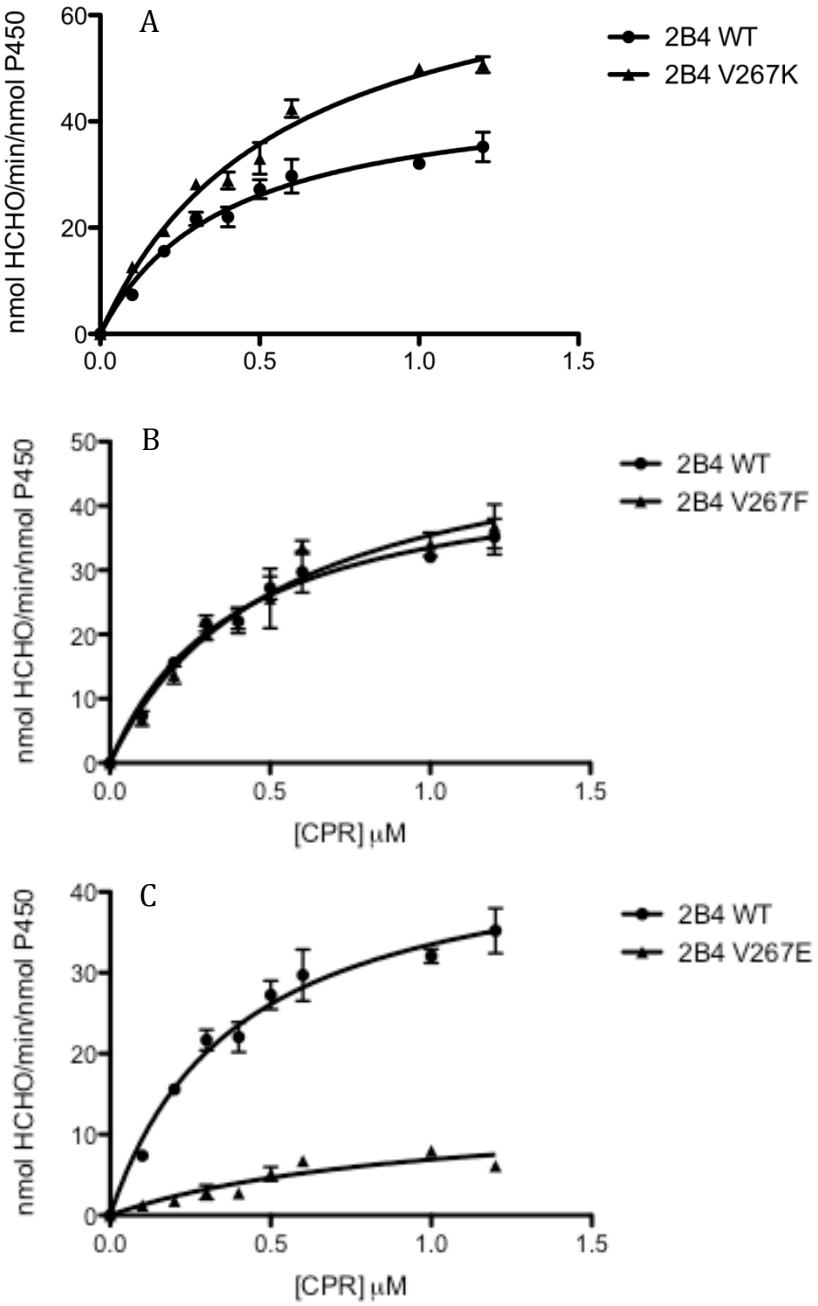

Figure 3.1: Determination of the apparent K_M and k_{cat} values of the CYP2B4 WT and the (A) V267K, (B) V267F and (C) V267E variants for CPR. The N-demethylation of benzphetamine to produce formaldehyde (HCHO) was measured at a constant concentration of CYP2B4 (0.2 μM) with increasing concentrations of CPR as described under "Materials and Methods". Error bars are the standard deviations from three measurements done in duplicate.

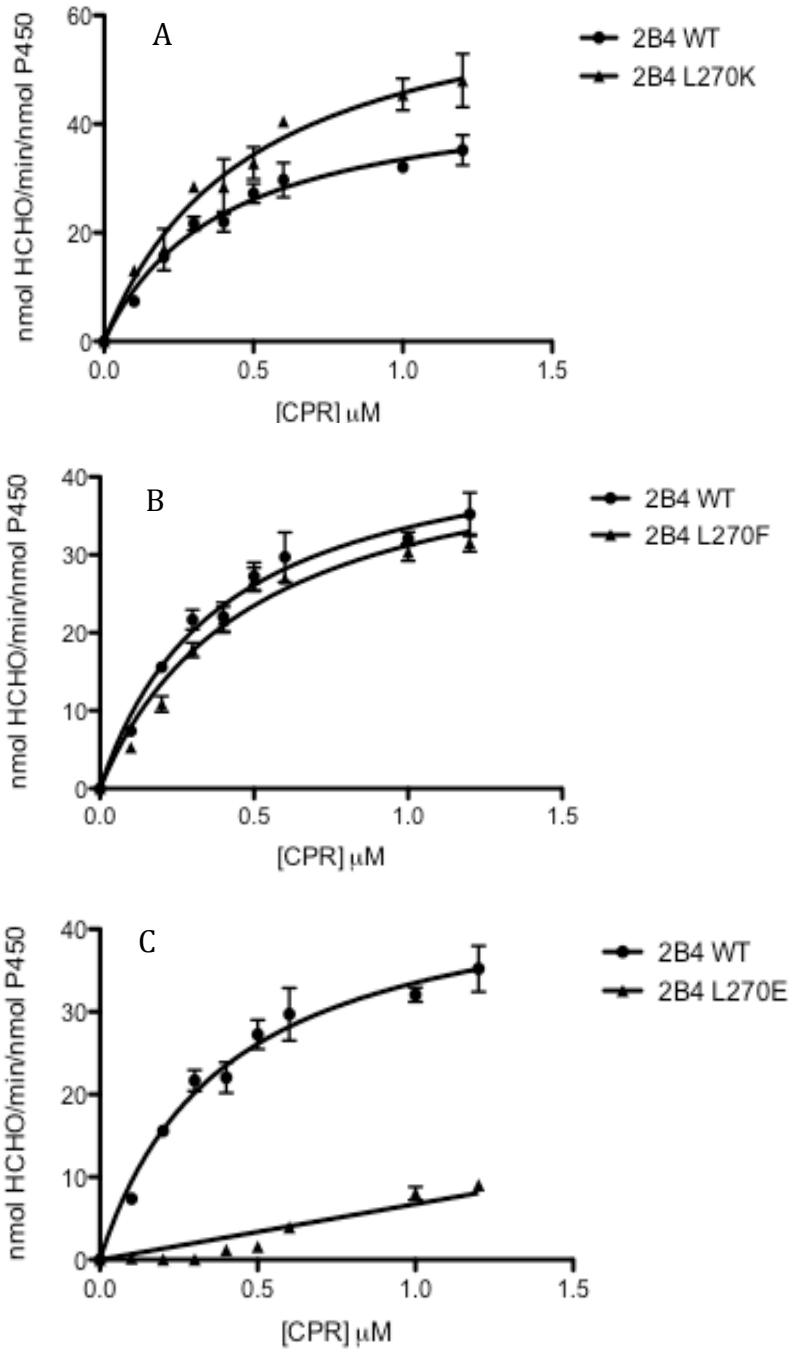

Figure 3.2: Determination of the apparent K_M and k_{cat} values of the CYP2B4 WT (A) L270K, (B) L270F and (C) L270E variants. The N-demethylation of benzphetamine to produce formaldehyde (HCHO) was measured at a constant concentration of CYP2B4 (0.2 μM) with increasing concentrations of CPR as described under "Materials and Methods". Error bars are the standard deviations from three measurements done in duplicate.

2B4	K_M (μM)	k_{cat} (min^{-1})	k_{cat}/K_M (min^{-1} μM^{-1})
WT	0.39±0.05	46±2.3	119
V267K	0.57±0.06	76±3.7	133
V267F	0.53±0.08	54±3.9	102
V267E	0.95±0.04	13±2.9	12.75
L270K	0.49±0.07	68±4.6	139
L270F	0.48±0.07	47±2.9	95
L270E	ND	ND	ND

ND = Not Determined

Table 3.2. K_M and k_{cat} values determined for CYP2B4 WT and its variants and CPR. As described under "Materials and Methods", the kinetic parameters were determined by measuring the rate of formaldehyde formation as a result of CYP2B4-mediated N-demethylation of benzphetamine under fixed concentrations of CYP2B4 and excess benzphetamine with increasing concentrations of CPR. The kinetics for the L270E variant did not accurately fit the Michealis-Menten equation due to poor activity at low concentrations of CPR, hence the kinetic parameters where not determined. The primary data from which these values are calculated are in Figures 3.1 and 3.2.

Determination of the Rate of tBHP-supported BNZ N-demethylation by CYP2B4 WT and Variants. The peroxide shunt in the P450 catalytic cycle can be used as a powerful tool to probe the catalytic integrity of the heme following site-directed mutagenesis. It is known that variations in the primary sequence of P450s, even those involving residues located in the periphery of the protein, may have a significant impact on activity (Domanski et al., 2001; Lin et al., 2003). Therefore, it is critical that the tBHP-supported activity of the P450 mutants under investigation is assessed because significant deviations in peroxide-supported activity will have a profound impact on the interpretation of CPR-supported activity data collected from any studies on the mutants. Furthermore, if significant changes are observed this would also signify that alternative residues should be pursued for the replacement of V267 and L270, e.g Asp instead of Glu or Arg instead of Lys. As shown in Figure 3.3 the mutations did not significantly alter the rate of BNZ metabolism compared to WT CYP2B4. As shown, all the variants are functional in *N*-demethylating BNZ to form formaldehyde, indicating that the heme and the active site environment of the variants are not adversely affected by these mutations.

Rates of Electron Transfer from CPR to Ferric CYP2B4 and its Variants. To further investigate the cause for the alterations in the catalytic activities of the variants, we investigated the rate of electron transfer from CPR to ferric CYP2B4, a critical step prior to substrate hydroxylation in the catalytic cycle of P450s. This is especially relevant to understand why V267E and L270E lose their catalytic activity when they retain an apparently fully functional heme and active site. This also tests the hypothesis that the enhancement in k_{cat} of V267K and L270K for CPR arises from faster electron transfer

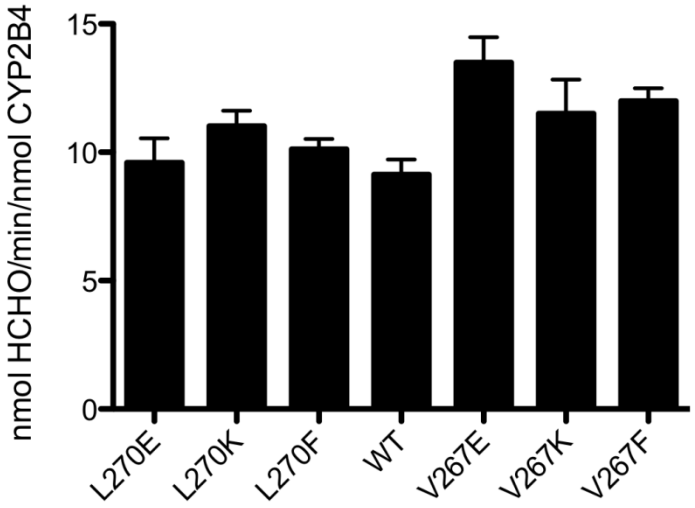

Figure 3.3. Comparison of the tBHP-supported metabolism of benzphetamine by CYP2B4 WT and variants. CYP2B4 WT and its variants were incubated with DLPC, potassium phosphate buffer, pH 7.4, and excess benzphetamine as described under "Experimental Procedures". The reactions were initiated by the addition of a 0.1 M final concentration of tBHP and the rate of formaldehyde formation was assessed spectrometrically after reaction with the Nash reagent. The data are an average of three experiments done in duplicate with the error bars representing standard deviation. the active site environment of the variants are not adversely affected by these mutations.

between CPR and these variants. The kinetic traces for electron transfer to reduce the P450s are depicted in Figure 3.4, and the rate constants and relative amplitudes for the fast and slow phases are summarized in Table 3.3. As shown, CPR transfers an electron to ferric CYP2B4 WT in the presence of NADPH with rate constants of 0.68 (72%) and 0.16 s^{-1} (28%) for the fast and slow phases, respectively. These rate constants are similar to those previously reported for CYP2B4 in the absence of BNZ (Chapter 2, this thesis). However, the rate constants for the variants either increased or decreased to various extents compared to the WT. The most dramatic change was observed when either Glu or Lys replaced the native residues at positions 267 and 270. For example, in CYP2B4 V267E and L270E the rate constants for the fast phases are 0.03 and 0.07 s^{-1}, respectively, which is approximately ~23-fold slower than that of WT CYP2B4. Glu also decreased the extent of reduction of V267E and L270E by CPR to 31% and 20% of the WT CYP2B4. The introduction of Lys at position 267 and 270 increased the rate of electron transfer of the fast phase by 2.2- and 2.5- fold compared to WT, respectively. Lys introduction also resulted in a slight shift in the percentage of P450 reduced in the fast phase. The Phe variants show reduction kinetics that are almost unchanged when compared to the WT protein.

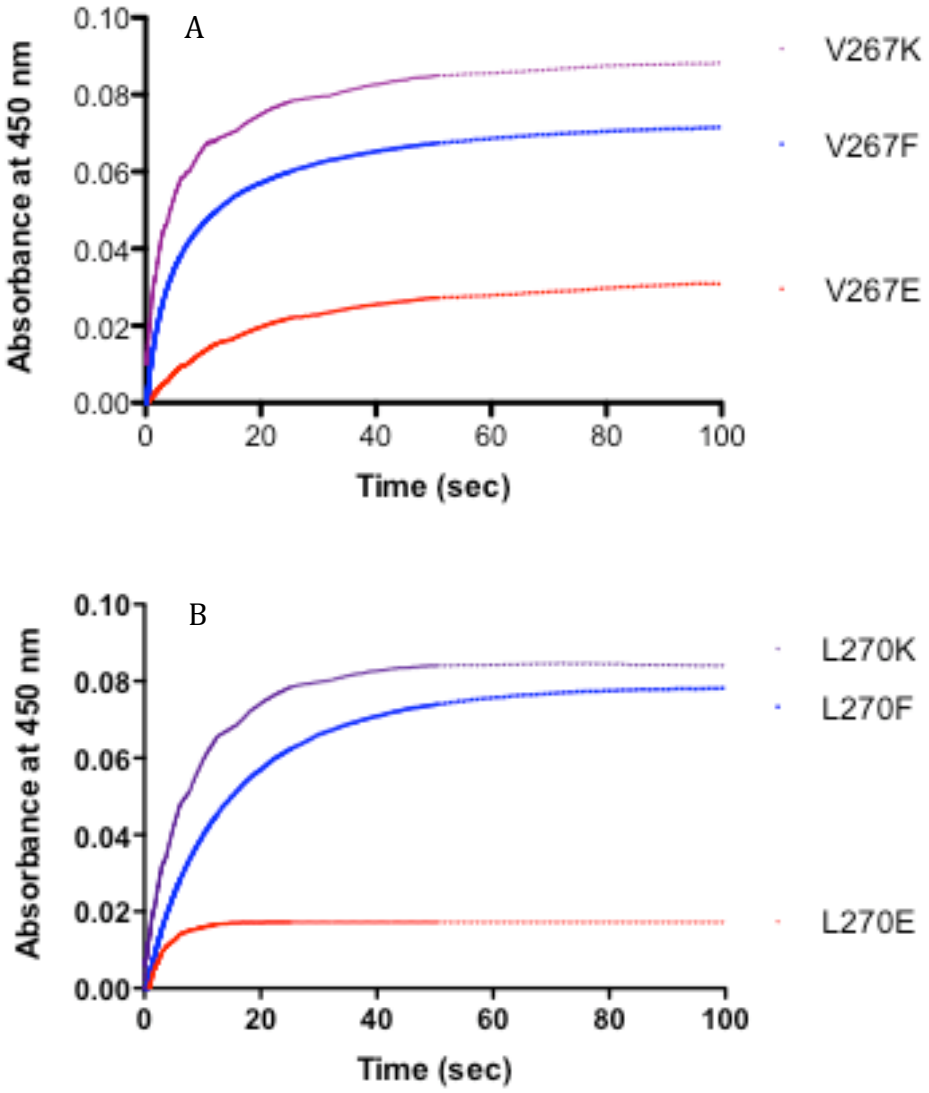

Figure 3.4. Kinetics for the reduction of the CYP2B4 variants at residue 267 (A) and 270 (B) by CPR. CYP2B4, CPR and DLPC were reconstituted for 1 hr on ice and mixed with NADPH in a stopped-flow apparatus. After mixing, the final concentrations of CYP2B4 and CPR were 1.5 μM and NADPH was 50 μM. Experiments were performed as described in "Materials and Methods" with a saturated solution of CO in both syringes. For convenience, all the absorbance data are offset to the same baseline.

2B4	Kinetic parameters				
	A_T	$A_1\%$	$k_{1,S}^{-1}$	$A_2\%$	$k_{2,S}^{-1}$
WT	0.090	72	0.68	28	0.16
V267K	0.085	87	1.5	13	0.11
V267F	0.070	68	0.72	32	0.24
V267E	0.028	34	0.03	66	0.08
L270K	0.080	78	1.68	22	0.19
L270F	0.078	59	0.67	41	0.33
L270E	0.018	62	0.07	38	0.01

Table 3.3. Rate constants and amplitudes observed for the reduction of CYP2B4 and its variants by CPR at 23^{o}C. The apparent rate constants for the two kinetic phases are k_1 and k_2, respectively, and the relative amplitudes for each phase are expressed as $A_1\%$ and $A_2\%$. The total absolute amplitude for the overall reduction is A_T.

Discussion

In this chapter we have extended the findings reported in Chapter II by investigating the role of charged residues at the CYP2B4-CPR binding interface. This objective was achieved by replacing V267 and L270 with Lys, Glu or Phe and characterizing their kinetics under steady-state and pre-steady-state conditions. Unlike previous studies, which have attempted (albeit unsuccessfully) to extend the high catalytic activity observed with $P450_{BM3}$ to mammalian P450s by covalently cross-linking P450 to CPR, we opted to take a different approach for the following reasons. One of the factors that contributes to CYP2B4 binding to CPR is complementary charge interactions between acidic residues in the FMN domain of CPR and basic residues on the proximal site of CYP2B4. Such electrostatic interactions are known to have relatively high dissociation energies and can play major roles in long-range interactions between protein pairs that are believed to be critical for steering and orienting protein partners (Schreiber, 2002). Since charge-charge interactions are significantly stronger that van der Waals interactions, they may also serve to minimize the distance between interacting redox-partner proteins, which is critical for efficient electron transfer. The properties of charge-charge interactions have been exploited in the past to engineer protein pairs with significantly improved association kinetics compared to their basal/native rates. For example, faster association kinetics were observed between barnase and barstar by introducing two Lys residues at the protein-protein interaction site (Schreiber and Fersht, 1996). Additionally, faster rates of electron transfer were observed between cytochrome b_5 and myoglobin when three aspartic residues were replaced with lysines (Xiong et al., 2009; Xiong et al., 2010). The question we sought to answer in this chapter is: “to what

extent can the properties of electrostatic interactions between proteins be harnessed to create a CYP2B4-CPR complex with a faster rate of electron transfer and higher catalytic activity?"

The effects of the mutations on the catalytic activity of the variants were relatively consistent between V267 and L270. Specifically, it was found that when a Lys residue was introduced into the proximal site of CYP2B4, the k_{cat} of the CYP2B4-CPR complex increased from 46 min^{-1} for the WT to 76 and 68 min^{-1} for the V267K and L270K variants, respectively, with a slight increase in the K_M values. Replacement of V267 and L270 with another hydrophobic residue, Phe, did not seem to perturb the k_{cat} of the complex, and like Lys, led to a slight increase in the K_M value. Interestingly, the introduction of Glu at residue position 267 led to a 9-fold decrease in the k_{cat} accompanied by 2.4-fold increase in the K_M. In the case of L270E, determination of K_M and k_{cat} was unsuccessful since poor CYP2B4 activity at low concentrations of CPR lead non-Michaelis-Menten kinetics that could not be fit to a rectangular hyperbolic equation.

The changes in activity observed in the presence of CPR were not due to changes in the catalytic integrity of the heme as a result of mutagenesis. This conclusion is supported by the results presented in Figure 3.3, which show that the tBHP-supported activity of the variants did not decrease compared to the WT. However, investigations into the effect of the mutations on electron transfer from CPR to the six CYP2B4 variants provided invaluable information regarding the effect of introducing more basic or acidic residues on the rate and extent of electron transfer.

When L270 and V267 were replaced by Phe, no major changes in the rate and extent of electron transfer were observed compared to WT, suggesting that the identity of

the hydrophobic residue at these positions in the protein is not likely to be critical for electron transfer or affinity for CPR. One would expect that replacing relatively small hydrophobic residues like Leu or Val with a bulkier hydrophobic side chain like Phe could lead to unfavorable steric interactions between CYP2B4 and CPR. However, the data presented in Tables 3.2 and 3.3 suggest that this is not the case since the introduction of Phe exerts almost no effect on the catalytic and reduction properties of CYP2B4. The rationale to study V267 and L270 springs from the observation that these two residues are situated in a relatively concentrated "patch" of hydrophobic residues located on the proximal site of CYP2B4 (Chapter II, Figure 2.1). Since it is believed that proteins often interact with each other at "hotspot" regions that are composed of several residues, it is possible that there exists an equivalent "patch" of hydrophobic residues in CPR. In this possible scenario, the single bond between the α- and β-carbons could allow the Phe at positions 267 or 270 to rotate freely and interact with other neutral residues present in the patch of hydrophobic residues in CPR. Thus, Phe may still interact with other hydrophobic residues on the surface of CPR and maintains a similar K_M, k_{cat} and rate of electron transfer as the WT protein.

Just like with the catalytic activity and apparent affinity, the most dramatic changes with respect to rates of electron transfer between CPR and CYP2B4 were observed with charged residues. Lys led to a modest but consistent enhancement in the rate of electron transfer while the Glu variants not only lowered the rate of electron transfer but also the extent of total reduction indicated by the A_T (Table 3.3). The agreement between the pre-steady-state results presented in Table 3.3 and those obtained under steady-state conditions (Table 3.2) strongly suggest that the perturbations observed

in K_M and k_{cat} stem from changes in the rate of electron transfer. These results therefore represent promising preliminary evidence that supports the hypothesis that modulating the maximal catalytic activity of redox-partner proteins can be achieved by enhancing the electron transfer process. This is especially encouraging in light of the numerous unsuccessful attempts by other labs to enhance catalytic activity by covalently tethering a P450 to CPR. Although these studies have been highly successful in enhancing the rate of electron transfer to levels that were not attainable in our study, the changes in catalytic activity of these engineered proteins are not proportionate to the changes in electron transfer (Fisher et al., 1992; Hayashi et al., 2000). In most cases, activity decreases significantly as a result of covalent cross-linking. This is most likely due to the observation that these covalent constructs are highly uncoupled compared to their native, untethered forms. Therefore, an obvious consequence of faster electron transfer as a result of covalent modification is an increase in autoxidation, which ultimately leads to a decrease in catalytic activity as measured by product formation.

How is it then that introduction of Lys enhances electron transfer without compromising catalytic activity? If Lys does not improve the affinity of CYP2B4 for CPR (as inferred from the K_M, Table 3.2) why does the rate of electron transfer improve? The rate of electron transfer is a function of the distance between redox partners. Dipole-dipole interactions are known to possess relatively high bond dissociation energies compared to other intermolecular interactions, e.g van der Waals. Because of this high dissociation energy, the intermolecular distance between a pair of atoms that share a charge-charge bond is likely to be short – of course, just like intramolecular bond lengths, intermolecular bond lengths are also a function of atomic radii. Since acidic residues in

the FMN domain of CPR likely form charge-charge interactions with basic residues on the proximal site of CYP2B4 including V267K and L270K, it is possible that introducing a Lys on the P450 leads to a reduction in the distance between CYP2B4 and CPR, facilitating the electron transfer process without significantly affecting protein affinity. Although speculative, this reasoning could also explain the substantial decrease in the k_{cat} observed for the V267E and L270E variants in this chapter and the R133C variant in Chapter 2, Table 2.3. If the charged residues modulated affinity, then one should be able to restore activity by using high concentrations of CPR, which would drive the binding equilibrium in the direction of complex formation. Yet, this is not the case with any of the Glu mutants. Instead, activity could not be recovered at saturating concentrations of CPR, likely because the distance between CYP2B4 and CPR was adversely and irreversibly altered as a result of either removing a basic residue or introducing an acidic residue in CYP2B4. Thus charged residues may play dual roles in controlling both protein-protein interaction affinity and interprotein distance.

References

Boddupalli SS, Pramanik BC, Slaughter CA, Estabrook RW and Peterson JA (1992) Fatty acid monooxygenation by P450BM-3: product identification and proposed mechanisms for the sequential hydroxylation reactions. *Arch Biochem Biophys* **292**:20-28.

Bridges A, Gruenke L, Chang YT, Vakser IA, Loew G and Waskell L (1998) Identification of the binding site on cytochrome P450 2B4 for cytochrome b5 and cytochrome P450 reductase. *J Biol Chem* **273**:17036-17049.

Buckle AM, Schreiber G and Fersht AR (1994) Protein-protein recognition: crystal structural analysis of a barnase-barstar complex at 2.0-A resolution. *Biochemistry* **33**:8878-8889.

Churbanova IY, Poulos TL and Sevrioukova IF (2010) Production and characterization of a functional putidaredoxin reductase-putidaredoxin covalent complex. *Biochemistry* **49**:58-67.

Deeni YY, Paine MJ, Ayrton AD, Clarke SE, Chenery R and Wolf CR (2001) Expression, purification, and biochemical characterization of a human cytochrome P450 CYP2D6-NADPH cytochrome P450 reductase fusion protein. *Arch Biochem Biophys* **396**:16-24.

de Montellano PO (2005) *Cytochrome P450 Structure, Mechanism and Biochemistry*, Plenum Publishers, New York, N.Y.

Domanski TL, He YQ, Scott EE, Wang Q and Halpert JR (2001) The role of cytochrome 2B1 substrate recognition site residues 115, 294, 297, 298, and 362 in the oxidation of steroids and 7-alkoxycoumarins. *Arch Biochem Biophys* **394**:21-28.

Fisher CW, Shet MS, Caudle DL, Martin-Wixtrom CA and Estabrook RW (1992) High-level expression in Escherichia coli of enzymatically active fusion proteins containing the domains of mammalian cytochromes P450 and NADPH-P450 reductase flavoprotein. *Proc Natl Acad Sci U S A* **89**:10817-10821.

Guengerich FP (2002) Cytochrome P450 enzymes in the generation of commercial products. *Nat Rev Drug Discov* **1**:359-366.

Hayashi K, Sakaki T, Kominami S, Inouye K and Yabusaki Y (2000) Coexpression of genetically engineered fused enzyme between yeast NADPH-P450 reductase and human cytochrome P450 3A4 and human cytochrome b5 in yeast. *Arch Biochem Biophys* **381**:164-170.

Ivkovic-Jensen MM, Ullmann GM, Young S, Hansson O, Crnogorac MM, Ejdeback M and Kostic NM (1998) Effects of single and double mutations in plastocyanin on the rate constant and activation parameters for the rearrangement gating the electron-transfer reaction between the triplet state of zinc cytochrome c and cupriplastocyanin. *Biochemistry* **37**:9557-9569.

Lin HL, Kent UM, Zhang H, Waskell L and Hollenberg PF (2003) Mutation of tyrosine 190 to alanine eliminates the inactivation of cytochrome P450 2B1 by peroxynitrite. *Chem Res Toxicol* **16**:129-136.

Miles JS, Munro AW, Rospendowski BN, Smith WE, McKnight J and Thomson AJ (1992) Domains of the catalytically self-sufficient cytochrome P-450 BM-3. Genetic construction, overexpression, purification and spectroscopic characterization. *Biochem J* **288 (Pt 2)**:503-509.

Miwa GT, West SB, Huang MT and Lu AY (1979) Studies on the association of cytochrome P-450 and NADPH-cytochrome c reductase during catalysis in a reconstituted hydroxylating system. *J Biol Chem* **254**:5695-5700.

Munro AW and Lindsay JG (1996) Bacterial cytochromes P-450. *Mol Microbiol* **20**:1115-1125.

Nash T (1953) The colorimetric estimation of formaldehyde by means of the Hantzech reaction. *Biochem J* **55**:416-421.

Omura T and Sato R (1964) The Carbon Monoxide-Binding Pigment of Liver Microsomes. Ii. Solubilization, Purification, and Properties. *J Biol Chem* **239**:2379-2385.

Ost TW, Clark J, Mowat CG, Miles CS, Walkinshaw MD, Reid GA, Chapman SK and Daff S (2003) Oxygen activation and electron transfer in flavocytochrome P450 BM3. *J Am Chem Soc* **125**:15010-15020.

Pearl NM, Jacobson T, Meyen C, Clementz AG, Ok EY, Choi E, Wilson K, Vitello LB and Erman JE (2008) Effect of single-site charge-reversal mutations on the catalytic properties of yeast cytochrome c peroxidase: evidence for a single, catalytically active, cytochrome c binding domain. *Biochemistry* **47**:2766-2775.

Schreiber G (2002) Kinetic studies of protein-protein interactions. *Curr Opin Struct Biol* **12**:41-47.

Schreiber G and Fersht AR (1996) Rapid, electrostatically assisted association of proteins. *Nat Struct Biol* **3**:427-431.

Schreiber G, Haran G and Zhou HX (2009) Fundamental aspects of protein-protein association kinetics. *Chem Rev* **109**:839-860.

Selzer T, Albeck S and Schreiber G (2000) Rational design of faster associating and tighter binding protein complexes. *Nat Struct Biol* **7**:537-541.

Sevrioukova IF, Poulos TL and Churbanova IY (2010) Crystal structure of the putidaredoxin reductase x putidaredoxin electron transfer complex. *J Biol Chem* **285**:13616-13620.

Shen S and Strobel HW (1992) The role of cytochrome P450 lysine residues in the interaction between cytochrome P450IA1 and NADPH-cytochrome P450 reductase. *Arch Biochem Biophys* **294**:83-90.

Shet MS, Fisher CW, Holmans PL and Estabrook RW (1993) Human cytochrome P450 3A4: enzymatic properties of a purified recombinant fusion protein containing NADPH-P450 reductase. *Proc Natl Acad Sci U S A* **90**:11748-11752.

Tetreault M, Cusanovich M, Meyer T, Axelrod H and Okamura MY (2002) Double mutant studies identify electrostatic interactions that are important for docking cytochrome c2 onto the bacterial reaction center. *Biochemistry* **41**:5807-5815.

Vermilion JL and Coon MJ (1978) Purified liver microsomal NADPH-cytochrome P-450 reductase. Spectral characterization of oxidation-reduction states. *J Biol Chem* **253**:2694-2704.

Xiong P, Nocek JM, Griffin AK, Wang J and Hoffman BM (2009) Electrostatic redesign of the [myoglobin, cytochrome b5] interface to create a well-defined docked complex with rapid interprotein electron transfer. *J Am Chem Soc* **131**:6938-6939.

Xiong P, Nocek JM, Vura-Weis J, Lockard JV, Wasielewski MR and Hoffman BM (2010) Faster interprotein electron transfer in a [myoglobin, b] complex with a redesigned interface. *Science* **330**:1075-1078.

Zhang H, Im SC and Waskell L (2007) Cytochrome b5 increases the rate of product formation by cytochrome P450 2B4 and competes with cytochrome P450 reductase for a binding site on cytochrome P450 2B4. *J Biol Chem* **282**:29766-29776.

Chapter IV

Interactions Between CYP2E1 and CYP2B4: Effects on Affinity for NADPH-cytochrome P450 Reductase and Substrate Metabolism

Abstract

Studies in both microsomal and reconstituted systems have shown that the presence of one P450 isoform can significantly influence the catalytic activity of another isoform. In this study, we assessed whether CYP2E1 could influence the catalytic properties of CYP2B4 under steady-state turnover conditions. The results show that CYP2E1 inhibits CYP2B4-mediated metabolism of benzphetamine (BNZ) with a K_i of 0.05 μM. However, CYP2B4 is not an inhibitor of CYP2E1-mediated p-nitrophenol hydroxylation. When these inhibition studies were performed with the artificial oxidant tert-butyl hydroperoxide, CYP2E1 did not inhibit CYP2B4 activity. Determinations of the apparent K_M and k_{cat} of CYP2B4 for CPR in the presence of increasing concentrations of CYP2E1 revealed a mixed competitive inhibition of CYP2B4 by CYP2E1. At low concentrations of CYP2E1, the apparent K_M of CYP2B4 for CPR increased up to 13-fold with virtually no change in k_{cat}, however, at higher concentrations of CYP2E1, the K_M of CYP2B4 for CPR decreased to levels similar to those observed in the absence of CYP2E1 and the k_{cat} also decreased by 10-fold. Additionally, CYP2E1 increased the apparent K_M of CYP2B4 for BNZ by 8-fold and the K_M did not decrease to its original value when saturating concentrations of CPR were used. While the individual K_M values of CYP2B4 and

CYP2E1 for CPR are virtually identical, the apparent K_M of CYP2E1 for CPR in the presence of CYP2B4 decreased significantly, thus suggesting that CYP2B4 enhances the affinity of CYP2E1 for CPR and this may allow CYP2E1 to out-compete CYP2B4 for CPR.

Introduction

In order to interrogate the catalytic properties of only the P450 under investigation, the majority of studies performed in reconstituted systems are generally conducted using saturating, or nearly saturating concentrations of CPR; however, in the endoplasmic reticulum (ER), P450s exist in vast excess (up to 20-fold) over CPR (Cawley et al., 1995; Backes and Kelley, 2003). Despite the plethora of information regarding the mechanisms by which CPR reduces P450s, very little is known about the spatial organization and interactions of the cytochromes (P450 and b_5) and flavoproteins (CPR and cytochome b_5 reductase) within the membrane of the ER.

Several models have been proposed to describe the distribution of P450s and their redox partners (CPR and cytochrome b_5) in the lipid membrane of the ER (Peterson et al., 1976; Backes and Kelley, 2003; Brignac-Huber et al., 2011). For example, it has been proposed that the N-terminal hydrophobic tail of CPR firmly anchors it in the membrane while its catalytic domain protrudes from the membrane into the cytosolic region of the cell. In this model, several P450's are envisioned to cluster around a central CPR molecule while a portion of the microsomal P450s are thought to be loosely associated with the CPR and may even be free-floating in the membrane matrix (Peterson et al., 1976). The disparity in the P450:CPR ratio combined with the likely organization of these microsomal proteins in the membrane suggests that at any given time only a portion

of the total microsomal P450s can be in functional complexes with CPR and thus capable of catalyzing the metabolism of drugs. For that reason, the outcome of the metabolism of a drug in a given tissue may not only be a function of the particular P450 that metabolizes the drug, but also its accessibility to CPR, which may be influenced by the presence and abundance of other P450s in the ER that may compete for the CPR (Eyer and Backes, 1992).

There have been a number of reports on the interaction of P450s not only with CPR but also with each other, leading to alterations in catalytic activity. For example, CYP3A4-mediated 6β-hydroxylation of testosterone is reported to be enhanced up to four-fold in the presence of human, rat and rabbit CYP1A2, although the extent of catalytic stimulation varied significantly depending on the species (Yamazaki et al., 1997). Interactions between the P450s have also been reported for several other major P450s including CYP2D6 and CYP2C9 (Subramanian et al., 2009). Specifically, coincubation of CYP2D6 with CYP2C9 resulted in a 50% decrease in the V_{max} for CYP2C9-mediated hydroxylation of flurbiprofen with almost no change in the K_M. In order to investigate the cause of the inhibition at the presteady-state level, the K_s of CYP2C9 for flurbiprofen was measured in the absence and presence of CYP2D6. The results showed that CYP2D6 increased the K_s of flurbiprofen for CYP2C9 by approximately 20-fold suggesting that the CYP2D6-mediated perturbation in CYP2C9 affinity for substrate results from conformational changes in the active site architecture of CYP2C9 (Subramanian et al., 2009). The physiological implications and relevance of such interactions have also been investigated. For example, CYP2C19 has been shown to be more active than CYP2C9 for the metabolism of methoxychlor in the purified

reconstituted system (Hazai and Kupfer, 2005). However, when the role of CYP2C19 in the metabolism of methoxychlor was assessed in human liver microsomes (HLM), by using monoclonal antibodies raised against CYP2C19, there was no change in methoxychlor metabolism, yet antibodies raised against CYP2C9 were efficient in inhibiting methoxychlor-O-demethylation (Hu et al., 2004). When the metabolism of methoxychlor was assessed in a reconstituted system containing both CYP2C9 and CYP2C19, the demethylation of methoxychlor by CYP2C19 was significantly inhibited, suggesting that interactions among P450 isoforms can modulate their catalytic activities and thereby confound *in vitro – in vivo* drug metabolism correlation predictions. In addition to the interactions between the P450 isoforms mentioned above, evidence also exists to support interactions between other P450s including CYP2B4 and CYP1A2 (Cawley et al., 1995; Backes et al., 1998; Cawley et al., 2001), CYP1A2 and CYP2E1 (Kelley et al., 2006), and CYP2C9 and CYP3A4 (Subramanian et al., 2010).

Among the many human P450s, CYP2E1 and CYP2B6 are known to play important roles in liver toxicity and drug metabolism, respectively. CYP2E1 is able to bioactivate low molecular weight compounds such as acetaminophen (Patten et al., 1993), N-ethyl nitrosamine (Levin et al., 1986) and carbon tetrachloride (Guengerich et al., 1991) into reactive metabolites that lead to chemical toxicity. Furthermore, CYP2E1 is known to be a highly uncoupled P450 and the induction of CYP2E1 by alcohol (Oneta et al., 2002) or fasting (Johansson et al., 1988) likely contributes to an increase in the generation of reactive oxygen species, which ultimately can lead to oxidative stress (Dey and Cederbaum, 2006). On average, CYP2B6 constitutes approximately 5% of the total P450 in the liver and plays an important role in the metabolism of a number of clinically

used drugs including bupropion, cyclophosphamide, efavirenz, and propofol (Walsky et al., 2006; Wang and Tompkins, 2008). It's highly polymorphic nature is of great importance in drug development, as differences in amino acid composition are known to affect drug efficacy and toxicity. However, the current heterologous expression system for recombinant human CYP2B6 in *E.coli* suffers from very low yield; therefore, the more highly expressing rabbit CYP2B4 (Scott et al., 2001; Oezguen et al., 2008), which shares approximately 80% sequence similarity with CYP2B6 and whose three-dimensional structure was recently shown to be virtually identical to that of CYP2B6 (Gay et al., 2010), may be used as a model system to better understand CYP2B6.

Although P450s CYP2E1 and CYP2B6 have been studied extensively for their individual roles in metabolism and toxicity, very little is known about how they may interact with each other to modulate each other's catalytic activity. Therefore, the objective of this study was to assess in a purified reconstituted system whether CYP2E1 and CYP2B4 could influence each other's catalytic activities, to characterize the kinetic nature of such interactions and to propose a preliminary model that explains the physical basis for the kinetic results.

Materials and Methods

Chemicals. All chemicals used are of ACS reagent grade unless otherwise specified and were obtained from commercial vendors. Benzphetamine (BNZ), p-nitrophenol (p-NP), NADPH, sodium dithionite, ascorbic acid and tert-butyl hydroperoxide were purchased from Sigma. Trifluoroacetic acid was purchased from Pierce Chemicals. Dilauroylphosphatidylcholine (DLPC) was purchased from Doosan

Serdary Research Laboratory (Toronto, Canada). Carbon monoxide gas (purity >99.5%) was purchased from Cryogenic Gases (Detroit, MI).

Construction of CYP2E1 Y422D variant. Site-directed mutagenesis was performed using a QuikChange site-directed mutagenesis kit according to the manufacturer's protocol (Stratagene). The forward and reverse mutagenic primers for Y422D were GGAAAGTTCAAGGACAGTGACTATTTCAAGCC and GGCTTGAAATAGTCACTGTCCT TGAACTTTCC, respectively. DNA sequencing performed at the University of Michigan DNA Sequencing Core confirmed the desired site-specific mutation.

Overexpression and Purification of Enzymes. The plasmids for the N-terminal truncated and C-terminal His-tagged CYP2B4dH (hereon referred to as CYP2B4) and human CYP2E1 were a generous gift from Dr. James Halpert. These two P450s and the CYP2E1 Y422D variant were over-expressed in *Escherichia coli* C41 (DE3) cells separately and purified using a Ni-NTA affinity column as described previously (Scott et al., 2003; Pratt-Hyatt et al., 2010). The concentrations of CYP2B4 and CYP2E1 were determined using an extinction coefficient of$\Delta\ \varepsilon_{450\text{-}490\ nm}$ of 91 mM cm^{-1} for the reduced CO-complex as described by Omura and Sato (Omura and Sato, 1964). NADPH-dependent cytochrome P450 reductase (CPR) was expressed and purified from *Escherichia coli* as described previously (Zhang et al., 2007). The concentration of CPR was determined using an extinction coefficient of 21 mM cm^{-1} at 456 nm for the oxidized enzyme (Vermilion and Coon, 1978).

Determination of the Inhibition of CYP2B4-Mediated N-demethylation of BNZ by CYP2E1 WT and the CYP2E1 Y422D Variant. The extent to which varying concentrations of either CYP2E1 WT or CYP2E1 Y422D inhibited the rate of formaldehyde formation by CYP2B4 (0.25 μM) was assessed at 37^{o}C using a fixed concentration of CPR and BNZ. CYP2B4 was reconstituted in triplicate with increasing concentrations of CYP2E1 WT or CYP2E1 Y422D (0.25, 0.5, 0.75, 1.0, 1.25, 1.50 μM), CPR (0.5 μM) and 0.03 mg/ml DLPC on ice for 1 h. The reconstituted mixtures were then added to 50 mM potassium phosphate buffer, pH 7.4, and BNZ (1.2 mM). After the samples were equilibrated at 37 ^{o}C for 15 min, the reactions were initiated by adding 7.5 μL of 20 mM NADPH to give a final reaction volume of 500 μL. The reactions were incubated for 5 min at 37 ^{o}C and then quenched by the addition of 25 μL of 50% TFA. The proteins were precipitated by centrifugation at 13.2k rpm in an Eppendorf 5415D microcentrifuge for 5 min and a 500 μL aliquot of the supernatant was assayed for formaldehyde using the Nash reaction(Nash, 1953).

Difference Spectra of the Carbon-Monoxy Ferrous WT CYP2E1 and Y422D Variant. WT CYP2E1 and the Y422D mutant (0.5 nmol) were reconstituted with CPR (1 nmol) at 22 °C for 30 min in 0.5 ml of suspension buffer (100 mM potassium phosphate buffer, 20% glycerol and 0.1 mM EDTA, pH 7.4). After adding 100 μM 4-methylpyrazole and 0.5 mM NADPH for the baseline, the samples were bubbled with CO, and the visible absorbance spectra were determined by scanning from 400 to 500 nm on a UV-2501PC spectrophotometer (Shimadzu Corporation, Kyoto, Japan) until a

steady-state was attained. A trace amount of sodium dithionite was added and additional scans were performed until no further changes were observed.

Determination of the Apparent K_M and k_{cat} Values for CYP2B4 for CPR Using the N-demethylation of BNZ in the Presence and Absence of CYP2E1. The K_M and k_{cat} values for CYP2B4 WT for CPR were determined at 37 ^oC by measuring the rate of formaldehyde formation as a result of the N-demethylation of benzphetamine at a constant P450 concentration with increasing concentrations of CPR as previously described (Kenaan et al., 2011). Briefly, CYP2B4 WT (0.25 µM) was reconstituted in triplicate with varying concentrations of CPR (0.1, 0.2, 0.3, 0.6, 0.8, 1.2 and 1.4 µM) and 0.03 mg/ml DLPC on ice for 1 h. The reconstituted mixtures were then added to 50 mM potassium phosphate buffer, pH 7.4, containing 1.2 mM BNZ. After the samples were equilibrated at 37 ^oC for 15 min, the reactions were initiated by adding 7.5 µL of 20 mM NADPH to give a final reaction volume of 500 µL. The reactions were incubated for 5 min at 37 ^{o} C and then quenched by the addition of 25 µL of 50% TFA. The proteins were precipitated by centrifugation at 13.2k rpm in an Eppendorf 5415D microcentrifuge for 5 min and a 500 µL aliquot of the supernatant was assayed for formaldehyde using the Nash reaction. The kinetic parameters were determined by fitting the data to the Michaelis-Menten equation using GraphPad Prism 5.0 from GraphPad software (La Jolla, CA). To determine the effect of CYP2E1 on the apparent K_M and k_{cat} of the CYP2B4 – CPR complex, the procedure outlined above was repeated in the presence of 0.125, 0.25, 0.75, 1.25, and 1.50 µM CYP2E1.

Graphical Analysis of Steady-State Activity Data. Using GraphPad Prism the inverse of the reaction velocities obtained for the determination of the apparent K_M and k_{cat} values for CYP2B4 and CPR were plotted against the inverse of the concentrations of CPR used in the presence of varying concentrations of CYP2E1 to obtain a Lineweaver-Burk plot. To obtain a K_i for CYP2E1 as a competitive inhibitor of the CYP2B4 – CPR complex, two methods were used. The first employed a non-linear global fitting analysis of the data to a mixed inhibition model using GraphPad Prism, and the second involved plotting $K_{M\ obs}$ against varying concentrations of CYP2E1 (0 – 0.75 μ). The K_i was obtained from the *x*-intercept of a linear regression analysis of this data (Kakkar et al., 1999).

Characterization of the tert-Butyl Hydroperoxide-supported Metabolism of BNZ by CYP2B4 WT in the Presence of Increasing Concentrations of CYP2E1 WT. To determine the rates for the tert-butyl hydroperoxide–supported metabolism of BNZ, a final concentration of 0.25 μM CYP2B4 WT was incubated with 0.03 mg/ml DLPC, 50 mM potassium phosphate buffer, pH 7.4, and 1.2 mM BNZ at 37 ^{o}C for 15 min. tert-Butyl hydroperoxide (52.5 μL of 1 M solution) was added to give a final volume of 500 μL and the reactions were incubated for 5 min and then terminated by the addition of 25 μL of 50% TFA. The samples were centrifuged at 13.2k rpm in an Eppendorf 5415D microcentrifuge for 5 min and 500 μL aliquots of the supernatants were assayed for formaldehyde using the Nash reaction. This procedure was then performed in the presence of 0.25, 0.5, 0.75, 1.0, 1.25, 1.50 μM CYP2E1 WT.

Determination of the K_M and k_{cat} Values for the Metabolism of BNZ by CYP2B4 in the Presence and Absence of CYP2E1 WT. The K_M and k_{cat} values for BNZ metabolism by CYP2B4 in the presence or absence of CYP2E1 were determined at 37 ^oC at constant P450 and CPR concentrations with increasing concentrations of benzphetamine. CYP2B4 WT (0.50 μM) was reconstituted in triplicate with an equal concentration of CPR and 0.03 mg/ml DLPC with or without 2 μM of CYP2E1 WT on ice for 1 h. The reconstituted mixtures were then added to 50 mM potassium phosphate buffer, pH 7.4, containing varying concentrations of BNZ (0.05, 0.1, 0.2, 0.4, 0.6, 0.8 μM). After the samples were equilibrated at 37^o C for 15 min, the reactions were initiated by adding 7.5 μL of 20 mM NADPH to give a final reaction volume of 500 μL. The reactions were incubated for 5 min at 37 ^{o} C and then quenched by the addition of 25 μL of 50% TFA. The protein was precipitated by centrifugation at 13.2k rpm in an Eppendorf 5415D microcentrifuge for 5 min and a 500 μL aliquot of the supernatant was assayed for formaldehyde using the Nash reaction. To determine whether the original K_M value in the absence of CYP2E1 could be observed by using saturating concentrations of CPR, this experiment was repeated in the presence of 2.5 μM CPR. The kinetic parameters were determined by fitting the data to the Michaelis-Menten equation using GraphPad Prism 5.0.

Spectral Dissociation Constant (K_s) for the Binding of BNZ to CYP2B4 in the Presence and Absence of CYP2E1. BNZ binding to ferric CYP2B4 was monitored spectrophotometrically as previously described by measuring the type I spectral changes (Zhang et al., 2009). Briefly, an equal volumes of the P450 solution containing 1 μM CYP2B4 in the presence or absence of 4 μM CYP2E1, 0.1 M potassium phosphate buffer

(pH 7.4) and 0.1 mg/ml DLPC were added to the sample and reference cuvettes in a UV-2501PC spectrophotometer (Shimadzu Corporation, Kyoto, Japan). A baseline was recorded after thermal equilibration at 30 ^{o}C for 5 min. CYP2B4 in the sample cuvette was titrated with aliquots of 20 mM BNZ while an equal volumes of water were added to the reference cuvette. The difference spectra were recorded from 350-500 nm, and the difference in absorbance between the wavelength maximum (386 nm) and minimum (421 nm) was plotted as a function of varying BNZ concentration (5 – 1200 μM). The data were then fit to Equation 1 to obtain the K_s.

$$\Delta A = \frac{\Delta A_{max} \times [BNZ]}{K_s + [BNZ]} \qquad \text{Eq. 1}$$

Determination of the Apparent K_M and k_{cat} Values of CYP2E1 for CPR using the Hydroxylation of p-NP in the Presence and Absence of CYP2B4. Saturating concentrations of p-NP, a fixed concentration of CYP2E1 and various concentrations of CPR were used to determine the apparent K_M and k_{cat} of CYP2E1 for CPR. CYP2E1 (0.1 μM) was reconstituted with varying concentrations of CPR (0.08, 0.12, 0.24, 0.72, 1.44, 2.00 μM) and 0.03 mg/ml DLPC in the presence or absence of 0.1 μM CYP2B4 on ice for 1 hr. The reconstituted mixtures were then added to 50 mM potassium phosphate buffer, pH 7.4, containing 0.3 mM p-NP and 2 mM ascorbic acid. After the samples were equilibrated at 37 ^{o}C for 15 min, the reactions were initiated by adding 20 μL of 20 mM NADPH to give a final reaction volume of 1000 μL. The reactions were incubated for 20 min at 37 ^{o}C before they were quenched with 300 μL 20% TCA. The samples were then incubated on ice for 10 min and centrifuged at 13.2k rpm in an Eppendorf 5415D microcentrifuge for 5 min. The absorbance at 510 nm was then measured by transferring

a 1000 μL aliquot of the reaction mixture to a cuvette containing 100 μL of 10 M NaOH.

Results

Effect of Increasing Concentrations of CYP2E1 on BNZ Metabolism by CYP2B4. In order to preclude the possibility that CYP2E1 metabolizes BNZ to form formaldehyde, or any other detectable product, the metabolism of BNZ by CYP2E1 was assessed using previously established methods (Kent et al., 2004). Our results showed that CYP2B4 metabolizes BNZ primarily to nor-benzphetamine and that metabolism by CYP2E1 is negligible compared to CYP2B4, even at high concentrations of CYP2E1 (data not shown). Conversely, CYP2E1 metabolizes p-NP relatively well whereas CYP2B4 shows very little activity towards p-NP, even at high concentrations (data not shown). Therefore, these control experiments demonstrate that the N-demethylation of BNZ activity to form formaldehyde and the hydroxylation of p-NP to form 4-NC are specific reporters of CYP2B4 and CYP2E1 activity, respectively in this system.

To assess the extent to which CYP2E1 could inhibit the catalytic activity of CYP2B4 toward its probe substrate (BNZ) under conditions of constant CPR, a series of concentrations of CYP2E1 were included with CYP2B4, CPR and DLPC. The results shown in Figure 4.1A illustrate that large concentrations of CYP2E1 can inhibit the activity of CYP2B4 up to approximately 80% of the activity observed in the absence of CYP2E1. The data can be fit to a rectangular hyperbolic function and are consistent with saturation kinetics. In order to determine whether the decrease in the CYP2B4 catalytic activity is due to a disruption of the interaction between CYP2B4 and CPR or to direct

interaction between CYP2B4 and CYP2E1, the catalytic activity of CYP2B4 for BNZ supported by tBHP was determined in the presence of increasing concentrations of CYP2E1. Although CYP2B4 exhibited a significant decrease in activity when titrated with CYP2E1, when BNZ demethylation was supported by tBHP, CYP2B4 was virtually resistant to inhibition by CYP2E1. Since hydroperoxides and other artificial oxygen donors are able to support substrate metabolism by P450s in the absence of redox partners such as CPR, the decrease in the CPR-supported BNZ activity with no change in the tBHP-supported activity suggests that inhibition is not due to direct CYP2B4-CYP2E1 interactions but rather due to an effect on the CPR-CYP2B4 interaction. The ability of CYP2B4 to inhibit or stimulate the metabolism of p-NP by CYP2E1 was also investigated and the results shown in Figure 4.1B demonstrate that CYP2B4 does not have any significant effect on the catalytic activity of CYP2E1. Therefore, the inhibition observed in the reconstituted system is solely due to an effect of CYP2E1 on CYP2B4 which is not reciprocated.

A.

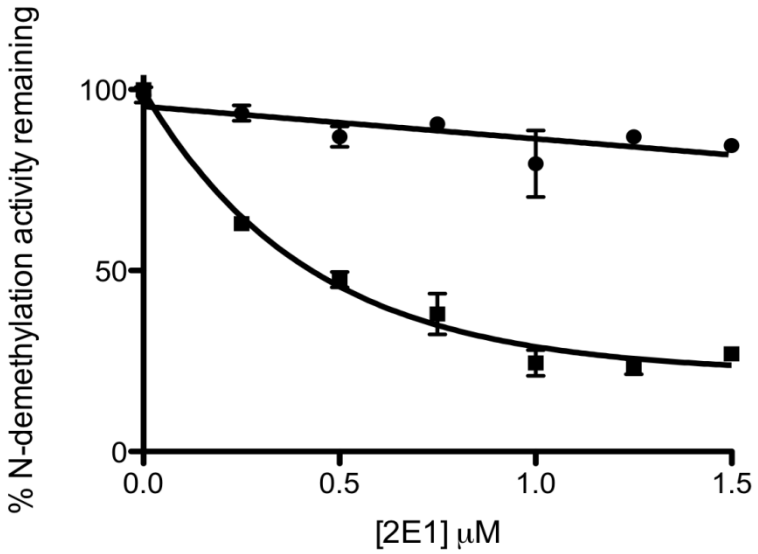

B.

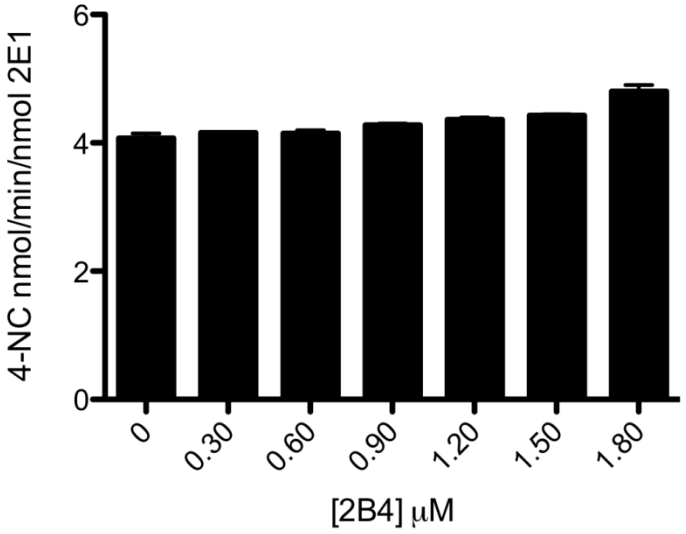

Figure 4.1. A. Effect of Increasing Concentrations of CYP2E1 on CYP2B4-catalyzed N-demethylation of BNZ. BNZ N-demethylation activity supported by t-BHP (•) and CPR/NADPH (■) was determined as described in Materials and Methods in attempts to differentiate the effect of direct CYP2E1-CYP2B4 interactions on CYP2B4 activity from competition for CPR as described in Materials and Methods. Excess BNZ (1.2 mM) was used in the incubations to compensate for possible perturbations in substrate binding affinity due to direct P450-P450 interactions. **B. Effect of Increasing Concentrations of CYP2B4 on CYP2E1-catalyzed p-NP hydroxylation.** To determine whether inhibition of CYP2B4 was observed with CYP2E1, the CYP2E1-catalyzed hydroxylation of p-NP was assessed in the presence of increasing concentrations of CYP2B4 and excess concentrations of p-NP. Data points for BNZ and p-NP metabolism represent the mean of three experiments, done at least in duplicate, while error bars represent the standard deviations.

Inhibition of CYP2B4 activity by the CYP2E1 Y422D variant. Previous studies by Lin et al. (Lin et al., 2007) led us to express and purify the CYP2E1 Y422D mutant in order to dissect out whether the inhibitory phenomenon observed in Figure 4.1 A was due to the CYP2E1 – CPR interaction. The Y422 residue of CYP2E1 can be nitrated by peroxynitrite and its modification results in a loss in the CPR-supported CYP2E1 activity when compared to tBHP-supported activity (Lin et al., 2007). Since the FMN domain of CPR, which is highly negatively charged, is believed to interact with the proximal side of CYP2E1, we hypothesized that replacing Tyr 422 with Asp using site-directed mutagenesis would create a charge repulsive interaction between the CYP2E1 Y422D and its residue counterpart in CPR that would perturb the apparent affinity of the two proteins for each other. Using stopped-flow studies we have previously shown that the extent of reduced CO-complex formation upon addition of NADPH is an indicator of the extent of formation of the P450-CPR complex and thus, it reflects the affinity of the P450 under investigation for CPR(Kenaan et al., 2011). The extent of reduction of the CYP2E1 Y422D mutant by CPR and NADPH relative to the reduction of WT CYP2E1 by CPR and NADPH can be determined by measuring the absorbance of Y422D-CO complex at 450 nm and comparing this to the absorbance of the WT-CO complex at the same wavelength. As shown in Figure 4.2A, the interaction of CYP2E1 Y422D with CPR

A.

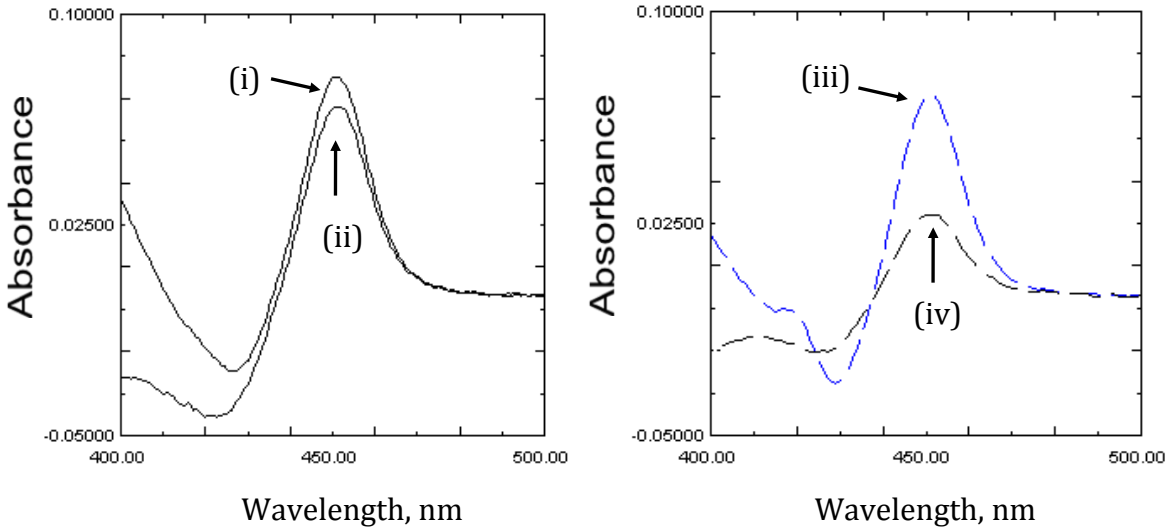

B.

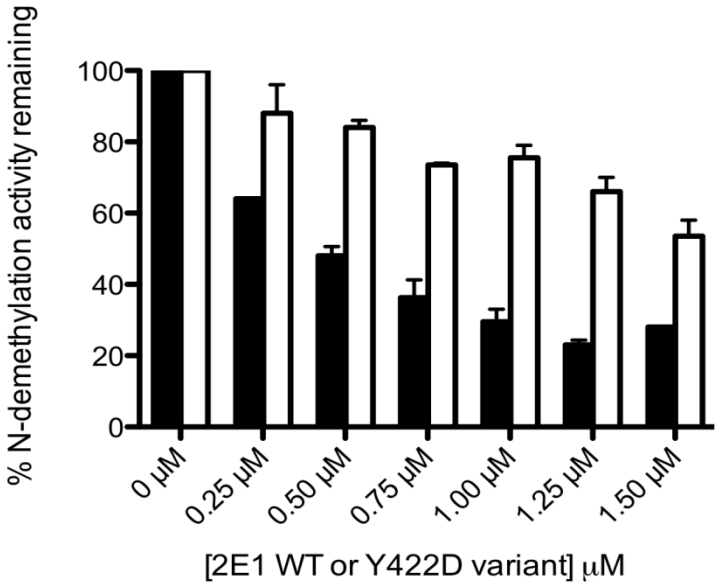

Figure 4.2. Effects of the Mutation of Y422 to D in CYP2E1 on its Ability to form the Reduced-CO Complex when Reduced with NADPH and for CYP2E1 WT or the Y422D Variant to Inhibit CYP2B4 Activity. A. Reduced CO spectrum of WT CYP2E1 (left panel) and CYP2E1 Y422D variant (right panel). The reduced CO difference spectra were measured in the following reconstitutions as described in Materials and Methods. Samples (i) and (iii) were chemically reduced with dithionite while samples (ii) and (iv) were reconstituted with CPR and reduced by the addition of NADPH. **B. Inhibition of CYP2B4 BNZ Activity by CYP2E1 WT and the Y422D Variant.** The ability of the Y422D variant was assessed with regard to its ability to inhibit CYP2B4 activity (open bars) and compared to WT CYP2E1 (filled bars) as described in Materials and Methods.

decreases by 50% compared to WT. Interestingly, when the inhibitory potential of this mutant for CYP2B4 was investigated, the results showed that it inhibited CYP2B4 activity to a significantly lesser extent than the WT CYP2E1 (Figure 4.2B).

Determination of the K_M and k_{cat} Values for the Interactions of CYP2B4 WT with CPR. Formation of a CPR-P450 complex is essential for the transfer of electrons to the heme that is required for substrate oxidation. The rate of substrate oxidation is believed to be directly proportional to the concentration of the CPR-CYP2B4 complex (Miwa et al., 1979; Bridges et al., 1998). Thus, by measuring the rate of BNZ oxidation in the presence of a fixed concentration of CYP2B4 and various concentrations of CPR, apparent K_M and k_{cat} values for CPR binding to CYP2B4 can be determined across a range of CYP2E1 concentrations. By comparing these kinetic parameters with various concentrations of CYP2E1, we can investigate the nature of the inhibitory interactions observed in Figure 4.1A. The competition between CYP2E1 and CYP2B4 for CPR should disrupt CYP2B4-CPR complex formation and decrease the concentration of complexed CYP2B4 that is able to oxidize BNZ. As shown in Figure 4.3, the rate of BNZ oxidation as a function of varying CPR concentrations follows a rectangular hyperbolic relationship which can be fit to the Michaelis-Menten equation. For CYP2E1 concentrations ranging from 0.125 – 0.75 μM, the apparent K_M of CYP2B4 for CPR increased by 14 fold while the k_{cat} remained virtually unchanged (Figure 4.3 and Table 4.1). For concentrations higher than 0.75 μM CYP2E1, an unusual non-competitive

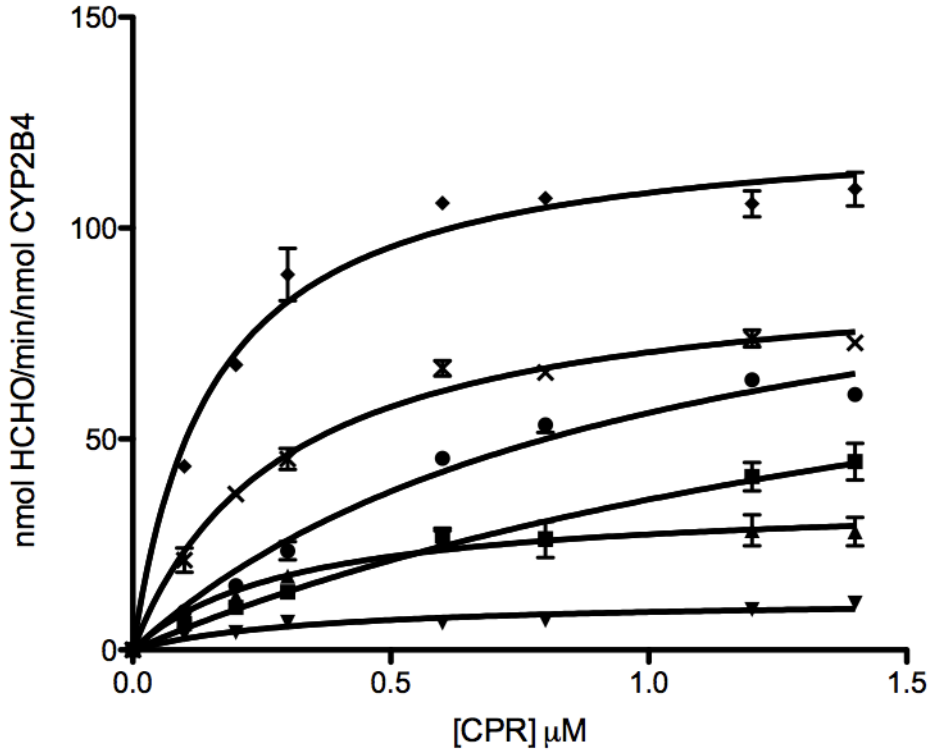

Figure 4.3. Determination of the Kinetics for the N-demethylation of BNZ by CYP2B4 in the Presence of Increasing Concentrations of CYP2E1 WT. The N-demethylation of BNZ to produce formaldehyde (HCHO) was measured at a constant concentration of CYP2B4 (0.2 μM) with increasing concentrations of CPR and the following concentrations of CYP2E1 WT: 0 (◆), 0.125 (**X**), 0.25 (●), 0.75 (■), 1.25 (▲), 1.50 μM (▼) as described under Materials and Methods. Error bars are the standard deviations from three measurements done at least in triplicate.

[2E1] μM	K_M (μM)	k_{cat} (min^{-1})
0	0.16±0.020	130±3.9
0.125	0.29±0.028	91±2.8
0.25	0.99±0.180	110±11
0.75	2.1±0.73	110±26
1.25	0.31±0.078	36±3.0
1.50	0.36±0.11	12±1.3

Table 4.1. K_M and k_{cat} values of CYP2B4 for CPR in the presence of increasing concentrations of CYP2E1 WT. The K_M and k_{cat} values of CYP2B4 for CPR were determined as described under Materials and Methods. Since CYP2E1 does not metabolize BNZ, the kinetic parameters for CPR binding to CYP2B4 could be determined by measuring the rate of formaldehyde formation using fixed concentrations of CYP2B4 and BNZ with increasing concentrations of CPR and CYP2E1. The kinetic values given here were derived from data as plotted in Figure 4.3.

kinetic behavior was observed with a 10-fold decrease in k_{cat} that was accompanied by a decrease in the apparent K_M value to 0.36 μM in the presence of 1.50 μM of CYP2E1.

Linear Regression Analysis of the Steady-state Activity Data. By plotting the inverse of the BNZ activity against the inverse of CPR concentrations as a function of varying CYP2E1 concentrations it was observed that this data could be divided into two sets (Figure 4.4). These data sets were grouped based on whether the linear regression analysis resulted in an intersection at a common value on the y-axis but diverged on the *x*-axis or whether the lines diverged on the y-axis and intersected on the *x*-axis. The data shown in Figure 4.4A clearly demonstrate that between 0 – 0.75 μM CYP2E1 the apparent K_M values change significantly while the k_{cat} values remain almost unchanged. This is indicative of a competitive interaction. Figure 4.4B illustrates the non-competitive nature of CYP2E1 inhibition as the apparent K_M values for 1.25 and 1.50 μM CYP2E1 are relatively similar to the K_M value observed in the absence of CYP2E1, yet the k_{cat} decreases significantly as evidenced by an increase in the y-intercept value compared to 0 μM CYP2E1. Therefore, under our experimental conditions it appears that CYP2E1 inhibits the formation of the CYP2B4-CPR complex by acting as a competitive inhibitor at low concentrations and as a noncompetitive inhibitor at higher concentrations.

To estimate a K_i for CYP2E1 as a competitive inhibitor of the CYP2B4-CPR complex we plotted the $K_{M\ obs}$ as a function of CYP2E1 concentration (Kakkar et al., 1999). These data were fit to a straight line that intersected the *x*-axis at an absolute value of 0.05 μM (Figure 4.5). Therefore, CYP2E1 is a potent CYP2B4 competitive inhibitor with a nanomolar affinity.

A. **B.**

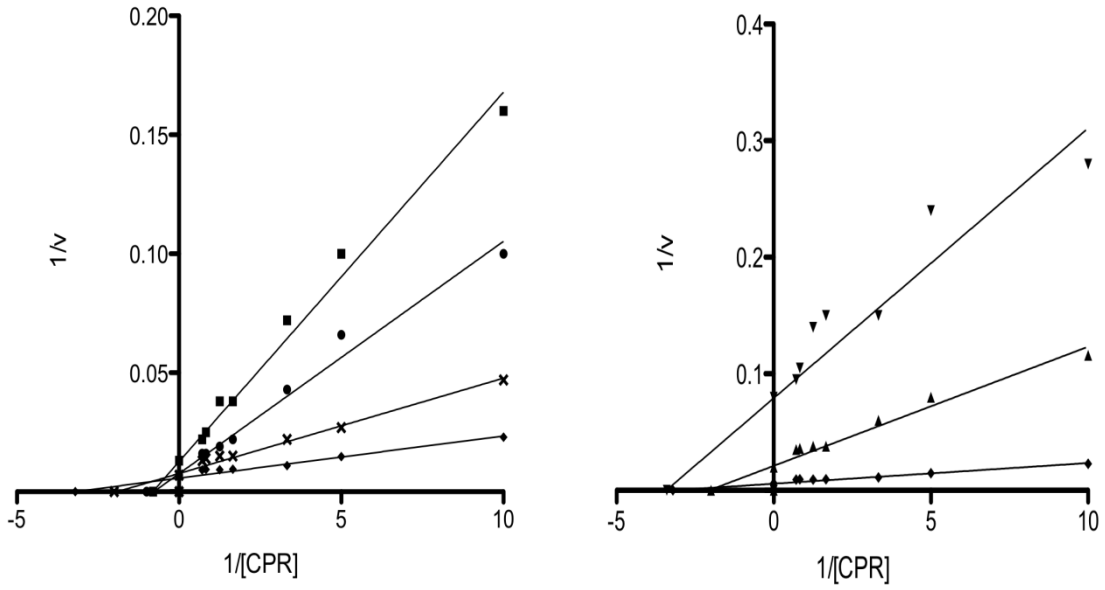

Figure 4.4. Lineweaver-Burk Plots of the Steady-state Activity Data Presented in Figure 4.3. The inverse of the rate of formaldehyde formation was plotted against the inverse of CPR concentrations (from Figure 4.3) as a function of varying CYP2E1 concentrations as indicated. These data were divided into two sets based on whether the linear regressions intersected at a common intercept or not. For the following concentrations of CYP2E1 WT: 0 (◆), 0.125 (**X**), 0.25 (●), 0.75 μM (■), CYP2E1 displayed competitive inhibition kinetics **(A)** while at higher concentrations, 1.25 (▲) and 1.50 μM (▼), CYP2E1 behaved as a noncompetitive inhibitor **(B)**.

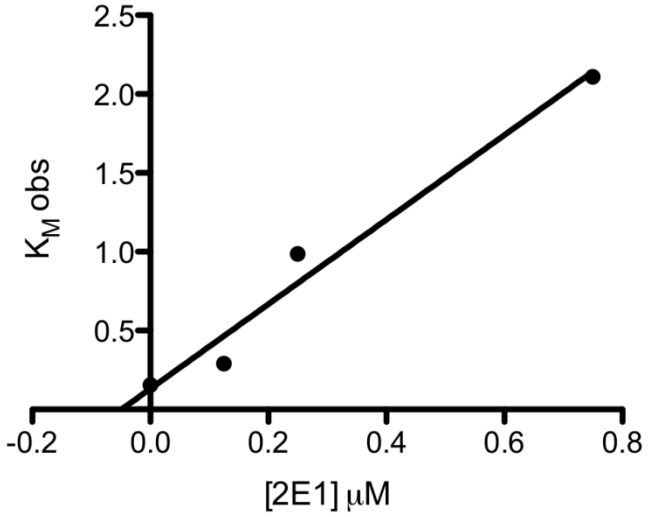

Figure 4.5. Plot of $K_{M\ obs}$ versus CYP2E1 Concentration used to Estimate the Inhibition Constant, K_i. Estimates of $K_{M\ app}$ were obtained from analysis of the activity data shown in Figure 4.3. The solid line is the linear regression analysis of data for CYP2E1 concentrations from 0 – 0.75 μM. The absolute value of the *x*-intercept of the line represents K_i (ca., 50 nM).

Steady-state activity of CYP2B4 for the Metabolism of BNZ in the Presence and Absence of CYP2E1. Previous reports have suggested an interplay between redox partner affinity and substrate affinity for P450s (French et al., 1980; Bonfils et al., 1981). Since the binding affinity of BNZ to CYP2B4 may be enhanced by the interaction between CYP2B4 and CPR (and vice-versa) we hypothesized that a perturbation in the formation of the CYP2B4-CPR complex by CYP2E1might lead to changes in the kinetic parameters of CYP2B4 for BNZ. The K_M and k_{cat} of CYP2B4 for BNZ were determined initially by increasing the concentrations of BNZ in the reaction mixture while keeping the concentrations of CYP2B4 and CPR constant and equal. This was then repeated in the presence of a four-fold excess in the concentration of CYP2E1 over CYP2B4. The data in Figure 4.6 and Table 4.2 show that the apparent K_M increases 8- fold while the k_{cat} remains essentially unchanged. If this increase in the apparent K_M for BNZ arises from a competition between CYP2E1 and CYP2B4 for reduction by CPR, then supplying saturating concentrations of CPR should shift the K_M back to favor the formation of the catalytically active CYP2B4-CPR complex as demonstrated by a decrease in the apparent K_M of CYP2B4 for BNZ activity at high concentrations of CPR (Figure 4.3 and Table 4.2). Therefore, the determination of K_M and k_{cat} of CYP2B4 for BNZ in the presence and absence of CYP2E1 was performed in the presence of high concentrations of CPR (5 fold over the concentration of CYP2B4). The results show that the presence of high concentrations of CPR enhanced the apparent K_M of CYP2B4 for BNZ by 20% and 72% in the absence and presence of CYP2E1, respectively, as compared to lower concentrations of CPR (Table 4.2). These data are consistent with the results shown in Figure 4.3, which taken together demonstrate that the presence of increased

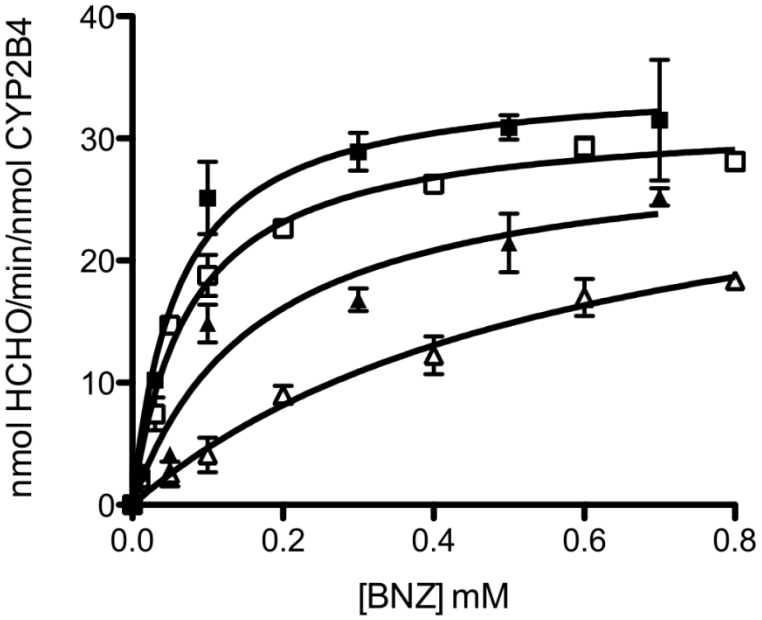

Figure 4.6. Effect of CYP2E1 and CPR on the Kinetics of BNZ Metabolism by CYP2B4. In order to investigate the effect of CYP2E1 on BNZ metabolism by CYP2B4, the K_M and k_{cat} values for BNZ metabolism were determined. The reaction mixtures contained 0.50 μM CYP2B4. They also contained increasing concentrations of BNZ and: 0.50 μM CPR (□), 0.50 μM CPR + 2 μM CYP2E1 (△), 2.50 μM CPR + 2 μM CYP2E1 (▲), and 2.50 μM CPR (■) as shown. Incubations and determinations of formaldehyde product formed were performed as described in Materials and Methods.

	CYP2B4			
	Control	**Plus CYP2E1**	**Plus saturating CPR**	**Plus CYP2E1 and saturating CPR**
K_M (mM)	0.075±0.010	0.60±0.13	0.060±0.012	0.17±0.051
k_{cat} (min^{-1})	32±0.78	33±3.7	35±1.6	30±3.0

Table 4.2. Effects of CYP2E1 and CPR on the K_M and k_{cat} of CYP2B4 for the metabolism of BNZ. The rate of BNZ N-demethylation by CYP2B4 was determined as described in Materials and Methods. All samples contained 0.50 μM CYP2B4 and increasing concentrations of BNZ. The "control" sample contained equal concentrations of CPR and CYP2B4, "plus CYP2E1" contained 2 μM CYP2E1 in addition to the components in the "control" sample, "plus CYP2E1 and excess CPR" contained 2.5 μM CPR in addition to the components in the "plus CYP2E1" sample and, "plus excess CPR" contained the same components as the "control" sample except for the addition of 2.5 μM CPR. The kinetic values given here were derived from data plotted in Figure 4.6.

concentrations of CPR reduce the inhibitory effect of CYP2E1 on CYP2B4. Alleviation of this inhibition leads to a significant decrease of the apparent K_M of CYP2B4 for BNZ back towards that observed in the absence of CYP2E1. account for this difference. Since previous studies on the inhibition of CYP2B4 by CYP2E1 were performed in the presence of excess BNZ (1.2 mM), a perturbation in the affinity of CYP2B4 affinity for BNZ by CYP2E1 may have eluded our detection in these studies. BNZ induces a type I spectral shift upon binding to CYP2B4 but not CYP2E1 (data not shown) and this can be exploited to determine the effect of CYP2E1 on the affinity of CYP2B4 for its substrate. The results in Figure 4.7 show that BNZ binds to CYP2B4 with a K_s of 11.4 μM and that in the presence of CYP2E1 this increases by approximately 30 fold to 339 μM. Thus, CYP2E1 not only inhibits the affinity of CYP2B4 for CPR but CYP2B4's affinity for BNZ.

Determination of the K_M and k_{cat} Values for the Interactions of CYP2E1 WT with CPR. The ability of CYP2E1 to out-compete CYP2B4 for CPR could be attributed to a higher affinity (low K_M) of CYP2E1 for CPR compared to CYP2B4 for CPR. However, our results show that CYP2E1 and CYP2B4 have virtually identical affinity for CPR with K_M values of 0.20 μM and 0.16 μM, respectively (Tables 4.1 and 4.3). Interestingly, when the K_M of CYP2E1 for CPR was measured in the presence of CYP2B4 we observed a 65% decrease in the K_M and an increase in the k_{cat} (Figure 4.8 and Table 4.3). The final K_M value, 0.08 μM, is close to the K_i of CYP2E1 for the CYP2B4 – CPR complex, which is 0.05 μM (Figure 4.5). This suggests that the presence of CYP2B4 leads to the formation of a CYP2E1-CPR complex with a higher affinity than the

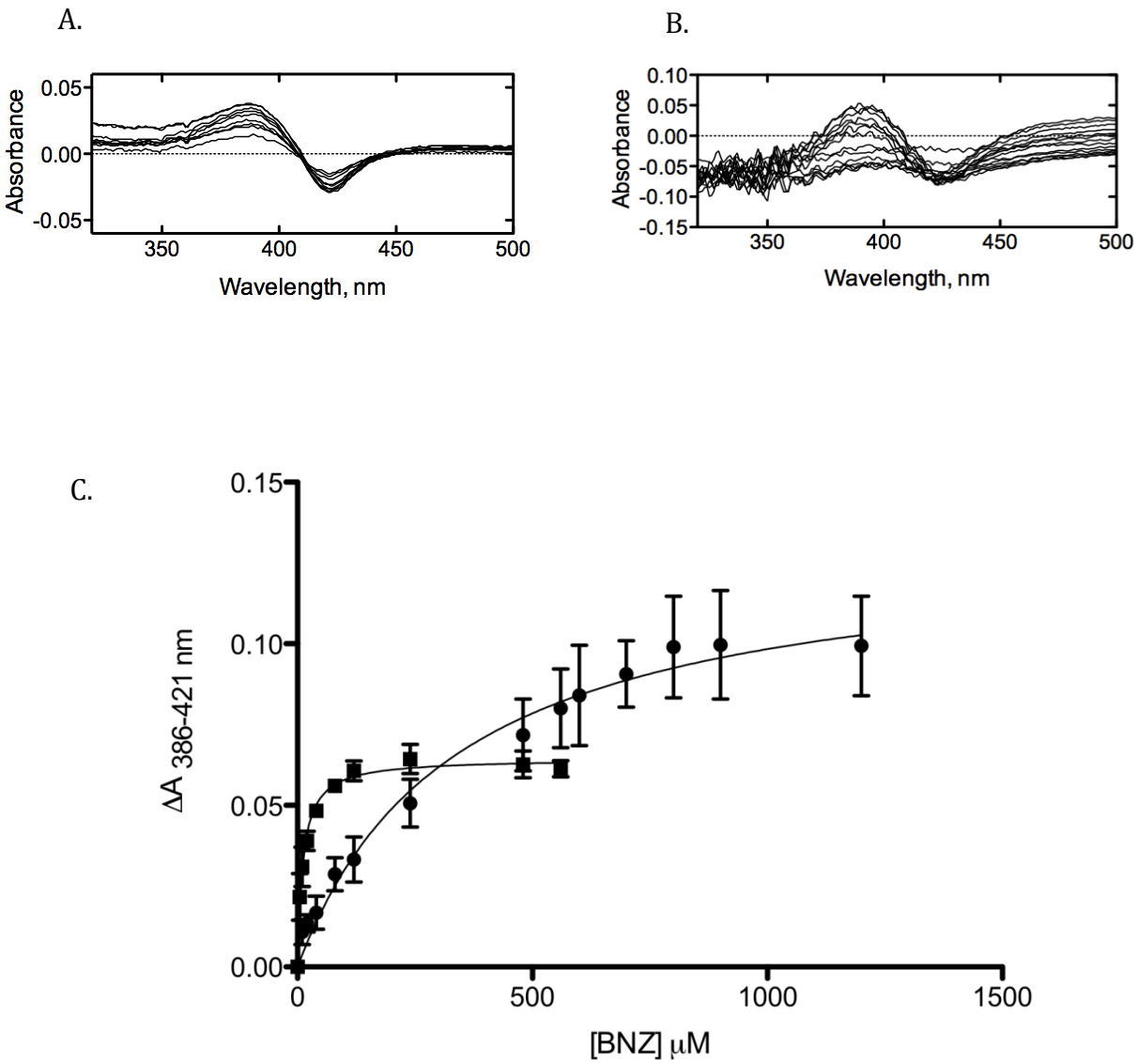

Figure 4.7. Spectral Binding Titrations of BNZ Binding to CYP2B4. Changes in the UV-visible spectrum of CYP2B4 induced by the addition of increasing concentrations of BNZ to CYP2B4 were recorded in the absence (A) and presence of 4 μM CYP2E1 (B) as described in Materials and Methods. Absorbance changes as measured by absorbance at 386 nm minus the absorbance at 421 nm were plotted as a function of BNZ concentration (C) to determine the K_s value for BNZ binding in the absence CYP2E1 (■) and the presence of CYP2E1 (●) as described in Materials and Methods. The values were 11.4 μM ± 1.10 and 339 μM ± 60.2, respectively.

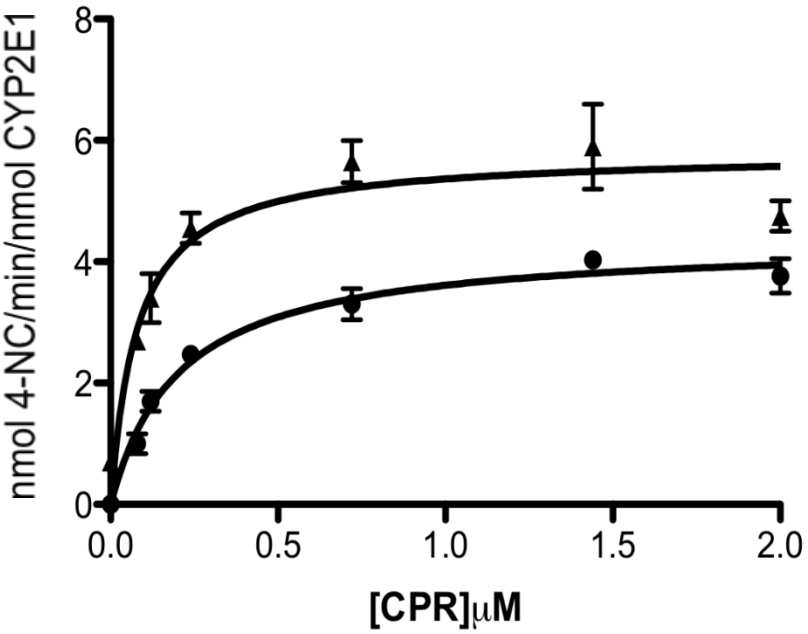

Figure 4.8. Effect of CYP2B4 on the K_M and k_{cat} of CYP2E1 for CPR. The hydroxylation of p-NP to produce 4-NC was measured at a constant concentration of CYP2E1 (0.1 μM) with increasing concentrations of CPR in the absence (●) or presence of 0.1 μM CYP2B4 (▲) as described under Materials and Methods. Error bars are the standard deviations from three measurements performed at least in duplicate.

	CYP2E1 WT	
	Control	**Plus CYP2B4**
K_M (μM)	0.21±0.030	0.080±0.022
k_{cat} (min^{-1})	4.4±0.020	5.8±0.033

Table 4.3. K_M and k_{cat} values of CYP2E1 WT for CPR as measured by p-NP hydroxylation in the absence and presence of CYP2B4. CYP2E1 (0.1 μM) was reconstituted with varying concentrations of CPR in the presence or absence of 0.1 μM of CYP2B4. The reconstituted mixtures were then added to 50 mM of potassium phosphate buffer, pH 7.4, containing 0.3 mM p-NP, and 2 mM ascorbic acid. The reactions were initiated by adding 0.4 mM NADPH and the incubations and determination of 4-NC formation were performed as described in Materials and Methods. The kinetic values given here were derived from the data plotted in Figure 4.8

CYP2B4-CPR complex.

Discussion

For almost four decades it has been known that P450s exist in significant excess (~ 20-fold) over CPR in the ER yet very little is known about their spatial distribution within the membrane (Cawley et al., 1995; Backes and Kelley, 2003). Even less is known about how the disparity in the molar ratio of P450s to CPR influences the catalytic activities of the various isoforms of the P450s and whether this impacts the pharmacokinetic profile of drugs that mainly undergo metabolism by specific P450s. Since CPR and P450 need to form 1:1 complexes for P450 catalytic function, it is highly unlikely that at any given time every P450 will be interacting with a molecule of CPR and functional. Although the overall tertiary structures of mammalian P450s are highly conserved, the amino acid compositions of the regions proposed to interact with CPR are highly variable. Therefore, it is likely that the significantly less than stoichiometric amounts of hepatic CPR relative to P450, coupled with differences in the nature of the interactions between the different P450s and CPR, may lead to favored status for some P450s in the competition between different P450s for binding to CPR. This will have a significant impact on the reduction of the P450 heme and its bound oxygen, and will ultimately lead to significant effects on xenobiotic metabolism.

P450s are capable of producing the ferrous hydro-peroxy intermediate, which is the precursor to compound I, by reaction with peroxides and hydroperoxides such as tert-butyl hydroperoxide (tBHP). The ability of peroxides and hydroperoxides to bypass the need for the delivery of two electrons from CPR makes tBHP a useful experimental tool to study the catalytic properties of the P450 heme in the absence of CPR. In order to

differentiate direct P450-P450 interactions from P450-CPR interactions that lead to inhibition, we measured CYP2B4 activity supported by CPR and tBHP. Furthermore, these studies were performed in the presence of saturating levels of substrate (1.2 mM BNZ) so that we could discern the effect of CYP2E1 on binding of CYP2B4 to CPR from its effect on the affinity of BNZ for CYP2B4. The data show that CYP2B4 was resistant to inhibition by CYP2E1 when BNZ metabolism was supported by tBHP, but lost up to 80% of its BNZ demethylase activity when supported by NADPH and CPR. These results suggest that competition for CPR is implicated in the inhibitory phenomenon observed in Figure 4.1A. To further interrogate the contribution of the CYP2E1 – CPR interaction to the inhibition of CYP2B4 we investigated whether a CYP2E1 variant (Y422D), which has a mutation in the proximal side that reduces binding to CPR by approximately 50%, could alter the extent of inhibition of CYP2B4 activity by CYP2E1. Our results show that the extent of CYP2B4 inhibition by CYP2E1 Y422D is significantly less than that observed with the WT CYP2E1, suggesting a role for the CYP2E1-CPR interaction in the inhibition of CYP2B4 activity supported by CPR.

The notion that CYP2E1 perturbs the formation of the CYP2B4-CPR complex is further supported by the data on the effect of CYP2E1 on the apparent K_M of CYP2B4 for CPR, which showed that low concentrations of CYP2E1 raised the apparent K_M for CPR by 13-fold with a negligible effect on k_{cat} compared to samples that did not contain CYP2E1. Higher CYP2E1 concentrations decreased the apparent K_M of CYP2B4 for CPR, but reduced the k_{cat} by 13-fold. Inverse plots of velocities as a function of CPR concentration revealed that CYP2E1 behaved both as a competitive (at low concentrations) and noncompetitive (at higher concentrations) inhibitor of CYP2B4-CPR.

To estimate a kinetic constant for the observed competitive inhibition component of CYP2E1 we plotted $K_{M\ obs}$ as a function of the CYP2E1 concentration that exhibited competitive inhibition kinetics. Linear regression analysis of these data produced a straight line, which intersected the *x*-axis at -0.05 μM, therefore indicating that inhibition of CYP2B4 by CYP2E1 is very potent. Global non-linear analysis of the same data by GraphPad Prism revealed a similar K_i (0.047 μM).

It is interesting to consider these results in light of the individual K_M values of these two P450s for CPR. If two P450s compete for the same functional binding site on CPR then the specificity, in the sense of discrimination between two P450s competing for CPR, should be determined by the respective K_M values for CPR. However, the measured K_M or k_d values of CYP2B4 and CYP2E1 for CPR are virtually identical; 0.16 μM and 0.20 μM, respectively (Table 4.1 and 4.3). Therefore, one would expect that both P450s could compete with each other for CPR with almost equal inhibitory potency, yet the data show that CYP2E1 can compete with CYP2B4 for CPR but CYP2B4 does not compete with CYP2E1 for reduction by CPR. This discrepancy led us to hypothesize that an alternative mechanism for the inhibition of CYP2B4-CPR complex formation by CYP2E1 likely confers a higher binding affinity of CYP2E1 for CPR.

Backes and co-workers have previously suggested that interactions between P450s and CPR may lead to changes in the affinity of P450s for CPR (Backes and Kelley, 2003; Reed and Backes, 2012). Determination of the apparent K_M and k_{cat} of CYP2E1 for CPR in the presence and absence of CYP2B4 revealed that the apparent K_M decreased by 65% to 0.08 μM while the k_{cat} increased by 1.4 fold to 5.8 min^{-1} in the presence of CYP2B4. Interestingly, the value of this enhanced apparent K_M is similar to

the K_i of CYP2E1 for the CYP2B4-CPR complex, thus supporting the notion that a decrease in the apparent K_M of CYP2E1 for CPR, due to the presence of CYP2B4, contributes to the inhibitory properties of CYP2E1.

In order to propose a tentative model to explain our kinetic data we took into account the following findings: 1) direct CYP2B4-CYP2E1 interactions alone do not lead to inhibition of CYP2B4 activity in the presence of saturating concentrations of BNZ (Figure 4.1A), 2) CYP2B4 and CYP2E1 interact directly to reduce the affinity of CYP2B4 for BNZ (Figure 4.7) and 3) CYP2E1 has a higher affinity for CPR in the presence of CYP2B4 (Figure 4.8). In light of these findings, one possible model that may explain the inhibitory behavior of CYP2E1 toward CYP2B4 is depicted in Figure 4.9. In this model, CYP2E1 and CYP2B4 interact to form a CYP2E1-CYP2B4 complex. This complex may then interact with CPR in such a way that CYP2E1, in the CYP2E1-CYP2B4 complex, interacts with the functional site of CPR with a higher affinity than CYP2E1 alone. A second, although unlikely scenario this model raises is the possibility that CYP2E1 lowers CYP2B4's affinity for CPR by binding directly to CPR's docking site on CYP2B4. While our tBHP studies (Figure 4.1A) excluded the likelihood that CYP2E1 inhibits CYP2B4 activity through direct P450-P450 interactions, it is possible that CYP2E1 may bind directly to CYP2B4 and sterically hinder CYP2B4's association with CPR. However, our studies with the CYP2E1 Y422D mutant point us to consider the opposite for the following reason. Replacing Tyr with Asp led to a decrease in the affinity of CYP2E1 interacting with CPR as well as a decrease in the extent of inhibition of CPR-supported CYP2B4 activity. If the interaction of CYP2E1 with CYP2B4, and not with CPR were responsible for the observed inhibition, then one should not seen any

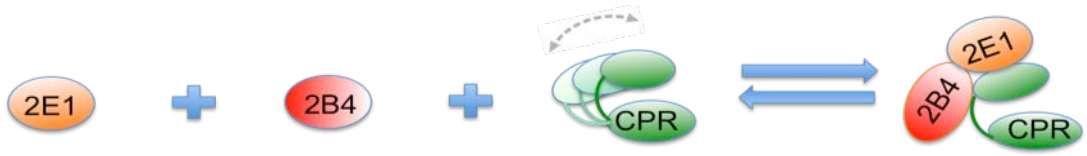

Figure 4.9. A Tentative Model for the CYP2B4-CYP2E1 interaction. Inhibition of CYP2B4 activity may arise from the formation of a CYP2E1-CYP2B4 complex. CPR is believed to be highly flexible (Hamdane et al., 2009; Xia et al., 2011) in solution and a CYP2E1-CYP2B4 complex could trap CPR in a particular conformation which makes it more favorable for CYP2E1, instead of CYP2B4, to bind at a functional site on CPR with a higher affinity than CYP2E1 or CYP2B4 alone.

change in the extent of CYP2B4 inhibition by the Y422D variant. Thus, although our data show that CYP2E1 interacts directly with CYP2B4 to perturb the affinity of CYP2B4 for BNZ, this interaction does not explain the modulation of CYP2B4's affinity for CPR by CYP2E1.

Despite earlier studies to investigate interactions between P450s, the inhibitory nature of CYP2E1 toward CYP2B4-mediated metabolism of BNZ and the enhancement of CYP2E1's apparent K_M for CPR by CYP2B4 (using pNP as a probe substrate for CYP2E1), has not previously been reported. For example, studies by (Kelley et al., 2006) demonstrated that interactions between CYP1A2 and CYP2E1 lead to significantly enhanced rates of 7-ethoxyresorufin (7-ER) and 7-pentoxyresorufin (7-PR). However, when interactions between CYP2E1 and CYP2B4 were investigated using 7-ER, 7-PR and aniline as substrates, functional interactions between these two P450s were not observed suggesting that they did not form P450-P450 complexes. Or, it is possible that complex formation had no effect on any of the activities measured. Therefore, the differences between our results and those of Kelly et al. are probably due to differences in the substrates used, as previous work has shown that interactions between P450s are highly dependent on the substrates under investigation (Cawley et al., 1995).

A significant amount of effort is expended by pharmaceutical and pharmacokinetic modeling companies to predict *in vivo* pharmacokinetic profiles of drugs from *in vitro* data (Rostami-Hodjegan and Tucker, 2007). Since protein-protein interactions in the P450 system may confound *in vitro – in vivo* drug metabolism extrapolations, it is important that in depth kinetic studies be conducted to determine the

kinetic basis and associated kinetic constants that govern these interactions. The information obtained from these types of studies is invaluable as it can play an important role in improving our ability to predict *in vivo* drug clearance and drug-drug interactions from *in vitro* data.

In conclusion, we have shown that the presence of CYP2E1 significantly reduces the N-demethylase activity of CYP2B4 for BNZ. This is not mediated through a simple competition for CPR since CYP2B4 does not decrease the catalytic activity of CYP2E1. It can be concluded from our studies that CYP2B4 and CYP2E1 interact to lower the apparent K_M of CYP2E1 for CPR, which may allow CYP2E1 to out-compete CYP2B4 for CPR. These findings warrant further physical and kinetic investigation to determine the precise structural basis for these interactions and the impact these types of interactions may have on drug-drug interactions.

Footnote

This chapter was under peer-review by the journal *Drug Metabolism and Disposition* during the completion of this thesis. The authors are Cesar Kenaan, Erin V. Shea, Hsia-lien Lin, Haoming Zhang, Matthew Pratt-Hyatt and Paul F. Hollenberg from the Chemical Biology Doctoral Program and Department of Pharmacology at The University of Michigan, Medical Sciences Research Building III, 1150 West Medical Center Drive, Ann Arbor, Michigan 48109, United States.

References

Backes WL, Batie CJ and Cawley GF (1998) Interactions among P450 enzymes when combined in reconstituted systems: formation of a 2B4-1A2 complex with a high affinity for NADPH-cytochrome P450 reductase. *Biochemistry* **37**:12852-12859.

Backes WL and Kelley RW (2003) Organization of multiple cytochrome P450s with NADPH-cytochrome P450 reductase in membranes. *Pharmacol Ther* **98**:221-233.

Bonfils C, Balny C and Maurel P (1981) Direct evidence for electron transfer from ferrous cytochrome b5 to the oxyferrous intermediate of liver microsomal cytochrome P-450 LM2. *J Biol Chem* **256**:9457-9465.

Bridges A, Gruenke L, Chang YT, Vakser IA, Loew G and Waskell L (1998) Identification of the binding site on cytochrome P450 2B4 for cytochrome b5 and cytochrome P450 reductase. *J Biol Chem* **273**:17036-17049.

Brignac-Huber L, Reed JR and Backes WL (2011) Organization of NADPH-cytochrome P450 reductase and CYP1A2 in the endoplasmic reticulum--microdomain localization affects monooxygenase function. *Mol Pharmacol* **79**:549-557.

Cawley GF, Batie CJ and Backes WL (1995) Substrate-dependent competition of different P450 isozymes for limiting NADPH-cytochrome P450 reductase. *Biochemistry* **34**:1244-1247.

Cawley GF, Zhang S, Kelley RW and Backes WL (2001) Evidence supporting the interaction of CYP2B4 and CYP1A2 in microsomal preparations. *Drug Metab Dispos* **29**:1529-1534.

Dey A and Cederbaum AI (2006) Alcohol and oxidative liver injury. *Hepatology* **43**:S63-74.

Eyer CS and Backes WL (1992) Relationship between the rate of reductase-cytochrome P450 complex formation and the rate of first electron transfer. *Arch Biochem Biophys* **293**:231-240.

French JS, Guengerich FP and Coon MJ (1980) Interactions of cytochrome P-450, NADPH-cytochrome P-450 reductase, phospholipid, and substrate in the reconstituted liver microsomal enzyme system. *J Biol Chem* **255**:4112-4119.

Gay SC, Shah MB, Talakad JC, Maekawa K, Roberts AG, Wilderman PR, Sun L, Yang JY, Huelga SC, Hong WX, Zhang Q, Stout CD and Halpert JR (2010) Crystal structure of a cytochrome P450 2B6 genetic variant in complex with the inhibitor 4-(4-chlorophenyl)imidazole at 2.0-A resolution. *Mol Pharmacol* **77**:529-538.

Guengerich FP, Kim DH and Iwasaki M (1991) Role of human cytochrome P-450 IIE1 in the oxidation of many low molecular weight cancer suspects. *Chem Res Toxicol* **4**:168-179.

Hamdane D, Xia C, Im SC, Zhang H, Kim JJ and Waskell L (2009) Structure and function of an NADPH-cytochrome P450 oxidoreductase in an open conformation capable of reducing cytochrome P450. *J Biol Chem* **284**:11374-11384.

Hazai E and Kupfer D (2005) Interactions between CYP2C9 and CYP2C19 in reconstituted binary systems influence their catalytic activity: possible rationale for the inability of CYP2C19 to catalyze methoxychlor demethylation in human liver microsomes. *Drug Metab Dispos* **33**:157-164.

Hu Y, Krausz K, Gelboin HV and Kupfer D (2004) CYP2C subfamily, primarily CYP2C9, catalyses the enantioselective demethylation of the endocrine disruptor pesticide methoxychlor in human liver microsomes: use of inhibitory monoclonal antibodies in P450 identification. *Xenobiotica* **34**:117-132.

Johansson I, Ekstrom G, Scholte B, Puzycki D, Jornvall H and Ingelman-Sundberg M (1988) Ethanol-, fasting-, and acetone-inducible cytochromes P-450 in rat liver: regulation and characteristics of enzymes belonging to the IIB and IIE gene subfamilies. *Biochemistry* **27**:1925-1934.

Kakkar T, Boxenbaum H and Mayersohn M (1999) Estimation of Ki in a competitive enzyme-inhibition model: comparisons among three methods of data analysis. *Drug Metab Dispos* **27**:756-762.

Kelley RW, Cheng D and Backes WL (2006) Heteromeric complex formation between CYP2E1 and CYP1A2: evidence for the involvement of electrostatic interactions. *Biochemistry* **45**:15807-15816.

Kenaan C, Zhang H, Shea EV and Hollenberg PF (2011) Uncovering the role of hydrophobic residues in cytochrome P450-cytochrome P450 reductase interactions. *Biochemistry* **50**:3957-3967.

Kent UM, Pascual L, Roof RA, Ballou DP and Hollenberg PF (2004) Mechanistic studies with N-benzyl-1-aminobenzotriazole-inactivated CYP2B1: differential effects on the metabolism of 7-ethoxy-4-(trifluoromethyl)coumarin, testosterone, and benzphetamine. *Arch Biochem Biophys* **423**:277-287.

Levin W, Thomas PE, Oldfield N and Ryan DE (1986) N-demethylation of N-nitrosodimethylamine catalyzed by purified rat hepatic microsomal cytochrome P-450: isozyme specificity and role of cytochrome b5. *Arch Biochem Biophys* **248**:158-165.

Lin HL, Myshkin E, Waskell L and Hollenberg PF (2007) Peroxynitrite inactivation of human cytochrome P450s 2B6 and 2E1: heme modification and site-specific nitrotyrosine formation. *Chem Res Toxicol* **20**:1612-1622.

Miwa GT, West SB, Huang MT and Lu AY (1979) Studies on the association of cytochrome P-450 and NADPH-cytochrome c reductase during catalysis in a reconstituted hydroxylating system. *J Biol Chem* **254**:5695-5700.

Nash T (1953) The colorimetric estimation of formaldehyde by means of the Hantzsch reaction. *Biochem J* **55**:416-421.

Oezguen N, Kumar S, Hindupur A, Braun W, Muralidhara BK and Halpert JR (2008) Identification and analysis of conserved sequence motifs in cytochrome P450 family 2. Functional and structural role of a motif 187RFDYKD192 in CYP2B enzymes. *J Biol Chem* **283**:21808-21816.

Omura T and Sato R (1964) The Carbon Monoxide-Binding Pigment of Liver Microsomes. Ii. Solubilization, Purification, and Properties. *J Biol Chem* **239**:2379-2385.

Oneta CM, Lieber CS, Li J, Ruttimann S, Schmid B, Lattmann J, Rosman AS and Seitz HK (2002) Dynamics of cytochrome P4502E1 activity in man: induction by ethanol and disappearance during withdrawal phase. *J Hepatol* **36**:47-52.

Patten CJ, Thomas PE, Guy RL, Lee M, Gonzalez FJ, Guengerich FP and Yang CS (1993) Cytochrome P450 enzymes involved in acetaminophen activation by rat and human liver microsomes and their kinetics. *Chem Res Toxicol* **6**:511-518.

Peterson JA, Ebel RE, O'Keeffe DH, Matsubara T and Estabrook RW (1976) Temperature dependence of cytochrome P-450 reduction. A model for NADPH-cytochrome P-450 reductase:cytochrome P-450 interaction. *J Biol Chem* **251**:4010-4016.

Pratt-Hyatt M, Lin HL and Hollenberg PF (2010) Mechanism-based inactivation of human CYP2E1 by diethyldithocarbamate. *Drug Metab Dispos* **38**:2286-2292.

Reed JR and Backes WL (2012) Formation of P450.P450 complexes and their effect on P450 function. *Pharmacol Ther* **133**:299-310.

Rostami-Hodjegan A and Tucker GT (2007) Simulation and prediction of in vivo drug metabolism in human populations from in vitro data. *Nat Rev Drug Discov* **6**:140-148.

Scott EE, He YA, Wester MR, White MA, Chin CC, Halpert JR, Johnson EF and Stout CD (2003) An open conformation of mammalian cytochrome P450 2B4 at 1.6-A resolution. *Proc Natl Acad Sci U S A* **100**:13196-13201.

Scott EE, Spatzenegger M and Halpert JR (2001) A truncation of 2B subfamily cytochromes P450 yields increased expression levels, increased solubility, and decreased aggregation while retaining function. *Arch Biochem Biophys* **395**:57-68.

Subramanian M, Low M, Locuson CW and Tracy TS (2009) CYP2D6-CYP2C9 protein-protein interactions and isoform-selective effects on substrate binding and catalysis. *Drug Metab Dispos* **37**:1682-1689.

Subramanian M, Tam H, Zheng H and Tracy TS (2010) CYP2C9-CYP3A4 protein-protein interactions: role of the hydrophobic N terminus. *Drug Metab Dispos* **38**:1003-1009.

Vermilion JL and Coon MJ (1978) Purified liver microsomal NADPH-cytochrome P-450 reductase. Spectral characterization of oxidation-reduction states. *J Biol Chem* **253**:2694-2704.

Walsky RL, Astuccio AV and Obach RS (2006) Evaluation of 227 drugs for in vitro inhibition of cytochrome P450 2B6. *J Clin Pharmacol* **46**:1426-1438.

Wang H and Tompkins LM (2008) CYP2B6: new insights into a historically overlooked cytochrome P450 isozyme. *Curr Drug Metab* **9**:598-610.

Xia C, Hamdane D, Shen AL, Choi V, Kasper CB, Pearl NM, Zhang H, Im SC, Waskell L and Kim JJ (2011) Conformational changes of NADPH-cytochrome P450 oxidoreductase are essential for catalysis and cofactor binding. *J Biol Chem* **286**:16246-16260.

Yamazaki H, Gillam EM, Dong MS, Johnson WW, Guengerich FP and Shimada T (1997) Reconstitution of recombinant cytochrome P450 2C10(2C9) and comparison with cytochrome P450 3A4 and other forms: effects of cytochrome P450-P450 and cytochrome P450-b5 interactions. *Arch Biochem Biophys* **342**:329-337.

Zhang H, Im SC and Waskell L (2007) Cytochrome b5 increases the rate of product formation by cytochrome P450 2B4 and competes with cytochrome P450 reductase for a binding site on cytochrome P450 2B4. *J Biol Chem* **282**:29766-29776.

Zhang H, Kenaan C, Hamdane D, Hoa GH and Hollenberg PF (2009) Effect of conformational dynamics on substrate recognition and specificity as probed by the

introduction of a de novo disulfide bond into cytochrome P450 2B1. *J Biol Chem* **284**:25678-25686.

Chapter V

Conclusions and Future Directions

Since the initial discovery that the critical components of the P450 system were phospholipid, P450 and CPR, there has been a continuing interest in elucidating the nature of the interactions between P450 and CPR. This interest has been compounded by the realization that microsomal P450s exist in a large excess over CPR (Cawley et al., 1995; Backes and Kelley, 2003). Since a single CPR molecule may be required to coordinate the reduction of 10-20 P450 molecules, rapid association and dissociation of the P450-CPR complex is likely to be important for the system to work effectively. Furthermore, the disparity in the P450:CPR ratio suggests that at any given time only a relatively small portion (5-10%) of the total microsomal P450s can be in functional complexes with CPR and thus capable of optimally catalyzing the metabolism of drugs. For that reason, the metabolism of a drug in a given tissue may not only be a function of the presence of a particular P450 that metabolizes the drug, but also the accessibility of the P450 to CPR, which may be influenced by the identity and abundance of other P450s present in the ER that may compete for the CPR (Eyer and Backes, 1992). To this end, there has been continued interest in delineating the biochemical and biophysical mechanism(s) of interaction of the P450s with CPR and the effect of P450-P450 interactions on the metabolism of various substrates.

Roles for hydrophobic and charged residues in mediating complex formation between CPR and P450 have been identified in the past (Black et al., 1979; Stayton and Sligar, 1990; Rodgers and Sligar, 1991; Shimizu et al., 1991; Voznesensky and Schenkman, 1992; Bridges et al., 1998; Bumpus and Hollenberg, 2010). However, most studies relied on steady-state turnover kinetics as ways to interrogate the residues present at the binding interface and thus could not distinguish perturbations in the electron transfer pathways from changes in the binding affinity. In chapter II, we uncovered novel roles for the surface-exposed residues V267 and L270 of CYP2B4 in mediating CYP2B4-CPR interactions by using a combination of site-directed mutagenesis, fluorescence labeling and stopped-flow spectroscopy techniques. In these studies, a single reactive cysteine was introduced in to a genetically engineered variant of CYP2B4 (C79SC152S) at each of 7 strategically selected surface-exposed positions. Each of these cysteine residues was modified by reaction with an environmentally sensitive fluorophore, fluorescein-5-maleimide (FM), and the CYP2B4-FM variants were then used to determine the K_d of the complex by monitoring fluorescence enhancement in the presence of increasing concentrations of CPR. Furthermore, the intrinsic K_M values of the CYP2B4 variants for CPR were measured and stopped-flow spectroscopy was used to determine the kinetics and the extent of reduction of the ferric P450 mutants to the ferrous P450-CO adduct by CPR. A comparison of the results from these three approaches revealed that the sites on P450 exhibiting the greatest changes in fluorescence intensity upon binding CPR were associated with the greatest increases in the K_M values of the P450 variants for CPR and with the greatest decreases in the rates and extents of reduced P450-CO formation. To our knowledge, the studies outlined in Chapter II are the

first to identify roles for L270 and V267 in the interaction between CYP2B4 and CPR. This was achieved, in part, by circumventing the limitations inherent in identifying residues at protein-protein interfaces exclusively by using mutagenesis and steady-state measurements by complementing those studies with stopped-flow and fluorescence spectroscopy.

In spite of the progress outlined in Chapter II in developing better methodologies to probe P450-CPR interactions, there remain several alternative approaches which may also provide direct measurement of protein-protein interactions but have yet to be explored in the study of mammalian P450 and CPR interactions. One such approach, isothermal titration calorimetry (ITC), has been used in the past to measure the equilibrium dissociation constant of small-molecules with their protein targets as well as the affinity of interacting proteins (Aoki et al., 1998; Muralidhara et al., 2006). Since the output measured by ITC relies on the heat released (and not catalytic activity) when two entities associate with one another, it represents a promising tool to understand the mechanism of interaction of P450 with CPR. For example, in order to obtain a more accurate K_d value for the CYP2B4-CPR complex, it would be of interest to compare the K_d values obtained across a range of independent techniques including ITC. It would also be of interest to study the effect of mutating Val 267 and Leu 270 to Cys on CYP2B4-CPR affinity. Although seemingly straightforward, ITC is likely to involve some degree of experimental optimization, especially when applied to mammalian P450s. Since mammalian P450s are known to exist as aggregates in solution, it is likely that in an ITC experiment where either CPR or P450 is gradually titrated against a constant concentration of CPR or P450 the degree of aggregation of either protein would increase

with an increase in the total concentration of protein in solution. The association of P450s with each other is also associated with a release in heat and this cannot be distinguished from the heat released from the association of CPR with P450. One way to circumvent this aggregation problem would be to employ a soluble CYP2B4 variant, for example CYP2B4dh H226Y which was recently shown to be monomeric at high concentrations (60 μM) and therefore suitable for ITC experiments (Muralidhara et al., 2006).

The conclusions reached in Chapter II regarding the role of V267 and L270 in binding of CYP2B4 to CPR could be further tested by the use of double-mutant cycles to investigate whether the interaction of these two residues with one another leads to effects on the K_d or K_M of CYP2B4 for CPR (Schreiber and Fersht, 1995; Horovitz, 1996). Briefly, a double-mutant cycle involves the comparison of the free energies of association between the wild-type protein, two single mutants, and a variant that contains both mutations. If the residues are not coupled, then the sum of the change in free energies of the single variants associated with binding a protein partner should be similar to the change in free energy associated with the binding of the double-mutant to the protein partner. For instance, although the crystal structure of CYP2B4 (PDB ID 1SUO) showed that V267 and L270 were not close enough for intermolecular interactions, CYP2B4 may be more flexible in solution, and subtle conformational changes may allow these two residues, as well as other residues in proximity and of critical importance for binding CPR (e.g., F135), to have intermolecular interactions. Therefore, the change in the apparent affinity of CYP2B4 for CPR when Val 267 or Leu 270 are replaced by Cys in CYP2B4 might not be a result of the individual roles these residues play in mediating CYP2B4-CPR interaction, but may arise from changes in interactions between the two

residues. This concern can be addressed by generating a CYP2B4 mutant that includes both the V267C and L270C mutations to determine whether the contributions from the V267C and L270C pair are additive or if the effects of mutations are coupled in some way. Therefore, the Gibbs free energy (ΔG), which will be calculated from the K_d for the association of the double mutant with CPR, would be compared to the sum of the ΔGs obtained for the individual L270C and V267C mutants interactions with CPR. If the ΔG value obtained for the double mutant is similar to the sum of the ΔG values obtained for the single-mutants, then V267 and L270 are not coupled, and therefore, the observations reported in Chapter II are specific to the roles of the individual residues which were mutated.

In the discussion section of Chapter II we mentioned that the total amplitude of reduction (A_T), which is a measure of the extent of reduced P450-CO complex formation is an indicator of the concentration of the pre-formed CYP2B4-CPR complex following reconstitution of in DLPC and a lengthy incubation on ice. Although the formation of the P450-CO species should thermodynamically drive the equilibrium between the uncomplexed and complexed CYP2B4 and CPR in favor of complex formation, the association of uncomplexed P450 with CPR is known to be a slow, rate-limiting process (Backes and Eyer, 1989) and was not detected in the timescales investigated in Chapters II and III. Since under our experimental conditions the P450-CO complex was only stable for approximately 400 seconds after reduction of CPR by NADPH in the stopped-flow, it would be valuable to use an FM-labeled CYP2B4 to monitor the association of CYP2B4 and CPR following the reduction of the CYP2B4 by CPR in the pre-formed complex. This experiment would allow direct monitoring of the slow association of CYP2B4 with

CPR and would ensure complete formation of a CYP2B4-CPR complex without the need to monitor the formation of the P450-CO complex, which is an indirect measure of complex formation.

In Chapter III we extended the findings reported in Chapter II by investigating the role of charged residues at the CYP2B4-CPR binding interface. This objective was achieved by replacing V267 and L270 with Lys, Glu and Phe, and characterizing their kinetics under steady-state and pre-steady-state conditions. Unlike previous studies, which have attempted to extend the high catalytic activity observed with $P450_{BM3}$ to mammalian P450s by covalently cross-linking P450 to CPR, we opted to take a non-covalent, reversible interaction approach. One of the factors that contributes to CYP2B4 binding to CPR is complementary charge interactions between acidic residues in the FMN domain of CPR and basic residues on the proximal site of CYP2B4. Such electrostatic interactions are known to have relatively high dissociation energies and can play major roles in long-range interactions between protein pairs that are believed to be critical for steering and orienting protein partners (Schreiber, 2002). Since dipole-dipole interactions are significantly stronger that van der Waals interactions, we hypothesized that they may also serve to minimize the distance between interacting redox-partner proteins, which is critical for efficient electron transfer.

It was found that when a Lys residue was introduced into the proximal CPR binding site of CYP2B4, the k_{cat} of the CYP2B4-CPR complex increased from 46 min^{-1} for the WT to 76 and 68 min^{-1} for the V267K and L270K variants, respectively with a slight increase in the K_M value. Additionally, the introduction of Lys at positions 267 and 270 increased the rate of electron transfer of the fast phase by 2.2 and 2.5 fold compared

to WT, respectively. Lys introduction also resulted in a slight shift in the amplitude of reduction rate toward to fast phase. Replacement of V267 and L270 with another hydrophobic residue, Phe, did not seem to perturb the k_{cat} of the complex and produced a slight increase in the K_m value. Interestingly, the introduction of Glu at residue position 267 led to a 9 fold decrease in the k_{cat} accompanied by a 2.4 fold increase in the K_m. In the case of L270E, accurate determination of the K_M and k_{cat} values was unsuccessful since poor CYP2B4 activity at low concentrations of CPR led to non-Michaelis-Menten kinetics that did not fit a rectangular hyperbolic equation. However, it is likely that mutating L270 to E significantly increased the K_M while greatly decreasing the k_{cat}.

The properties of dipole-dipole interactions have been exploited in the past to engineer protein pairs with significantly improved association kinetics compared to their basal/native rates. For example, faster association kinetics were observed between barnase and barstar by introducing two Lys residues at the protein-protein interaction site in barnase (Schreiber and Fersht, 1996). Additionally, faster rates of electron transfer were observed between cytochrome b_5 and myoglobin when three aspartic residues were replaced with Lys in myoglobin (Xiong et al., 2009; Xiong et al., 2010). Since the studies in Chapter III explored the effect of mutating a single residue to Lys, it would be beneficial to investigate the effect of mutating both Val 267 and Leu 270 to Lys to determine if even faster rates of electron transfer or catalytic activity can be attained for the CYP2B4-CPR complex.

Since introducing a Lys at positions 267 and 270 resulted in a differential increase in the rate of first electron transfer compared to the k_{cat} value for the 2B4-CPR complex, it would be of interest to investigate the extent of uncoupling in the CYP2B4 variants.

Determination of the degree of uncoupling is particularly interesting in light of previous attempts to covalently tether P450 to CPR. These studies were very successful in enhancing the rate of electron transfer beyond levels attained in Chapter III; however, the changes in catalytic activity of these engineered proteins were very far from proportionate to the changes in electron transfer (Fisher et al., 1992; Hayashi et al., 2000). In most cases, activity decreased significantly as a result of covalent cross-linking and this was attributed to higher extents of uncoupling compared to the native, untethered forms. Since the Lys variants reported in Chapter III showed a 2.5 fold increase in electron transfer and a 1.6 fold increase in catalytic activity, an increase in the extent of uncoupling might account for the discrepancy between electron transfer and catalytic activity.

While the studies described in Chapter II and III investigated the mechanism of interaction between CYP2B4 and CPR, the studies described in Chapter IV focused on the effect of interactions between CYP2B4 and CYP2E1 on the affinity of both P450s for CPR and substrate metabolism. The key findings reported in this chapter were the following: 1) CYP2E1 increases the K_M of CYP2B4 for CPR, 2) CYP2B4 and CYP2E1 interact directly to reduce the affinity of CYP2B4 for BNZ and 3) CYP2E1 has a higher affinity for CPR in the presence of CYP2B4. We proposed a tentative model to attempt to explain the kinetic behavior of CYP2B4 and CYP2E1 at less than stoichiometric ratios of CPR. In this model, CYP2E1 and CYP2B4 interact to form a CYP2E1-CYP2B4 complex. This complex may then interact with CPR in such a way that CYP2E1, in the CYP2E1-CYP2B4 complex, interacts with the functional site of CPR with a higher affinity than CYP2E1 alone.

In spite of the progress made in understanding the effect of P450-P450 interactions on substrate metabolism and CPR affinity, several questions remain unanswered with regard to the physical basis and physiological relevance of such interactions. For example the model proposed in Chapter IV to explain the physical basis for the interactions between CYP2B4 and CYP2E1 relies on measurements of the catalytic activities of CYP2B4 and CYP2E1. The major assumption of this approach is that the rate of substrate oxidation is directly proportional to the concentration of the P450-CPR complex (Miwa et al., 1979; Bridges et al., 1998). Since this approach relies on catalytic activity to infer the concentration of the P450-CPR complex, it is therefore an indirect measure of the association of P450 with CPR and does not directly examine the P450-CPR binding process to P450 and subsequent reduction of the P450 by CPR.

The development of methods to specifically probe the effects of CYP2E1 on the reduction of CYP2B4 by CPR would shed important light on the mechanism of P450-P450 interactions. For example, using stopped-flow spectroscopy one could measure the rates of electron transfer from CPR to P450 (as shown in Chapters II and III). However, a major problem with this approach is that both CYP2B4 and CYP2E1 absorb at the same wavelength (450 nm) when reduced and bound to CO making it impossible to distinguish the effect of increasing CYP2E1 concentrations on the rate of reduction of CYP2B4 by CPR. One way around this would be to replace CYP2E1's heme iron with another transition metal, like manganese (Mn), that does not undergo oxidation state changes under the conditions used for stopped-flow studies and would not form a reduced CO complex absorbing at 450 nm. This would negate the absorbance due to CYP2E1 at 450 nm in the presence of CO and would simplify the interpretation of CYP2B4 reduction

kinetics by CPR in the presence of increasing concentrations of CYP2E1.

In the past, attempts to introduce modified porphyrins have been limited to proteins like cytochrome b_5 (cyt b_5) that can withstand removal of the heme-prosthetic group under partially denaturing conditions that are readily reversible (Zhang et al., 2008). For example, Zhang et al. used manganese-containing cyt b_5 (Mn-cyt b_5) to show that cyt b5 inhibits the reduction of CYP2B4 by occupying the binding site of CPR on CYP2B4 (Zhang et al., 2008). They showed that the rate and extent of electron transfer from CPR to CYP2B4 was decreased by Mn-cyt b_5 in a concentration-dependent manner. It would be interesting to apply this approach to the study of CYP2B4 reduction by CPR in the presence of increasing concentrations of Mn-CYP2E1. The preparation of Mn-cyt b_5 from WT cyt b_5 involves dissociating the native heme from cyt b_5 under acidic conditions and then removing it from aqueous solution by extraction with butanone (Morgan and Coon, 1984; Gruenke et al., 1997). The exposure of P450s to acid and organic solvents required to remove the heme leads to protein denaturation and conditions to prevent or reverse this have not yet been determined. This has been a major challenge to efforts directed at substituting the native P450 heme with artificial protoporphyrins while maintaining the native P450 fold. An attractive alternative to the use of harsh denaturing conditions to replace native hemes in proteins involves the use of *E. coli* strain RP523 (Woodward et al., 2007). This method, developed by Woodward et al., exploits the inability of RP523 to synthesize heme as well as membrane permeability of this *E.coli* to large molecules including substituted porphyrins. Briefly, the RP523 cells were grown under anaerobic fermentation conditions and protein expression was induced under aerobic conditions in the presence of Mn-substituted heme. Since

Woodward et al. have shown that this method could replace the native heme of nitric oxide synthase (a P450-like protein) with Mn-porphyrin, it represents a promising tool to substitute CYP2E1's heme iron with Mn. If successful, the use of Mn-substituted heme would provide unambiguous information regarding the effect of CYP2E1 on the K_M of CYP2B4 for CPR and its effect on the reduction of CYP2B4 by CPR.

Thus far, the majority of P450-P450 interaction studies have used purified proteins and were conducted in liposomes. Although the insights gained from studies in purified reconstituted systems are highly valuable, it would be beneficial to extend these studies to systems that more closely resemble the conditions present in the endoplasmic reticulum of the liver. Therefore, studies in hepatocytes or liver microsomes could shed important light on the physiological relevance of the findings reported in Chapter IV. Evidence exists to suggest that the interactions observed between CYP2B4 and CYP1A2 in a purified system also exist in rabbit liver microsomes (Cawley et al., 1995; Backes et al., 1998; Cawley et al., 2001). Since ethanol (Oneta et al., 2002) is known to elevate levels of CYP2E1 it can be used to selectively increase the expression of CYP2E1 relative to CYP2B4 (Pantuck et al., 1985). The N-demethylation of BNZ by CYP2B4 in the presence of elevated protein levels of CYP2E1 can then be measured to determine if CYP2E1 inhibits the activity of CYP2B4 in rabbit liver microsomes. This study will be of great value in determining the potential biological relevance of P450-P450 interactions.

It is important to note that while the widely used methodology to reconstitute P450s and CPR in DLPC is a useful empirical tool to solubilize these proteins and enhance P450 activity *in vitro*, it is not a suitable model to investigate the interactions of

monomeric forms of P450 with CPR. When reconstituted in lipid using methods similar to those employed in studies described in this thesis, P450 and CPR exist as higher state homo-oligomers (Kawato et al., 1982; Reed et al., 2006). Despite the awareness of the existence of P450s as homo- and heterooligomers in membranes, very little is known about the functional importnace of oligomerization on mono-oxygenase activity. To study the association of monomeric forms of CYP2B4, CYP2E1 and CPR future studies would benefit from the use of phospholipid bilayer nanodiscs (Bayburt and Sligar, 2003; Nath et al., 2007a). Nanodiscs are essentially discoidal high-density lipoprotein particles that are composed of a lipid bilayer surrounded by a membrane scaffold protein. Adjusting the ratio of lipid to membrane scaffold protein allows the incorporation of P450s, like CYP3A4 (Nath et al., 2007b), into Nanodiscs and prevents its oligomerization, which can affect reduction kinetics (Davydov et al., 2005).

In conclusion, the work presented in this thesis provides a better understanding of the mechanisms and effects of protein-protein interactions in the cytochrome P450 system by developing methodology to probe CYP2B4-CPR interactions, identifying novel roles for specific hydrophobic residues in binding CPR, harnessing the knowledge obtained in these studies to enhance the rate of electron transfer from CPR to CYP2B4, and determining that interactions between CYP2B4 and CYP2E1 lead to changes in the affinity of CPR for CYP2B4 and CYP2E1. It is our hope that this work will be informative for future studies aimed at acquiring a detailed molecular understanding of protein-protein interactions between not only other P450 isoforms and CPR but other redox-partner proteins as well. Additionally, we hope that the findings will provide valuable insights into the potential for protein-protein interactions in the P450 system to

confound *in vitro – in vivo* drug metabolism extrapolations and may play an important role in improving our ability to predict *in vivo* drug clearance and drug-drug interactions from *in vitro* data.

References

Aoki M, Ishimori K, Fukada H, Takahashi K and Morishima I (1998) Isothermal titration calorimetric studies on the associations of putidaredoxin to NADH-putidaredoxin reductase and P450cam. *Biochim Biophys Acta* **1384**:180-188.

Backes WL, Batie CJ and Cawley GF (1998) Interactions among P450 enzymes when combined in reconstituted systems: formation of a 2B4-1A2 complex with a high affinity for NADPH-cytochrome P450 reductase. *Biochemistry* **37**:12852-12859.

Backes WL and Eyer CS (1989) Cytochrome P-450 LM2 reduction. Substrate effects on the rate of reductase-LM2 association. *J Biol Chem* **264**:6252-6259.

Backes WL and Kelley RW (2003) Organization of multiple cytochrome P450s with NADPH-cytochrome P450 reductase in membranes. *Pharmacol Ther* **98**:221-233.

Bayburt TH and Sligar SG (2003) Self-assembly of single integral membrane proteins into soluble nanoscale phospholipid bilayers. *Protein Sci* **12**:2476-2481.

Black SD, French JS, Williams CH, Jr. and Coon MJ (1979) Role of a hydrophobic polypeptide in the N-terminal region of NADPH-cytochrome P-450 reductase in complex formation with P-450LM. *Biochem Biophys Res Commun* **91**:1528-1535.

Bridges A, Gruenke L, Chang YT, Vakser IA, Loew G and Waskell L (1998) Identification of the binding site on cytochrome P450 2B4 for cytochrome b5 and cytochrome P450 reductase. *J Biol Chem* **273**:17036-17049.

Bumpus NN and Hollenberg PF (2010) Cross-linking of human cytochrome P450 2B6 to NADPH-cytochrome P450 reductase: Identification of a potential site of interaction. *J Inorg Biochem* **104**:485-488.

Cawley GF, Batie CJ and Backes WL (1995) Substrate-dependent competition of different P450 isozymes for limiting NADPH-cytochrome P450 reductase. *Biochemistry* **34**:1244-1247.

Cawley GF, Zhang S, Kelley RW and Backes WL (2001) Evidence supporting the interaction of CYP2B4 and CYP1A2 in microsomal preparations. *Drug Metab Dispos* **29**:1529-1534.

Davydov DR, Fernando H, Baas BJ, Sligar SG and Halpert JR (2005) Kinetics of dithionite-dependent reduction of cytochrome P450 3A4: heterogeneity of the enzyme caused by its oligomerization. *Biochemistry* **44**:13902-13913.

Eyer CS and Backes WL (1992) Relationship between the rate of reductase-cytochrome P450 complex formation and the rate of first electron transfer. *Arch Biochem Biophys* **293**:231-240.

Fisher CW, Shet MS, Caudle DL, Martin-Wixtrom CA and Estabrook RW (1992) High-level expression in Escherichia coli of enzymatically active fusion proteins containing the domains of mammalian cytochromes P450 and NADPH-P450 reductase flavoprotein. *Proc Natl Acad Sci U S A* **89**:10817-10821.

Gruenke LD, Sun J, Loehr TM and Waskell L (1997) Resonance Raman spectral properties and stability of manganese protoporphyrin IX cytochrome b5. *Biochemistry* **36**:7114-7125.

Hayashi K, Sakaki T, Kominami S, Inouye K and Yabusaki Y (2000) Coexpression of genetically engineered fused enzyme between yeast NADPH-P450 reductase and human cytochrome P450 3A4 and human cytochrome b5 in yeast. *Arch Biochem Biophys* **381**:164-170.

Horovitz A (1996) Double-mutant cycles: a powerful tool for analyzing protein structure and function. *Fold Des* **1**:R121-126.

Kawato S, Gut J, Cherry RJ, Winterhalter KH and Richter C (1982) Rotation of cytochrome P-450. I. Investigations of protein-protein interactions of cytochrome P-450 in phospholipid vesicles and liver microsomes. *J Biol Chem* **257**:7023-7029.

Miwa GT, West SB, Huang MT and Lu AY (1979) Studies on the association of cytochrome P-450 and NADPH-cytochrome c reductase during catalysis in a reconstituted hydroxylating system. *J Biol Chem* **254**:5695-5700.

Morgan ET and Coon MJ (1984) Effects of cytochrome b5 on cytochrome P-450-catalyzed reactions. Studies with manganese-substituted cytochrome b5. *Drug Metab Dispos* **12**:358-364.

Muralidhara BK, Negi S, Chin CC, Braun W and Halpert JR (2006) Conformational flexibility of mammalian cytochrome P450 2B4 in binding imidazole inhibitors with different ring chemistry and side chains. Solution thermodynamics and molecular modeling. *J Biol Chem* **281**:8051-8061.

Nath A, Atkins WM and Sligar SG (2007a) Applications of phospholipid bilayer nanodiscs in the study of membranes and membrane proteins. *Biochemistry* **46**:2059-2069.

Nath A, Grinkova YV, Sligar SG and Atkins WM (2007b) Ligand binding to cytochrome P450 3A4 in phospholipid bilayer nanodiscs: the effect of model membranes. *J Biol Chem* **282**:28309-28320.

Oneta CM, Lieber CS, Li J, Ruttimann S, Schmid B, Lattmann J, Rosman AS and Seitz HK (2002) Dynamics of cytochrome P4502E1 activity in man: induction by ethanol and disappearance during withdrawal phase. *J Hepatol* **36**:47-52.

Pantuck EJ, Pantuck CB, Ryan DE and Conney AH (1985) Inhibition and stimulation of enflurane metabolism in the rat following a single dose or chronic administration of ethanol. *Anesthesiology* **62**:255-262.

Reed JR, Kelley RW and Backes WL (2006) An evaluation of methods for the reconstitution of cytochromes P450 and NADPH P450 reductase into lipid vesicles. *Drug Metab Dispos* **34**:660-666.

Rodgers KK and Sligar SG (1991) Mapping electrostatic interactions in macromolecular associations. *J Mol Biol* **221**:1453-1460.

Schreiber G (2002) Kinetic studies of protein-protein interactions. *Curr Opin Struct Biol* **12**:41-47.

Schreiber G and Fersht AR (1995) Energetics of protein-protein interactions: analysis of the barnase-barstar interface by single mutations and double mutant cycles. *J Mol Biol* **248**:478-486.

Schreiber G and Fersht AR (1996) Rapid, electrostatically assisted association of proteins. *Nat Struct Biol* **3**:427-431.

Shimizu T, Tateishi T, Hatano M and Fujii-Kuriyama Y (1991) Probing the role of lysines and arginines in the catalytic function of cytochrome P450d by site-directed mutagenesis. Interaction with NADPH-cytochrome P450 reductase. *J Biol Chem* **266**:3372-3375.

Stayton PS and Sligar SG (1990) The cytochrome P-450cam binding surface as defined by site-directed mutagenesis and electrostatic modeling. *Biochemistry* **29**:7381-7386.

Voznesensky AI and Schenkman JB (1992) The cytochrome P450 2B4-NADPH cytochrome P450 reductase electron transfer complex is not formed by charge-pairing. *J Biol Chem* **267**:14669-14676.

Woodward JJ, Martin NI and Marletta MA (2007) An Escherichia coli expression-based method for heme substitution. *Nat Methods* **4**:43-45.

Xiong P, Nocek JM, Griffin AK, Wang J and Hoffman BM (2009) Electrostatic redesign of the [myoglobin, cytochrome b5] interface to create a well-defined docked complex with rapid interprotein electron transfer. *J Am Chem Soc* **131**:6938-6939.

Xiong P, Nocek JM, Vura-Weis J, Lockard JV, Wasielewski MR and Hoffman BM (2010) Faster interprotein electron transfer in a [myoglobin, b] complex with a redesigned interface. *Science* **330**:1075-1078.

Zhang H, Hamdane D, Im SC and Waskell L (2008) Cytochrome b5 inhibits electron transfer from NADPH-cytochrome P450 reductase to ferric cytochrome P450 2B4. *J Biol Chem* **283**:5217-5225.